Title

Structural and Physiological Studies on the Crystalline Membrane Particles in the Yeast Saccharomyces cerevisiae

Author

Sosinsky, Gina E

Publication Date

1983-04-01

STRUCTURAL AND PHYSIOLOGICAL STUDIES ON THE CRYSTALLINE MEMBRANE PARTICLES IN THE YEAST *Saccharomyces cerevisiae*

Gina E. Sosinsky
(Ph.D. Thesis)

April 1983

Prepared for the U.S. Department of Energy under Contract DE-AC03-76SF00098

DISCLAIMER

LBL-16007

STRUCTURAL AND PHYSIOLOLGICAL STUDIES ON THE CRYSTALLINE MEMBRANE PARTICLES IN THE YEAST *Saccharomyces cerevisiae*

Gina E. Sosinsky
(Ph.D. Thesis)

April 1983

Lawrence Berkeley Laboratory
University of California
Berkeley, California 94720

This work was supported by the U.S. Department of Energy under Contract Number DE-AC03-76SF00098.

ABSTRACT

Structural and Physiological Studies on the Crystalline Membrane Particles in the Yeast Saccharomyces cerevisiae

by

Gina E. Sosinsky

The two-dimensional crystalline particles which are found in the plasma membrane when a stationary state yeast cell is freeze fractured have been studied. These intramembranous particles have previously been seen only by freeze fracture electron microscopy.

The first section involves the characterization of the cellular mechanism of particle crystallization in vivo. Two inhibitors, cycloheximide and sodium azide, were tested to see if they would either prevent or induce the crystallization of the particles. Freeze fracture was used as the assay for crystallization. It has been hypothesized that the reason crystals were found in stationary state yeast cells was that metabolic starvation occurred when the yeast reached stationary phase. Experiments are described which show that metabolic starvation itself was not the only reason for crystal formation, but that protein synthesis was also necessary. The most probable mechanism for patch formation is the saturation of the membrane with these particular proteins and the subsequent precipitation of the membrane proteins as crystalline patches in the plasma mem-

brane.

The bulk isolation of these arrays and the development of a freeze fracture assay to test the morphological purity of the preparation of the membranes are described. The preparation method gives good morphological purity as assayed by a modified monolayer freeze fracture technique, but exact molecular weights of the proteins comprising the crystalline arrays could not be determined. The morphological purity is good enough to image these paracrystals using other electron microscopic techniques besides freeze fracture.

The last part of the research describes attempts made at high resolution imaging of negatively stained and unstained frozen hydrated samples. Deep etching of yeast protoplasts and surface replication of isolated membranes has shown that there is no obvious surface structure that negative stains can penetrate or surround. The failure of negative stains to "outline" morphological features of the crystalline array was confirmed experimentally. Unstained membranes, which were frozen to keep the structures hydrated in the electron microscope vacuum, were imaged. The images of frozen hydrated membranes did not show strong optical diffraction intensities. In rare cases, spots could be seen, but only to a resolution of about 82 Å. In contrast to these disappointing results, the same techniques of imaging frozen hydrated purple membrane were used repeatedly to obtain images of that specimen to greater than 15 Å. It is concluded that the difficulty of obtaining good images of this frozen hydrated membrane is due to an arrangement of the lipids and

the proteins which results in inherent low contrast and minimal surface structure of the specimen.

Acknowledgements

The author wishes to thank many people. First and foremost is my thesis advisor, Dr. Robert Glaeser, whose standards of excellence in science have always been a goal for his students to strive for, and whose dedication to his students is undaunting.

I would also like to thank Dr. Randy Schekman for his kind gifts of the enzyme, lyticase, his insightful conversations, and his reading of this thesis. I would also to thank Dr. John Owicki for reading this thesis.

There are many people at Donner Lab who deserve special mention. Among them, the Yeast Genetic Stock Center, Dr. Robert Mortimer, Rebecca Contopoulou, and Dr. David Schild, for not only their generous gift of Saccharomyces cerevisiae X2180-1a, but their patience as I often used them as a reference source. In my own laboratory group, Dr. Ken Downing, Dr. Bing Jap, Dr. Jules Jaffe, and Dr. Chung Fu Chang deserve special mention for their help and support. The author thanks Ms. Thea Scott-Garner for her technical assistance. I am also grateful to Brian Knittel for his help through the maze called the UNIX system.

Finally, I would like to thank my immediate family and close friends who have provided support and encouragement through this sometimes uphill effort.

TABLE OF CONTENTS

CHAPTER 1

Introduction

Hexagonal arrays of intramembranous particles found in the plasma membrane of the common brewer's yeast, Saccharomyces cerevisiae have long been a favorite object to study for freeze fracture electron microscopists. Yeast cells are easily grown or bought and just as easily prepared for freeze fracture. These freeze fracture particles are affected by common freeze fracture artifacts. Because of these three features, the yeast plasma membrane makes a perfect test specimen for freeze fracture. Yet very little is known about the paracrystals themselves.

The goal of this thesis is to enrich and enlarge the present information about this crystalline membrane not only through freeze fracture, but by other biochemical and electron microscopic techniques. These paracrystalline particles have only been previously observed using the freeze fracture technique and, therefore, a great deal of this thesis will be based on the technique of freeze fracture. Because these particles form two dimensional crystalline arrays in vivo, the hexagonal patches in the yeast plasma membrane are suitable specimens for applying Fourier techniques of image processing in order to enhance higher resolution structural information than freeze fracture can provide.

Throughout this dissertation, I shall be using the freeze fracture nomenclature of Branton et al. (1975) for the plasma membrane surfaces and fracture faces. The plasma membrane has two hydrophilic surfaces: the extracellular, also known as the exoplasmic or external surface, and the protoplasmic surface. The external surface, abbreviated ES, faces the extracellular medium. In the case of yeast cells, the ES faces the periplasmic space. The protoplasmic surface, PS, faces the cytoplasm of the yeast cell. When a plasma membrane is freeze fractured, the membrane is divided into two half-bilayers. The hydrophobic surface, or fracture face, associated with the exoplasmic surface is called the E face or EF. Similarly, the face associated with the protoplasmic surface is called the P face and abbreviated PF.

Chapter 1 contains a broad introduction to the problem presented in the thesis. It contains background on the yeast paracrystals themselves, as well as the electron microscopic techniques used in subsequent chapters. To be specific, Chapter 1 describes previously published work in three areas. The first section reviews the freeze fracture morphology of the paracrystals, the physiology of the particular plasma membrane particles, methods of biochemical isolation of these freeze fracture particles, their protein composition, carbohydrate composition, surface protrusions of these integral membrane proteins, and possible functions for these membrane particles. The second literature review describes previously published work about what has been learned about the structure of the intramembranous par-

tic es from the use of these hexagonal arrays of particles as a freeze fracture test specimen. The last part of the introduction describes the history of the frozen hydrated technique for examining unstained hydrated biological structures as an introduction to "going beyond freeze fracture" with the isolated crystalline yeast membranes. All three sections of this review are relevant with respect the experimental data presented in Chapters 2 through 4.

I. Present Knowledge of the Morphology, Physiology, and Biochemistry of the Paracrystals

A. Morphology: Lattice Size, Particle Size, and Membrane Thickness

When a stationary state yeast cell is freeze fractured, hexagonal arrays are found on the plasma membrane fracture faces. These hexagonal arrays consist of 100 Å particles (Takeo, 1976, Kübler, Gross, and Moor, 1978) on the P face arranged in a 160-165 Å lattice. In artifact-free replicas each particle resembles a volcano, and contains a 50 Å crater in the center of the particle. Larger lattice spacings and particle diameter sizes have been reported but are probably due to artifacts associated with the freeze fracture technique. The complementary E face contains both a ringlike depression, when the replicas are uncontaminated by water vapor, and particles 40 Å in diameter. Takeo has reported that the center-to-center spacing for the E face is 90 Å, one half the spacing found for the P face, which he reported as being 180 Å (Takeo, 1976). However, most other authors find the center-to-center spacing on the E face to be 160-165

Å, equal to that on the P face.

The membrane thickness is average for eucaryotic cell membranes, 80-100 Å as estimated from thin sections of isolated membranes. The thickness has also been reported to be slightly more than 100 Å thick (Fuhrmann, Wehrli, and Boehm, 1974), which may be due to the staining of carbohydrate groups on the external surface of the membrane. Maurer and Mühlethaler (1981a) have estimated that the membrane thickness of freeze dried membranes is 70 Å from the heights of shadows in their replicas of isolated membranes. The P face particle itself stands about 40 to 50 Å high (Maurer and Mühlethaler, 1981a, Gross, 1979), so it may be a transmembrane protein.

B. Physiology: Particle Distribution

The appearance and distribution of the volcano-like intramembranous particles in a population of cells do not remain static throughout the time course of cell culture. The particles are aggregated into paracrystals in stationary state cells, but are found dispersed and in monomeric form in exponential phase (Steere, Erbe, and Moseley, 1980). Late exponential and early stationary state cells contain a mixture of populations in which some cells contain hexagonal arrays but the rest of the population does not. Mixtures of stationary and exponential state cells cultured for 15 minutes show the same appearance as before mixing, although the hexagonal arrays have begun to decrease (Takeo, Shigeta, and Takagi, 1976). The second change in the membrane faces, as visualized by freeze fracture, is that invaginations in the membrane P faces or the ridges

in the E faces normally found to be deep and long in stationary state cells are short and shallow in exponential cells.

In stationary state cells, 20 to 50 PF particles are associated in each hexagonal patch. There is an average of 10 patches per μ^2, but there can be as many as 40 patches per μ^2 found on a particular P fracture face. In stationary phase, the particles average about 20 patches per μ^2 as reported by Osumi, Nagano, and Yanagida (1979) which by their estimation is about 8% of the membrane surface area. The total number of particles found in these arrays varies from 500 to 800 per μ^2. Inhibitors such as sodium azide and dinitrophenol increase the number of patches per unit area as much as by ten times while inhibitors such as ouabain or oligomycin do not affect the freeze fracture appearance of the plasma membrane (Osumi, Nagano, and Yanagida, 1979).

An attempt has been made by Sleytr and Messner (1978) to define two states of the cells according to the physiological conditions under which the cells were prepared for freeze fracture. The authors define a yeast culture to be "resting" if the culture was allowed to grow to stationary phase and remain in the media before being processed for freeze fracture, and "starved" if the culture was resuspended in distilled water and remained for 24 hours at 20 to 23°C with a sterile airflow in the culture. It was their contention at that time that there was a difference in the appearance of the particles in the fractured membrane faces between the two states of the yeast cell. The resting state would not show a volcanic appear-

ance but the starved yeast cell would. Since the time that Sleytr and Messner published this hypothesis, it has been shown by Steere et al. (1980) that it is the fracturing conditions, not the "starved" versus "resting" state of the cells that accounts for the difference in the fracture faces. Sleytr and Messner's paper provides reasonable definitions for two different culture conditions, but the different feature appearing on their freeze fracture faces are artifacts. It has always been assumed that starved cells and stationary state cells would show crystalline arrays in all cells.

C. Biochemistry

1. Isolation Attempts

Attempts to isolate the crystalline arrays involves two methods to remove the outer cell wall which forms the great barrier to the plasma membrane. The first utilizes enzymes containing glucanases which are able to digest the glucan layer forming the major structural support for the cell. The second method uses glass beads which mechanically disrupt the cell wall and plasma membrane at the same time. Both methods have their advantages and disadvantages.

The first method of cell wall removal was historically the first attempted. For example, Boulton (1965) isolated the membrane of the yeast Candida utilis, a genus close to that of Saccharomyces cerevisiae, by first removing the cell wall by using the enzyme streptozyme as the glucanase. Protoplasts were then osmotically lysed and the membrane isolated by differential centrifugation. At that time, Boulton noted that the preparations of membranes isolated by this

method contained about twice as much contaminating membranes from internal sources compared to the plasma membrane. In later publications, protoplasts were prepared using the enzyme helicase as well as streptozyme (Schibechi, Rattray, and Kidby, 1973). Helicase, also known as snail gut enzyme, disintegrates the cell wall completely, while streptozyme appears to make a large hole in the equatorial region of the cell through which the protoplast could escape. In all cases, protoplasts were prepared using exponential phase cells since the glucanases involved function optimally on exponential cells.

There are major advantages and disadvantages to using lytic enzymes to digest the cell wall. The advantage of using the enzyme and osmotic lysis protocol is that one can isolate membrane sheets rather than membrane vesicles, which seems to be the predominant species in cell disruption procedures. The major disadvantage to using lytic enzymes to isolate plasma membrane has been that the commercially available enzyme preparations contain large amounts of proteases which are liable to nick and damage the proteins which are exposed at the plasma membrane exterior. For example, the ratio of lytic (glucanase) to proteolytic activities for glusulase (the commercial preparation currently available) is 66 to 1. Only recently, Scott and Schekman (1979) were able to purify a lytic enzyme preparation which has a lytic to proteolytic ratio of approximately 1500:1. The second disadvantage has been that the enzyme has optimum potency during exponential phase, at times when the size and number of patches is at a minimum. For these two reasons, most patch isolation

attempts have used the mechanical disruption method of cell wall removal for the membrane isolation.

Matile et al. (1967) originally devised the mechanical disruption method upon which Fuhrmann et al. (1974) refined. Fuhrmann et al. starved yeast cells, this time Saccharomyces cerevisiae, under aeration for 15 hours in distilled water and washed with distilled water. The cells were ground with glass beads in a mortar. The cell free extract was osmotically stabilized (Fuhrmann, Boehm, and Theuvenet, 1976). In a later publication, they refined their procedure by using a cell homogenizer which increased the yield of membranes. Subsequent authors who have modified Fuhrmann et al.'s procedure have used mainly glass beads for cell disruption (Baumgartner et al., 1980, Maurer and Mühlethaler, 1981a).

After the cell has been disrupted the isolation of the plasma membrane fragments is rather standard. Fuhrmann et al. (1974) first centrifuged at low speed (2000 x g) and then at higher speeds (5000 x g). The cell extract was run on a continuous sucrose gradient at concentrations of sucrose of 10 to 60%. The membrane separated into two bands. Band 1 was found at a sucrose concentration of 30 to 40%, consisted mainly of mitochondrial vesicles, while band 2 equilibrated at 55 to 60 % sucrose and consisted mainly of plasma membrane vesicles. One assay used to identify the plasma membrane fraction was freeze fracture of the two membrane bands and the occurrence of hexagonal arrays in the fracture faces. The second band was instantly recognizable as containing plasma membranes because hexagonal arrays

were found in the fracture faces of the vesicles. The plasma membrane vesicles contained a mixture of hexagonal arrays and non-hexagonal array fracture faces. In their refined method, Fuhrmann, Boehm, and Theuvenet (1976) found that the two membrane bands had two different surface and isoelectric charges. Mitochondrial vesicles aggregate at pH 4, as seen by an increase in turbidity. Plasma membrane vesicles do not aggregate as the pH is changed. They wanted to avoid using a sucrose gradient because they believed the sucrose gradient was too osmotically stressful for their plasma membrane vesicles. Instead, they first aggregated the mitochondrial vesicles at pH 4 and then, separated the aggregates out at low centrifugation speeds.

Schibeci, Rattray, and Kidby (1973) made protoplasts by lytic enzyme removal of the cell wall using log phase cells and incubated in 0.2 M mercaptoethanol to reduce the disulfide bonds in the cell wall, 0.5% pronase to dissolve the proteins found in the cell wall, and 1.5% helicase. They lysed the protoplasts in the presence of Mg^{++}. Membranes ruptured in the presence of Mg^{++} are stable but may form aggregates. The membranes were layered on a discontinuous sucrose gradient of 60/40/36/32/25% sucrose. They found seven bands, but the predominant plasma membrane band was found in Fraction 7 with a density range of 1.18 to 1.29 gms/cc. The assay used to identify the plasma membrane fraction was the detection of a radioactive label that was reacted only with the external surface of the protoplast plasma membrane. Further centrifugation on a finer sucrose gradient

of the Fraction 7 band gave membrane bands at 1.18 to 1.21, 1.21 to 1.23, and 1.23-1.29 gm/cc. Unfortunately, since no morphological assay of these bands was done, it is not known where the array membranes equilibrated.

Matile et al. (1967) found that cell-free extracts layered on discontinuous sucrose gradients at steps of 55/40/30 at 48,000 X g for 3 hours gave a plasma membrane band contaminated with glycogen and mitochondrial membranes, but the contamination could be reduced by resuspending the material in amylase for 2 hours at $4^{o}C$. The membranes were run on a urograffin gradient and a membrane band was collected at 1.175 gm/cc. Deoxycholate solubilized only part of the membrane fraction. The membranes remaining after DOC treatment had a density of 1.16 gm/cc. The composition, as measured by plasma membrane enzyme activities, differed significantly from one would expect for pure plasma membrane material.

In a later publication, Matile (1970) used instead of a sucrose gradient, a urografin gradient in the range of 1.165 to 1.170 gm/cc. Plasma membranes collected from this gradient partially dissolved in Triton X-100 or DOC. The detergent-treated membranes showed a strong band at 1.23 gm/cc when centrifuged on a urografin gradient of 1.07 to 1.323 gm/cc.

The most recent attempts to isolate the crystalline arrays have been done by Maurer and Mühlethaler (1981a, 1982). They isolated membranes by modifying the Fuhrmann et al. procedure, using cell disruption techniques followed by a modification of the membrane

isolation procedure of Baumgartner et al. Again, the membranes were purified by centrifugation on a continuous density gradient of 20 to 60% sucrose sedimenting at 190,000 g for 150 min. The plasma membrane fraction containing hexagonal arrays sedimented to a density of 1.18 gms/cc. In a later publication (1981b), the authors tried affinity density perturbation for isolating the paracrystalline membranes by conjugating the membrane to Concanavalin A (Con A) coated glass beads. The plasma membrane is known to contain Con A binding sites. The binding of the conjugated beads to the membranes was so strong that the membrane could not be separated from the beads by the addition of a competitor for the binding site, alpha methyl mannose, and therefore, was unsuccessful in terms of bulk isolation. However, the proteins could be isolated for gel electrophoresis by stripping them off the beads with hot SDS.

2. Protein Composition

In all membrane preparations, the problem of cross contamination from internal membranes has prevented identifying the particular plasma membrane bands on polyacrylamide gels (Baumgartner et al. 1980, Maurer and Mühlethaler, 1980, Fuhrmann et al. 1974). Several investigators have found as many as 15 to 20 protein bands of molecular weights in the range of 15,000 to 200,000 in their polyacrylamide gels. Fuhrmann et al. (1974) found that there were four main protein peaks occurring on the gel. These peaks corresponded to molecular weights of 150,000, 90,000, 40,000, and 17,000. They noted that there was contamination from their membrane band 1, the mitochondrial

vesicle fraction, because the 40,000 molecular weight protein was common to both bands and the protein banding profiles of both the plasma membrane and the mitochondrial vesicles were similar.

In spite of this cross contamination problem, several authors have estimated the protein content of their isolated membranes. Fuhrmann et al. maintain that the amount of dry weight of protein is 30 to 45%, while Matile (1970) claims there is only 26% protein. Longley et al. (1968), using the osmotic lysis of protoplasts to isolate the plasma membranes, states that 49% of the membrane fraction is made up of protein.

3. Carbohydrate composition

The carbohydrate content of the yeast plasma membrane patches has been reported to be quite significant and important. The polysaccharides found in the isolated membranes have been shown to be exclusively mannan because the hydrolysis of the residues yields only mannose (Matile, Moor, and Mühlethaler, 1967). In fact, the ratio of mannose to protein by weight is about 3 to 4. This corresponds to the membrane being made up of approximately 15% mannose. In a later publication, Matile (1970) maintains that the total carbohydrate content of the plasma membrane is lower than 5% by weight. Maurer and Mühlethaler (1981a) claim that when membrane proteins are electrophoresed and stained for carbohydrates, four major peaks are seen. There are two large molecular weight glycoproteins at 160,000 and 240,000 and two smaller peaks seen at 60,000 and 70,000, but since their membrane contained mixtures of areas of patch and nonpatch

particles, their assertion that the crystalline particles are composed of glycoproteins is rather speculative.

4. Surface Structures

Labeling of the sugar residues with electron-dense markers has been one way to test the asymmetry of the membrane. Silver staining of protoplasts reveals, in thin sections, dense silver stain granules, which are due to the presence of the carbohydrate groups on the external surface of the membrane.

The external surface usually appears very smooth after deep etching of freeze fractured membranes (Kopp, 1973, Streiblova, 1968). However, when Con A, the lectin whose binding sites are specific for glucose and mannose, is added to protoplasts, the Con A markers are clustered into small domains on the outside of the plasma membranes. Maurer and Mühlethaler (1981b) believe that these small domains are coincident with the small domains of the hexagonal arrays in spite of the fact that the Con A molecules themselves do not form hexagonal arrays on the outside of the cell.

Maurer and Mühlethaler (1981b) claim that in contrast to the smooth outer surface of the ES, the PS contains exposed portions of the crystalline membrane particles. They obtained this result by surface replication of membrane vesicles which were adhered to alcian blue-treated glass and lysed with a shearing stream of buffer. The particles on the PS had the same lattice spacing and approximately the same size as the intramembranous proteins. It is interesting to

note that fibrils were also seen on the PS which were interpreted as cytoskeletal elements.

Immunochemical analysis of the isolated crystalline-noncrystalline mixed membranes revealed 17 discrete antigens in Triton X-100 extracts of the plasma membrane (Baumgartner et al., 1980). Baumgartner et al. made antibodes directed against antigenic determinants on the ES only, the PS and the ES, and the PS only. Cross immunoelectrophoresis of antigens produced by three surface labeling experiments showed that there were 17 distinct antigenic determinants on the surfaces of the yeast plasma membrane. Seven antigenic determinants are exposed on the external surface and 8 are on the protoplasmic surface. Two of the 17 antigenic determinants are on transmembrane proteins and four determinants are exposed only on the ES.

5. Possible functions of the proteins in the paracrystalline arrays

The lack of knowledge about the function of the crystalline arrays can be explained by the two important problems involved in the isolation of the crystalline arrays. The first one has been the cross contamination from other internal membranes. The second problem is the membrane preparations contain crystalline and noncrystalline membrane particles. In spite of this, several researchers have ventured their speculations on the function of these membrane proteins.

Moor and Mühlethaler first speculated in, 1963 that the intramembranous particles were involved in the synthesis of glucan and the transport and insertion of the glucan fibrils into the cell wall. Their speculation relied on their original freeze fracture studies on the fine structure of yeast showing the hexagonal arrays were penetrated by fibrils of short length about 50 Å in diameter, which appeared to be close to the fractured cell walls. It has later been shown by Sleytr and Robards (1977) that the fibrils are due to plastic deformation, an artifact of the freeze fracture process.

Proteins identified by their biochemical activity in the plasma membrane fractions are the Mg^{++}-dependent ATPase, mannan synthetase, glucan synthetase, membrane bound invertase, and NADH dehydrogenase (Maurer and Mühlethaler, 1981b). Baumgartner et al. (1980) showed that of the 17 immunoprecipitates found on the CIE, four possess the enzymatic activities of the ATPase or the NAHD dehydrogenase.

The best studied of the known proteins is the Mg^{++}-dependent ATPase. Matile, Moor, and Mühlethaler (1967) showed that the ATPase activity is 35 to 40 times higher in isolated plasma membrane than in cell free extracts. The ATPase is distinctly different from the mitochondrial ATPase because the former is oligomycin resistant while the mitochondrial ATPase is oligomycin sensitive. (Matile et al., 1967, Fuhrmann et al., 1976). The ATPase is not inhibited by EDAC (N-ethyl-N'-(3-dimethylaminopropyl)-dicarbodiimide hydrochloride), known to inhibit transport ATPase, or inhibited by ouabain, which inhibits the Na^{+}/K^{+} ATPase, nor does it generate cyclic AMP (Fuhrmann

et al., 1976). Recently, it has been shown that a Saccharomyces cerevisiae membrane ATPase is involved in creating a pH gradient across the plasma membrane required for solute transport (Schekman, personal communication). A membrane ATPase isolated from the yeast, Schizosaccharomyces pombe, has been shown to be a proton pumping ATPase (Dufour et al., 1978). This ATPase has similar properties to the Saccharomyces cerevisiae Mg^{++}-dependent ATPase. The Mg^{++}-dependent ATPase is therefore a candidate for these membrane particles because it has been used many times as a marker enzyme for plasma membrane fractions containing these hexagonal arrays. Unfortunately, previous researchers' correlations have been contradictory.

The most recent speculation on the function of paracrystals is by Maurer and Mühlethaler (1982). Their isolated vesicles containing crystalline and noncrystalline areas exhibit invertase activity. Invertase, also known as β-furofructosidase, is the enzyme which catalyzes the cleavage of sucrose and other sugars at the fructosidic linkage (Arnold, 1982). Gels stained for glycoproteins reveal that the two glycoproteins of 160,000 and 240,000 exhibit invertase activity. Protoplasts, labeled with antibodies against soluble invertase and deep etched, exhibit a clumping pattern on the external surface. Again, as was the case with labeling with Con A, the authors felt that the clumped label was overlying the crystalline arrays even though the markers did not exhibit any crystallinity itself.

To summarize, there is not much that is known that is definite about the molecular weight, composition, and function of the proteins making up the crystalline arrays. So far, isolated membrane preparations have not been clean enough, with respect to biochemical purity, to determine the molecular weights, composition, or a possible function for these proteins.

II. Present knowledge of the yeast paracrystals as ascertained by freeze fracture electron microscopy

The greatest amount of information about the paracrystal structure has been obtained by freeze fracture techniques. At the resolution of freeze fracture, e.g. 20 to 50 Å, the structure of these hexagonal arrays has been well documented.

A. Use of the paracrystals as a test specimen for freeze fracture

What makes the arrays so well worth studying is their ease of preparation and their sensitivity to freeze fracture artifacts. In fact, McNutt and Weinstein (1971) recommended using the yeast paracrystals as an ideal test specimen for freeze fracture. Using a cold block cleaving device, they noticed that the EF had numerous ring-like depressions which were readily obscured by freeze fracture artifacts such as specimen contamination or improper platinum-carbon evaporation. McNutt and Weinstein recommended that due to the ease of handling yeast cells and their susceptibility to freeze fracture artifacts, including yeast cells in the internal matrix of a sample could provide a useful internal resolution standard for freeze

fracture replicas. Sleytr and Umrath (1974) have also recommended using these particles as a test of the performance of a freeze fracturing device.

B. First documented study of the paracrystals

The first documented study of the paracrystalline particles was by Moor and Mühlethaler (1963). In their initial study on the fine structure of yeast as observed by freeze fracture, the PF particles appeared as blobs, and the ring-like depressions described by McNutt and Weinstein appeared as pits. Fibrils leading to the cell wall from the particles were observed.

C. Effect of Freeze Fracture Conditions or Artifacts on Morphological Appearance

We now know that the PF particles appear as volcanoes in freeze fracture replicas, through the work of many researchers (e.g. Steere, Bullivant, Moor, and Sleytr) who used the yeast plasma membrane as the test specimen for the two predominant artifacts of freeze fracture. The two artifacts are water vapor condensation and plastic deformation. Both degrade the resolution of the freeze fracture replica by altering the structure of the intramembranous particle before replication and can mislead the investigator to interpret the structure incorrectly.

Water vapor contamination arises by four causes: 1) the hoar frost surrounding the cold specimen as it is transferred into the chamber, 2) residual water vapor in the bell jar, 3) specimen chips

left on the knife edge, which are in poor thermal contact with the knife edge after repeated microtoming, and 4) subliming water vapor from the sample itself. Of these factors, the last two are the major causes of the artifact. A less serious condensation artifact is gas condensation from the evaporators, but is not as well documented (Gross, Bas, and Moor, 1978).

Plastic deformation arises during fracturing when the considerable amount of energy due to the fracturing process itself is transferred to the proteins in the membrane (Sleytr and Robards, 1977). The proteins change their appearance because this energy of dissipation is so great.

The result of these two artifacts is to either fill in pits, enhance the particles or both (Bullivant, 1973). Until recently, it was believed that these two artifacts could not be decreased except through high technological advances.

1. Vacuum Conditions and Water Vapor Contamination

Gross, Bas, and Moor (1978), in an effort to decrease plastic deformation by fracturing at low temperatures (-196^{o}C), modified a standard Balzer's freeze fracture device BA350 to obtain ultrahigh vacuum (UHV). Ultrahigh vacuum is desirable because when a sample is fractured at low temperature, the water vapor contamination increases relative to the amount of water vapor contamination at normal fracturing temperatures, unless an ultrahigh vacuum system is used. The standard Balzers machine consists of a cold microtome arm in a high

vacuum chamber which cuts through specimens kept at a desired temperature on a cold stage. Their apparatus contained an airlock into which specimens devoid of the hoar frost could be put directly into an evacuated bell jar.

Under normal vacuum conditions (10^{-6} torr) and at low fracturing temperatures, the decreased vapor pressure of water favors condensation onto the fresh fracture face rather than evaporation from the sample. At a specimen temperature of -110°C, the partial pressure of water is 10^{-6} torr. Decreasing the pressure to 10^{-9} torr will decrease the contamination rate 1000 fold. At a fracture temperature of -100°C and conventional vacuum conditions, no volcano appearance was found. At a fracture temperature of -196°C and 10^{-9} torr vacuum, the particles clearly appear volcano-like. When the yeast is fractured at -100°C and 10^{-9} torr, an intermediate appearance is found, where volcano structures and non-volcano particles are seen in the hexagonal arrays. In addition, a previously unseen substructure was found on the PF in the threefold position of the hexagonal lattice.

Sleytr and Messner claimed later in 1978 that under normal vacuum conditions, the particles in starved yeast cells resemble volcanoes but the particles in resting yeast cells did not. Although their interpretation has been shown to be incorrect by Steere, Erbe, and Moseley (1980) and Bullivant, Metcalf, and Warne (1979), Sleytr and Messner did demonstrate that the volcanic appearance could be obtained under normal vacuum conditions if a liquid nitrogen cooled shroud was used. It appears that the local, not the global vacuum

conditions around the specimen are the most important in reducing water vapor contamination. If the cells were cleaved under liquid nitrogen, warmed to -108°C, and the shroud kept on until just before replication, the PF particles were still uncontaminated by water vapor.

The volcano appearance and its complementary ring-like depressions had been shown earlier than 1978. In fact, McNutt and Weinstein demonstrated the ring-like depressions in 1971, when they recommended the yeast paracrystals as a test specimen. They had used a variation of the Bullivant and Ames freeze fracturing device type II. The advantage of using the Bullivant and Ames device is the simplicity of the system (Bullivant, 1973). Yeast cells are spun down into a pre-nicked capillary tube, frozen in an appropriate freezing agent, and fractured by breaking the tube under liquid nitrogen. The tube is placed into a hole in a solid metal block and covered with two blocks of metal. The first block contains two tunnels, one at a 90° angle for the carbon shadowing to the fracture face and the other tunnel at 45° for the platinum shadowing. The top metal block acts as a cover to protect against water vapor and other contaminating vapors from entering the tunnels to deposit on the exposed fracture face. The device is transferred to a vacuum evaporator where the top cover is removed and the fracture face can now be replicated. The fracture face is so extremely well shrouded by the metal blocks that freeze fracture replicas reveal optical diffraction spots out to fifth order (approximately 30 Å). When the plasma membrane is frac-

tured by the Bullivant and Ames system, the EF appears as ring-like depressions complementary to the volcano PF particles. An additional "substructure" appears. The major disadvantages of this system, as opposed to the Moor (Balzer) system, are the decreased versatility, i.e. no cold stage, controlled microtoming of the sample, and a decrease in the size of the replicas.

Water vapor contamination is deleterious because it condenses on the yeast plasma membrane so that the water crystallites deposited on the surface appear to look like membrane particles when replicated (Gross, Bas, and Moor, 1978). Gross, Kübler, Bas, and Moor (1978) used their UHV Balzers apparatus to examine how water vapor decorates the paracrystal fracture face. They added to the UHV Balzers an inlet valve through which pure water vapor could be injected. They correlated this with the variation of the partial pressure of water inside the bell jar. Outbursts of water vapor were recorded during successive fracturing. When the fracture temperature was -196°C, the vacuum was 10^{-9} torr, and the partial pressure of water released into the bell jar was 10^{-6} torr, some volcano-like PF particles were found but water condensates were again found mostly outside the paracrystalline regions. The E face rings appeared as heightened particles and water vapor condensates were found outside the crystalline patch area. Increased impingement rates ($ppH_2O=10^{-5}$ torr) caused condensates on the main ring structure of the E face, while low impingement rates (10^{-7} torr) caused contamination on the E face substructure.

Steere, Erbe, and Moseley (1980) showed that replicas where immediate replication had taken place after fracturing with a liquid nitrogen cold shroud revealed volcano particles. Fracturing at -196°C, etching for 5 minutes at -95 °C, and recooling to -196°C, also gave volcanoes. If the cold shroud was kept warm, but the specimen was fractured under the previous conditions, heavy water vapor contamination occurred. In order to confirm that the contamination was indeed from water vapor, they injected nitrogen gas, carbon dioxide gas, room air, or water vapor into the evacuated bell jar. Of these gasses, water vapor caused globular deposits on fracture faces, although room air did cause light contamination. If the fracture temperature was raised to -120°C and room air injected, there was an increase in the water vapor contamination which obscured the membrane and nonmembrane surfaces.

2. Plastic Deformation

Experiments to reduce plastic deformation of the yeast paracrystals have shown what the structures look like after being plastically deformed and how they can be misinterpreted or obscured. An example of the effect of plastic deformation on model systems is the freeze fracture of latex spheres. The glass transition temperature is defined to be the temperature at which a bulk polymer, e.g. latex, will exhibit a brittle fracture rather than an elastic or plastic deformation. The behavior of individual particles can be quite different (Sleytr and Robards, 1977). The glass transition temperature of the latex polymer can be greater than 200 degrees above the freeze

cleavage temperature yet plastic deformation of individual spheres occurs. When plastic deformation of the spheres occurs, the latex spheres resemble long horn-like structures. Fracturing of the spheres at temperatures as low as -258°C still results in specimens that show plastic deformation (Sleytr and Robards, 1977).

For yeast cells, fibrils are found near the cross-fractured wall on one side of the fracture face but no fibrils or depressions which could be caused by fibrils are found on either the opposite side of the face or on complementary halves. Originally, these fibrils were thought to be strands of glucan being transported through the intramembranous particles for cell wall synthesis (Moor and Mühlethaler, 1963). Whenever structures are found non-complementary, it is indicative of plastic deformation. There is an increase in the number of fibrils on both sides of the fracture faces when nonglycerinated (i.e. noncryoprotected) cells are fractured in temperature ranges of -196°C to liquid helium temperatures. It has been hypothesized that during the subsequent shadowing process, only those deformed particles that are in close thermal contact with large dominant structures such as a cell wall or plasma membrane invaginations remain deformed (Sleytr and Robards, 1977). The other deformed particles collapse by radiant heat, heat of condensation during replication, or are destroyed. Thermal vibrations cause deformed particles to collapse to the nearest surface. It is possible that the lipids deform, causing flat spaces where a complementary particle should fit into a pit. The only test for minimized or no plastic deformation is

if the two complementary halves are a perfect fit.

3. High Temperature versus Low Temperature Freeze Fracture

It was hoped by many researchers in the field of freeze fracture electron microscopy that, by going to lower fracturing temperatures, the amount of plasticdeformation would be reduced because at lower temperature the proteins and lipids would be harder and much more likely to keep their shape upon cleaving. This has not been the case. In fact, Steere, Erbe, and Moseley (1980) found that hexagonal arrays of volcano particles without the fibrils indicative of plastic deformation were found on the PF of cells that had been "prefractured", a term invented by Steere to describe fracturing that takes place during cooling of the specimen, before one had intended to fracture. For example, when samples of yeast cells were frozen in Freon 22, visible cracks or fissures arose within the sample as the water in the sample expands during the freezing. They noticed that specimens frozen in Freon 22 contained cubic ice crystals on some of the fracture faces if replicated immediately after fracturing, whereas those samples etched for more than one minute at -100°C were devoid of these ice crystals. Since Steere's apparatus contains an extremely efficient cold shroud, it is doubtful that the ice crystals could have arisen from any decoration phenomenon during fracturing in the bell jar. A more likely explanation was that the ice crystals decorated the membrane face after prefracturing. Only arrays either devoid of fibrils or with a few fibrils were found associated with cubic ice crystals. In the same replica, they found arrays that did

not have cubic ice crystals and contained fibrils. These faces, they named "cold fracture" faces. Prefracture faces are formed at high temperatures (e.g. -60°C) whereas cold fractures occur at temperatures much lower than -60°C. Intermediate temperature fractures also take place.

Bullivant et al. (1979) noticed local differences in fracturing caused different appearances in the PF particles. On the same replica, distinct volcano particles were found in those areas where mostly membrane fractures occurred, while in areas where cross fractures predominated, PF particles lacked craters and had a more irregular shape due to plastic deformation. Bullivant hypothesized that cross fractures are indicative of higher deformations because the plane of least resistance should go through the membrane and therefore, membrane fractures in these areas are likely to be much more plastically deformed. What can be hypothesized about the fracturing of proteins from these studies is that under high temperature conditions proteins are more fluid and will flow back to their original shape, whereas at low temperatures, the more rigid protein particles retain a plastically deformed appearance. It is interesting to note that the debate about high versus low temperature fracturing still exists (see further Sleytr and Robards, 1982).

4. Image Processing of the Freeze Fracture Paracrystal Replicas

Gross and his coworkers used image processing (computer filtration) techniques in order to obtain complementary fracture faces without complementary replicas (Kübler, Gross, and Moor, 1978).

Plastic deformation causes a lack of correspondence between structures seen in the complementary fracture faces. Membranes fractured at low temperatures under ultrahigh vacuum show optical diffraction out to 4th order. These diffraction spots lie on a hexagonal lattice. When computer filtering of the lattice is done, the volcano particles have obvious counterparts in the ringlike depressions on the EF whereas in unprocessed micrographs the complementarity is not apparent. Each ring is surrounded by a hexagonal arrangement of depressions which lie on the threefold axis. This "substructure" should have a particle counterpart on the PF, but it was obscured by the much larger volcano particle. The combination of UHV freeze fracture and image processing techniques produced structures on the PF and EF complementary to each other at a resolution of 20 Å. In the original replicas, the complementary structures were obscured by noise. From these image processed electron micrographs of freeze fracture replicas, a model of the structure emerges. There is a 100 Å volcano particle on the PF, a 50 Å crater particle on the EF, and a depression on the EF which should correspond to a particle on the PF of about 50 Å. Figure 1.1 is a reconstruction from freeze fracture replicas of the present model of the yeast plasma membrane paracrystal.

Image processing was also used as a tool for examining water vapor decoration on these structures (Gross, Kübler, Bas, and Moor, 1978). For example, the image processed structure was known before the introduction of water vapor into the UHV Balzers. Image process-

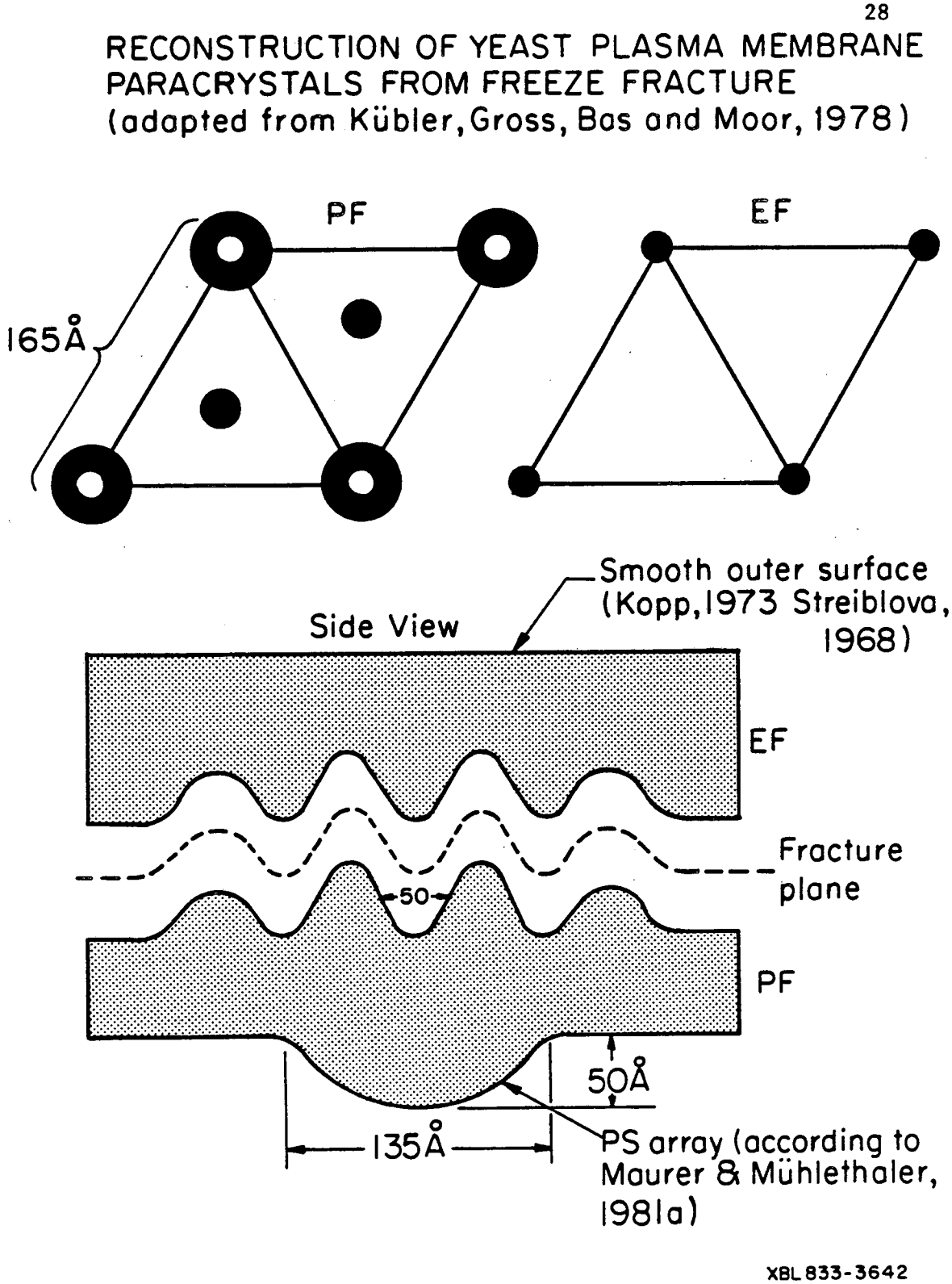

Figure 1.1 A reconstruction of the paracrystalline structure from artifact minimized freeze fracture replicas.

ing was done after decoration to obtain specific sites of water vapor contamination.

5. Complementary Freeze Fracture Replicas

Efforts to obtain complementary replicas have been successful with minimization of plastic deformation and water vapor condensation. Complementary replicas have been produced by two methods: 1) the specimen is fractured under high vacuum at temperatures between -196°C and -100°C and shadowing is done immediately after fracturing or after etching; or 2) the specimen is fractured under liquid nitrogen, liquid helium, or "melting" nitrogen (-210°C) and is transferred carefully under high vacuum for shadowing. In both cases, complementary yeast faces show that the cell wall is cross fractured and numerous fibrils originating from the cell wall occur but no fibrils are found on the corresponding concave fracture face. Fibrils may also be seen bridging the invaginations in the membranes, while fibrillar depressions associate with corresponding ridges on the concave face (Sleytr and Umrath, 1974). Complementary fracture faces have shown that there is a unique plane of fracture through the membrane (Moor, 1971).

III. Going beyond freeze fracture

The motivation for this thesis has always been to isolate the paracrystals in bulk and to examine the paracrystals by electron microscopic techniques other than freeze fracture. The limitations on the resolution of freeze fracture replicas are the artifacts in

the freeze fracture process and the size of the shadowing grains in the replica. Any replication technique, e.g. freeze fracture or surface replication, has a resolution limit of about 20 Å because the resolution of the replica is limited by the size of the shadowing grains, e.g. platinum or tungsten, and not necessarily by the order of the specimen.

A. Limitations to the electron microscopy of unstained biological structures.

It is more advantageous to look at the unstained membrane structure itself, not the surface relief of a fractured membrane. The two main obstacles to studying unstained membrane structure have always been the radiation damage incurred by the electron beam and specimen dehydration due to the electron microscope vacuum. In the case of radiation damage, most biological specimens can only tolerate 1 to 5 $e^-/Å^2$ (Glaeser and Taylor, 1978). Normal focusing and picture taking use doses of more than 1000 times higher than the critical dose. A high dose irradiation of a membrane under normal imaging conditions will definitely destroy almost all substructure. Specimen dehydration can be equally as limiting a problem. For example, crystalline catalase will lose its electron diffraction intensities if there is less than 90% hydration (Taylor, 1978).

B. Circumventing Radiation Damage: Spatial Averaging and Low Temperature

Fortunately, there are ways of getting around radiation damage. The spatial redundancy of biological crystals can be used to reduce the incident dose needed to form the image by using the the method of Williams and Fisher (1970) and employing computer spatial averaging techniques (see Glaeser, 1971). Unwin and Henderson (1975) used computer techniques on "invisible images" of purple membrane taken at safe doses of 0.5 e-/Å^2 to obtain a 7 Å map of purple membrane.

In addition, radiation damage can be significantly reduced at low temperatures. The loss of electron diffraction intensities is a very good measurement of the radiation sensitivity of a biological macromolecule. There is a ten fold increase in the critical dose (the dose required for the complete fading of diffraction spots) of catalase at low temperatures (Taylor and Glaeser, 1976) compared to room temperature and a three fold improvement at low temperature for frozen hydrated catalase as opposed to glucose embedded catalase at room temperature. The critical dose for purple membrane at liquid nitrogen temperatures increases by a factor of 5 to 7 (Hayward and Glaeser, 1979).

C. Maintaining specimen hydration

The problem of maintaining specimen hydration in the electron microscope vacuum has been attacked in many ways. Previous methods are worthy of mention because of their limitations to maintain high resolution structural features even before the specimen is placed into the microscope vacuum.

One of the earliest methods of specimen preservation was the critical point drying technique of Anderson (1952). Specimens being prepared for electron microscopy are dehydrated by gradually replacing the water in the sample with another liquid; either acetone or alcohol is routinely used. The sample is passed through an increasing concentration of alcohol, and the alcohol is subsequently replaced by amyl acetate. The specimen is placed into a bomb and the amyl acetate is flushed out with liquid carbon dioxide. The liquid CO_2 is brought up to its critical temperature and the pressure is brought back down to atmospheric pressure, at which time the liquid CO_2 turns to gaseous CO_2 and the specimen is totally dehydrated. In addition to the fact that the solvents used to replace the water also extract membrane lipids, specimens dried by the critical point drying method exhibit drying artifacts. For example, flagella exhibit thermal collapse, e.g. fibrous structures which were suspended freely from cells vibrate freely under vacuum and collapse irreversibly onto the support and may even break under the tension (Kistler and Kellenberger, 1977).

The same thermal collapse is seen in samples that have been dehydrated by freeze drying. Freeze drying involves the fast freezing of the specimen into either liquid nitrogen or liquid freon and the slow sublimation of water under high vacuum with increasing temperature (Steere, 1957). Freeze drying also introduces a distortion due to increasing salt concentrations upon dehydration. Small particles that are rigid in an ice matrix become displaced by the receding

surface of ice. These particles may then attach to the surface of other particles, or may even be removed entirely upon complete sublimation of the background ice (Steere, 1957). T4 heads, for instance, will collapse to different degrees depending upon whether the heads are filled with DNA as a structural support (Kistler and Kellenberger, 1977). T layer tubes of Bacillis brevis flatten also after freeze drying. Because the T layers are two dimensional crystals the resolution can be measured by optical diffraction. The limiting resolution for freeze dried and shadowed T layers is about 25 to 30 Å, which is about the same as negative staining (Kistler, Aebi, and Kellenberger, 1977). Recently, Lepault and Dubochet (1980) have reported, however, that freeze dried catalase crystals kept in a dry atmosphere at room temperature will show electron diffraction intensities to a resolution of 6 Å.

Negative staining has also been used as a method of preventing specimen collapse as well as its original purpose of enhancing specimen contrast. In this technique, a 1 to 2% solution of a heavy salt such as uranyl acetate or phosphotungstic acid is mixed with the sample. The bulk water is drained off and the sample is air dried. The result is a specimen which is embedded in a heavy salt. According to current theories, the heavy ion penetrates and fills either the surface structure or the water channels, thereby preventing thermal collapse. Shadowing of negatively stained specimens showed very flat surfaces (Kellenberger and Kistler, 1979). The most attractive feature of negative staining is the ease of preparation and the high

contrast of the negative stain, although nonuniform stain penetration is an uncontrollable problem. The best resolution attainable by negative staining is only about 15 Å. Under electron irradiation, the negative stain migrates and changes the structure to a final stable endpoint (Glaeser, 1971). The redistribution and aggregation of stain molecules may involve the formation of microcrystalline regions of stain (Unwin, 1974). At a resolution of less than 10 Å, the negatively stained structure will bear a close resemblance to the original structure, but at higher resolutions the similarity diverges (Unwin, 1974).

Another solution to the specimen hydration problem has been to build a hydration chamber in the specimen area. Two approaches to build chambers are the environmental cell (Kalman et al., 1976) and the differentially pumped (aperture limited) hydration chamber (DPC) (Parsons et al., 1972).

The environmental cell consists of a closed chamber with two thin films forming the roof and floor of the chamber. The films should be thin enough to let the electron beam pass through, but unfortunately films with this requirement are usually too fragile to accommodate constant electron bombardment and when breakage of the films occurs, the specimen hydration is lost. Environmental chambers have mainly been used to image whole cells (Kalman et al., 1976).

The other approach spearheaded by Parsons and his coworkers is that of the differentially pumped hydration stage (DPC). This setup consists of the specimen being sandwiched between two 100 μ

apertures, 1.2 mm apart, which form the floor and ceiling of the chamber. Therefore, the electron beam passes through the aperture. There are also two 200 μ apertures above and below the two 100 μ apertures, which are colinear. The outer chamber is pumped independently while a combination of water vapor, oxygen, and helium is pumped into the inner chamber in order to keep the specimen hydrated (Parsons et al., 1972). The DPC has been used successfully in combination with high voltage to obtain images of wet whole tissue culture cells (Parsons, Uydess, and Matricardi, 1974) and cancer cells (Parsons et al., 1972) and electron diffraction of retina rod disc (Hui, Matricardi, and Parsons, 1973), catalase (Dorset and Parsons, 1975), rat hemoglobin (Dobbs, Pangborn, and Parsons, 1975), and red blood cell phospholipid bilayers (Hui and Parsons, 1974). While the resolution obtained by electron diffraction using the DPC can extend as as far as 3.2 Å as in the case of catalase, the DPC stage is too mechanically unstable to provide good quality images.

The technique of glucose embedment was invented by Unwin and Henderson (1975) in order to get around the specimen dehydration using existing equipment. The procedure of glucose embedment is very similar to that of negative staining except that a 1 to 2% solution of glucose or other sugars is mixed with the specimen and air dried. Crystalline order as measured by electron diffraction was preserved to 3.5 Å for both catalase and purple membrane. Unwin and Henderson, using extremely low specimen doses (0.5 e-/Å^2), were able to record images of catalase and purple membrane to resolutions of 9 and 7 Å,

respectively. The three dimensional structure of purple membrane to 7 Å resolution was determined using the glucose embedment to preserve specimen hydration (Henderson and Unwin, 1975). By combining the glucose technique with low temperatures and refining the phases by probability distributions, Hayward and Stroud (1981) were able to extend the projected structure of purple membrane to 3.7 Å. Glucose embedment, like negative staining, may only fill water spaces and is dependent on the accessibility of the water spaces to the glucose. Therefore, glucose embedment does not work with all specimens. An exception to this hypothesis is the case of purple membrane. Negative staining does not work very well with purple membrane, but glucose embedment does. The major disadvantage of glucose embedment is that the density of the glucose is very close to that of proteins and at low and moderate resolution the map may be uninterpretable (Hayward and Glaeser, 1980).

There are two benefits in using low temperatures with respect to specimen hydration. The first advantage is the increase in radiation resistance and the second is the increased contrast between the protein and the ice. In our own laboratory, the frozen hydrated technique has been a major focus.

Controlling the thickness of the bulk ice can be difficult because of the reproducibility of the layer of ice. The bulk ice must be thin enough for the electron beam to penetrate, but not too thin for the specimen to be dehydrated before freezing in liquid nitrogen. Two methods tried by Taylor and Glaeser (1976) consisted

of a) sandwiching the specimen between two formvar carbon coated folding grids or b) controlling the evaporation of water in a humidity box as monitored by the interference fringes of the bulk water. However, these techniques gave inconsistent results. Two other techniques have been developed within this laboratory for frozen hydrated specimens, one of which is relevant to this thesis.

The first technique is known as the fatty acid monolayer technique, developed by Hayward et al. (1978). It was first used to determine the orientation of purple membrane. Purple membrane binds preferentially to polylysine according to pH. At low pH, the extracellular side binds and at neutral pH, the majority of the purple membranes are found with the cytoplasmic side attached to the polylysine. Unfortunately, purple membranes which have been attached to a polylysine grid and then glucose embedded rarely diffracted. In order to keep the membrane hydrated, a submerged purple membrane-polylysine-carbon coated formvar grid is pulled through a surface film of stearic acid and frozen. The surface film squeezes the bulk water out while retaining the water bound to the purple membrane. Frozen hydrated purple membrane prepared in this manner diffracted to about 4 Å while catalase, which may have been partially disordered, diffracted to at best only 4.2 Å.

The other frozen hydrated technique which I will describe in detail in Chapter 4 is the double carbon film technique (Jaffe, 1982). In the double carbon method, carbon is evaporated onto freshly cleaved mica. The carbon film is floated off on water and a

tabbed grid is pulled through the carbon layer and dried. Purple membrane is applied to the grid and allowed to settle for an appropriate length of time. The grid is immersed into the water, thereby washing off the excess membranes, and brought up a second time through the carbon film. The result is a carbon film sandwich. The back of the grid is dried with filter paper and the evaporation of water from the space between the two carbon films as monitored by the appearance of the drying top carbon film, e.g. the change from shiny to dull. At the correct moment, the grid is immediately frozen. Frozen hydrated purple membrane prepared by the double carbon film technique shows electron diffraction intensities to a resolution of 3.8 Å. Success has recently been attained with images of gap junctions using this method (Unwin, personal communication).

IV. Introduction to thesis research

It has always been a puzzle as to why the freeze fracture paracrystalline membrane proteins are so well loved by freeze fracture electron microscopists and yet have been relatively untapped by membrane biophysicists and biochemists. The most probable answer is a combination of the function of these intramembranous particles being unknown and the complexity in probing the function. While this thesis will not answer the question of the function of these membrane proteins, it will, in the following chapters, describe my research on the yeast paracrystals in the following three areas: 1) the timing and mechanism of patch occurrence and disappearance, 2) the biochemical bulk isolation of the paracrystals, and the 3) the imaging of the

paracrystals by freeze fracture and by electron microscopic techniques other than freeze fracture. Chapter 5 will discuss and integrate the experimental data with previously published research on the yeast paracrystals. Finally, a model of the mechanism of patch formation and paracrystal structure will be proposed.

CHAPTER 2

Experiments on Whole Cells Using Freeze Fracture as the Assay

Freeze fracture can be used as an easy assay for studying the physiological conditions which will cause the formation of crystalline arrays of particles found in the yeast plasma membrane. In this chapter, I will describe three sets of freeze fracture experiments designed to probe the conditions necessary for either patch formation or dissolution. The ultimate goal is to understand the mechanism involved in the crystallization of these membrane proteins. The three sections consist of A) the natural breakup of the crystalline arrays, B) artificial induction of the formation of crystalline arrays by starvation, and C) artificial induction of crystalline arrays by metabolic inhibitors, or lack of effect of these metabolic inhibitors to elicit patch formation.

At the beginning of this project, it was postulated that there were three probable mechanisms of patch formation. These consist of: 1) the precipitation mechanism, 2) the particle deactivation mechanism, and 3) the cytoskeletal deactivation mechanism.

The first, the "precipitation" mechanism, states that the yeast cell keeps overproducing and inserting new particle proteins into the membrane until the "solubility limit" within the plane of the membrane of the proteins is reached. The inserted membrane proteins

which constitute the crystalline arrays are insoluble in the aqueous phase, but once inserted in the plane of the membrane, these proteins can diffuse around freely. If the number of monomers exceeds the solubility limit for free diffusion, oligomers may form. In this case, the higher aggregates are two dimensional crystals. Therefore, there is a definite solubility limit of the crystalline membrane proteins with increasing concentration of the proteins. During patch dissolution, the reverse process occurs. As the amount of plasma membrane increases during cell growth, the crystalline arrays "dissolve" because of the addition of new membrane components, especially the membrane lipids.

The second mechanism is a variation on the precipitation mechanism, named the "particle deactivation" mechanism. In this case, it is postulated that there is a change in the state of either the particle proteins or the membrane lipids that alters the solubility of the particle in the plane of the membrane. The solubility limit of the membrane proteins changes, even though the concentration of the membrane proteins already inserted into the membrane may not have changed. For example, changes in ionic gradients, cyclic AMP levels, and phosphorylation of the proteins themselves may cause association or dissociation of the arrays and thereby change the particle-particle interactions. If there is a change in the state of the particles, this may cause the particles to either repel each other, in which case there is dissociation of the crystalline arrays, or may cause the particles to attract each other, resulting the formation of

crystalline arrays. Alternatively, the state of the lipids in the membrane, which act as a solvent for the intramembranous particles, may change, depending on the metabolic state of the cell, causing aggregation or deaggregation of crystalline arrays.

The third mechanism, the "cytoskeleton deactivation" mechanism, postulates that an activated cytoskeletal structure or similar external constraints, lying beneath the plasma membrane, is required to hold the particles apart. As the metabolic energy sources are used up, the forces holding the membrane particles apart (through the cytoskeletal elements) are deactivated and the paracystalline arrays form spontaneously. Addition of energy again causes the arrays to disperse by moving the cytoskeletal elements beneath the particles.

The experiments reported below in sections A (natural dissolution), B (starvation), and C (metabolic inhibitors) help to elucidate the most probable mechanism of crystalline particle formation.

A. Distribution of Patches Through Lag Phase

Several preliminary studies were done to quantify the disappearance of the crystalline arrays as the cells entered into exponential growth. It was known before these experiments were started that there were patches always present in stationary state yeast cells, while there were no patches present in exponentially growing cells. There were two important questions that were asked, which the following experiments will answer. The first question was whether the change in appearance of the fracture faces was gradual or abrupt.

Secondly, how does the dissolution coincide with the timing of the cell growth curve, especially as a yeast cell proceeds from lag phase to exponential growth?

1. Materials and Methods

Timed samples were taken from a culture grown under the following conditions. A starter culture of wild type haploid yeast, 2180X-1a, was inoculated with a single colony from a streaked YEPD-agar Petri dish into YEPD liquid media (1% yeast extract, 2% bacto-peptone, and 2% dextrose or glucose) and placed into a 30°C incubator with aeration for 24 to 48 hours. Stationary state starter cultures which resulted after this time period were checked for an absorbance at 600 nm of 30 to 40 "O.D. units" (30 O.D. units means that 1 ml of a 1/25 dilution of the yeast culture yielded an absorbance of 1.2 at 600 nm). The effect of letting the culture grow to stationary phase for this long a time interval was to "synchronize" the the cells in the culture, so an inoculum of cells would all have crystalline arrays. A larger culture was inoculated with 1/40 volume of starter culture per volume of new YEPD media and placed back into the 30°C incubator. Samples were taken in the time span of 0 to 5 hours at intervals of 15 to 30 minutes. The samples were assayed for cell growth by measuring the absorbance at 600 nm using a Zeiss PM2 or a Perkin Elmer λ3 spectrophotometer and at the same time aliquots were prepared for freeze fracture.

The same freeze fracture specimen preparation method was used for all the experiments in this chapter. The yeast cells were first

washed twice with 50 mM potassium phosphate buffer (pH 7.5) at 4° C, and then, fixed with 2% glutaraldehyde in 50 mM phosphate buffer (pH 7.5) at room temperature for 30 minutes. The yeast cells were then washed with 20% glycerol in double distilled water and resuspended in 20% glycerol at 4°C for adequate cryoprotection. The yeast were spun down and resuspended in a minimum of 20% glycerol to make a paste. Yeast paste (3 to 5 µl) was applied to 3 mm cardboard discs and frozen in liquid freon or liquid nitrogen slush. The sample discs were then freeze fractured using a Balzers 400 or 301 at -115°C and replicated immediately using ~25 A of Pt-C at a 45° shadowing angle. Carbon was immediately applied after the Pt-C shadow and the replicas were floated off in liquid bleach and cleaned for a minimum of two days. The replicas were rinsed twice with distilled water washes for a minimum of 20 minutes each. Replicas were mounted on either flamed naked 400 mesh grids or carbon backed formvar coated 200 mesh grids.

Replicas were examined in an AEI 802 or JEOL 100CX electron microscope at 80 KV or 100 KV, respectively. Micrographs were usually taken at magnifications of either 25,000 or 40,000 for the AEI 802, and 26,000 or 33,000 for the JEOL 100CX. These particular magnifications were used because fracture faces of yeast usually fill most of the area of the film. P faces were considered preferable to E faces for picture taking because they are less susceptible to freeze fracture artifacts such as plastic deformation or water vapor contamination than E faces. However, in every sample of fracture faces taken, a few E face pictures were also taken for the sake of

completeness. Between twenty and thirty micrographs were usually taken for adequate sampling as a subjective but consistent criterion. An eight by ten enlargement of each negative was printed to provide quick visual inspection of the occurrence of the paracrystalline arrays on the membrane fracture face. The fracture faces were divided into two categories: those containing hexagonal arrays and fracture faces devoid of hexagonal arrays.

2. Results

Under the conditions of this experiment, the cells remained in lag phase for approximately 2 1/4 hours and then proceeded into exponential growth. The crystalline arrays as measured by freeze fracture begin to disappear about 30 to 45 minutes before the onset of exponential growth.

A cell growth curve is shown in Figure 2.1. The arrow denotes the time at which the number of fracture faces revealing patches has significantly decreased. A summary of this experiment is shown in Table I and a gallery of P fracture faces representing the results for each of the sampling times is shown in Figure 2.2.

The cells reveal many small patches at 5 minutes, 30 minutes, and 1 hour, but show either reduced size and numbers of crystalline arrays, or the paracrystals are nonexistent, at 90 minutes. It is interesting to note that 90 minutes is about one generation time for yeast in a rich medium such as YEPD. Therefore, at 90 minutes, all yeast cells in this culture should have progressed from their dormant

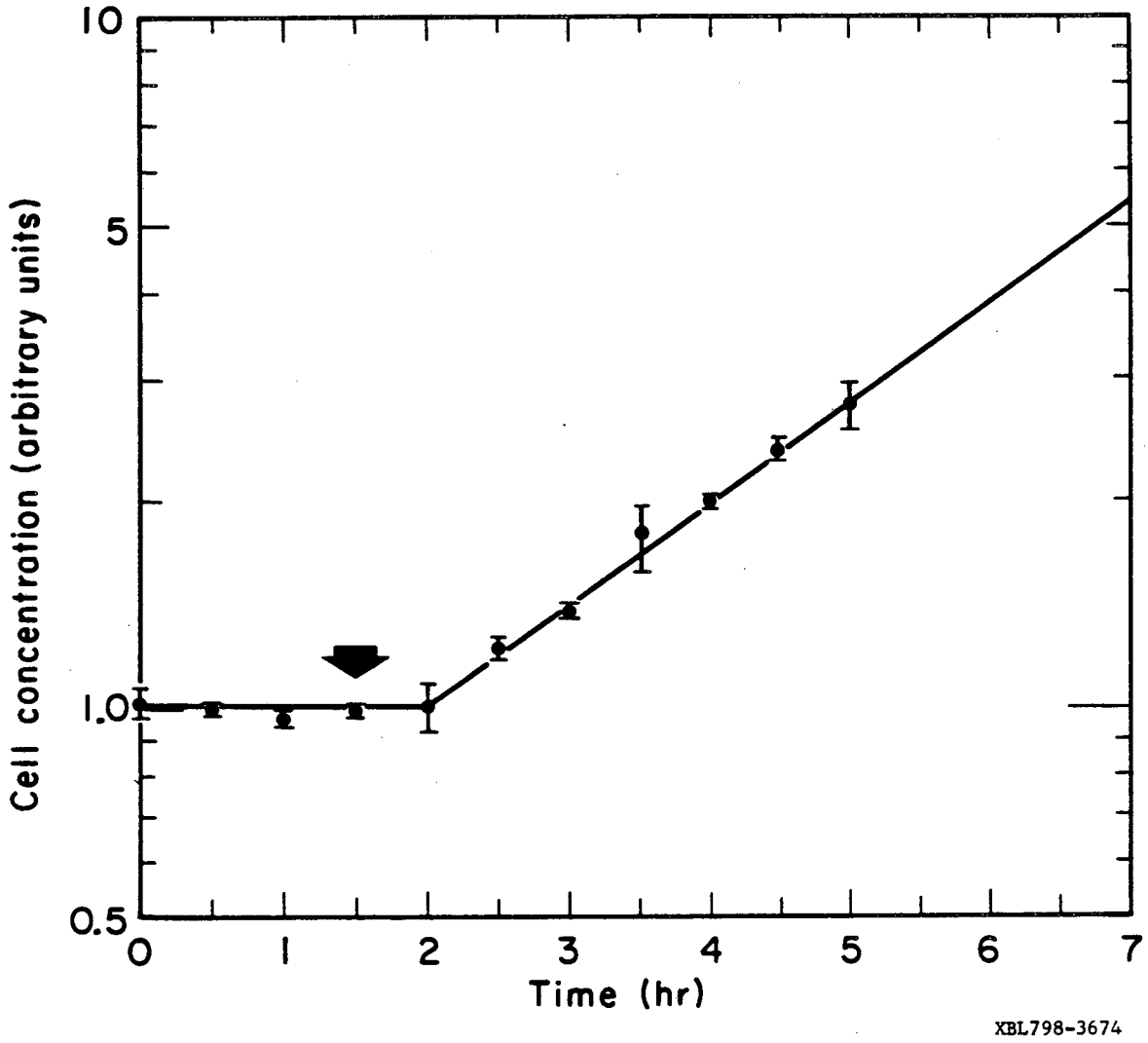

Figure 2.1. Cell growth versus time for the experiments probing the distribution of patches through lag phase. The arrow indicates the time at which populations of cells which have crystalline arrays on their fracture faces have significantly decreased.

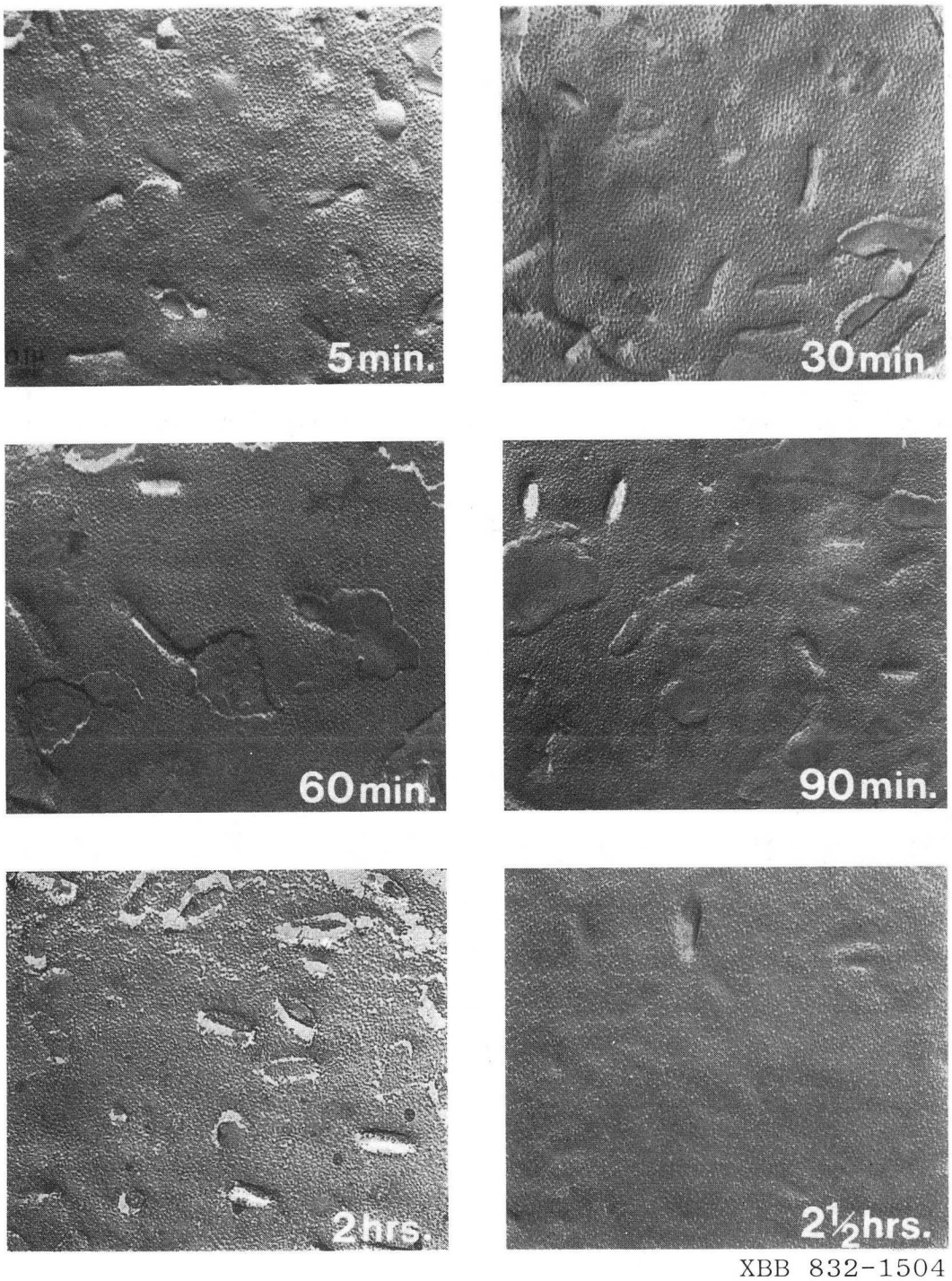

XBB 832-1504

Figure 2.2. Representative P fracture faces for each of the sampling times in the experiments probing the distribution of patches through lag phase experiment. The magnifications for all of the fracture faces are the same.

TABLE I. SUMMARY OF THE EXPERIMENTS PROBING THE DISTRIBUTION OF PATCHES THROUGH LAG PHASE

Time After Inoculation	% Cells With Patches	% Cells Without Patches	# Cells (Pictures)
5 Min	100	0	7
30 Min	100	0	16
60 Min	100	0	24
90 Min	45	55	20
2 Hrs	4	96	25
2 1/2 Hrs	5	95	22
Late Log Phase	62	38	13

state to one of active growth. By 2 1/2 hours, the predominant population of yeast cells does not reveal any patches in their fracture faces. At a sample time of about 4 hours, no yeast cells were found containing crystalline arrays in their fracture faces. Samples taken during late exponential phase (A_{600} greater than 14 OD units) contained mixed populations of fracture faces which contained paracrystals and fracture faces which did not show paracrystals. A decreasing rate of cell growth occurs in late log phase due to density dependent inhibition. Late log phase cultures contain mixed populations of the two different types of fracture faces.

B. Starvation Experiments

An interesting question arose about the difference in numbers of fracture faces containing crystalline arrays in cells which had been starved and stationary phase cells. Before this set of experiments, it was thought that there was no difference between the two states with respect to patch formation, i.e. patches were always found in all cells in stationary phase and in starved cells. It was thought that stationary state cultures exhibited close to 100% fracture faces containing patches because depletion of the nutrients in the medium induced a starved state condition. If this is true then it is important to determine how long the starvation period must be in order for a culture to exhibit crystalline arrays on 100% of the plasma membranes. For these reasons the following sets of experiments were done.

1. Materials and Methods

A starter culture was inoculated from a single colony and allowed to grow for 24 to 48 hours to stationary phase as monitored by the absorbance at 600 nm. A flask containing liquid YEPD was inoculated at an inoculation ratio of 1:250. The cultures grew for about 10 hours to an absorbance at 600 nm of about 2. Cells grown under these conditions should have no crystalline arrays when they are freeze fractured. The cells were then collected by centrifugation and washed free of the media with 50 mM potassium phosphate buffer at a pH of 7.5. The cells were resuspended in 50 mM phosphate buffer and placed back on the 30°C incubator with aeration and allowed to "starve". Samples were taken at various times and prepared for freeze fracture using the same procedure as the described in section A.

A second YEPD culture was used as a control to compare the growth of yeast cells when maintained in nutrient rich media. The second culture was taken out of the incubator at the same time as the first and placed on ice in order to keep it coincident with the first. When the starved culture was placed back into the incubator, the control culture, i.e. cells still in YEPD, was also returned to the incubator and samples were taken out at the same times as the starved culture, prepared for freeze fracture, but were never fractured. The A_{600} was measured in order to compare the cell growth in rich media with that in starvation media.

2. Results

The results of the experiment dealing with the length of time of starvation are shown in Table II. Yeast cells starved for only 1 hour showed complete lack of crystalline arrays, but by 2 hours after starvation patches do occur in significant quantities. Comparing the cell growth in the starvation media versus cell growth in the rich media, the cells in rich media grew at a much faster rate than those in starvation media, as expected.

Several unexpected results of this experiment occurred. First, there were two populations of cells, one with patches and another devoid of patches. Whether a given cell develops crystalline patches or not may depend upon where in the cell cycle that particular cell is just prior to starvation. For example, two different trials of this experiment gave two different ratios of the two types of fracture faces at the same time period (see the 10 hour sample). Cells capable of forming patches proceed to form crystalline arrays in their plasma membrane, but another set of cells remain in a condition whose freeze fracture appearance is similar to log phase fracture faces. The starvation time at which crystalline arrays form is between 1 and 2 hours, which is coincident with the lag phase timing experiments of section 2A where 90 minutes was the time at which a large percentage of the cells were devoid of crystalline arrays. Also unexpected was the observation that crystalline arrays never formed in 100% of the cells even at very long intervals of starvation such as 24 and 48 hours. Also, the ratio of fracture faces devoid of crystalline arrays increased, as did the number of cells, as yeast

TABLE II. SUMMARY OF STARVATION EXPERIMENTS

Starvation Times	% Cells With Patches	% Cells Without Patches	# Cells (Pictures)	OD_{600} of Starved Cells	OD_{600} of Cells in YEPD
0 Hours a)**	NF*	NF	NF	2.095	2.070
b)	NF	NF	NF	2.520	2.360
1 Hour a)	0	100	24	2.115	2.205
b)	0	100	29	2.530	2.422
2 Hours a)	NF	NF	NF	2.133	2.500
b)	45	55	27	2.510	2.625
5 Hours a)	21	79	23	2.157	2.820
b)	NF	NF	NF	2.520	2.940
10 Hours a)	25	75	24	2.253	3.061
b)	63	37	32	2.590	3.482
24 Hours b)	48	52	29	8.180	14.300
48 Hours b)	7	93	28	7.730	17.350

* denotes a sample was collected but not fractured.
** a) and b) denote two different trials of these experiments.

cells turned on alternative metabolic pathways. It is interesting that the crystalline arrays almost completely dispersed upon long intervals of starvation. Under these long starvation conditions, it is likely that the cells ceased membrane protein synthesis and insertion.

Therefore, to answer the questions asked at the beginning of this section, there is no minimum time of starvation which will yield a 100% population of fracture faces bearing crystalline arrays. Rather an optimum starvation time occurs somewhere between 5 and 10 hours which yields a maximum population of cells revealing crystalline arrays on their fracture faces. There does seem to be a difference between stationary state and starvation with respect to the ratio of the two different fracture faces. Although the two states were expected to both have yeast cells whose membranes fracture faces all contain crystalline arrays, this does not occur. Perhaps the definition of stationary state should be one in which the yeast cell is resting. Protein synthesis has been completed and the metabolic resources have been depleted. Starvation is a state in which metabolic resources are not present and protein synthesis may have not been completed in all cells.

C. Effect of Metabolic Inhibitors on Patch Formation

Two types of metabolic inhibitors were used to test their ability to influence patch formation. Cycloheximide is a well known inhibitor of protein synthesis in yeast. Sodium azide inhibits the formation of ATP by binding to cytochrome oxidase in mitochondria

(Boyer et al., 1977). Unfortunately, there was no inhibitor available that would affect cytoskeletal elements underlying the cell plasma membrane in yeast cells, so hypothesis three, activation/deactivation of the cytoskeleton, cannot be totally eliminated.

1. Materials and Methods

Again, a starter culture was grown for two to three days to stationary phase in order to start the experiment with an inoculum of yeast cells with 100% patch containing fracture faces. The absorbance at 600 nm was usually measured to be about 30 to 40. A portion of this starter culture (0.5 ml) was added to each of six flasks containing 100 ml of YEPD at 30°C with aeration and allowed to grow for 10 hours in order to reach a mid-log phase. The six flasks were designated in the following manner:

Sample A. Log phase control

B. Starved Culture

C1. Cycloheximide treated but not starved

C2. Cycloheximide treated and starved in the presence of cycloheximide

D1. Azide treated but not starved

D2. Azide treated and starved in the presence of azide

For the log phase control (sample A), yeast cells were collected after 10 hours of growth, washed free of the medium, and prepared for freeze fracture. At the time of collection, the absorbance at 600 nm

was measured to be 9.9 O.D. units, which is indicative of a culture in mid log phase.

Cells in sample B were collected after ten hours, washed free of medium with a 50 mM pH 7.5 potassium phosphate buffer and resuspended in this buffer. The cell suspension was incubated on the 30°C shaker for 4 1/2 hours. The cells were then collected, washed with the phosphate buffer, and prepared for freeze fracture.

After 10 hours of growth, 11.4 mg (solid) of cycloheximide were added to the yeast culture designated C1 to give a final concentration of 100 µg/ml. The flask was returned to the 30°C incubator for 1 1/2 hours, after which the cells were collected, washed, and prepared for freeze fracture. Sample C2 was treated with cycloheximide in the same manner except that after 1 1/2 hours on the 30°C shaker, the cells were collected, washed with phosphate buffer containing cycloheximide and resuspended in phosphate buffer containing cycloheximide. Concentrations of cycloheximide were also kept at 100 µg/ml. The cell suspension was put back onto the incubator. After two hours, the cells were collected and washed with buffer containing inhibitor and prepared for freeze fracture using the procedure mentioned above.

For the last two sample cultures, after 10 hours of growth, 0.2 M of sodium azide (final concentration) was added to the two flasks. The culture was returned to the 30°C incubator for 1 1/2 hours. After 1 1/2 hours, the cells in one flask, which was designated D1, were collected by centrifugation, washed with phosphate buffer

containing the same concentration of sodium azide and prepared for freeze fracture. The yeast cells in the last culture, D2, were collected by centrifugation after the 1 1/2 hour azide treatment in media, but were washed and resuspended in phosphate buffer containing 0.2 M sodium azide and put back in the incubator for 2 hours of starvation. After the two hours, the cells were collected, washed with buffer containing the inhibitor and prepared for freeze fracture.

2. Results

A summary of this experiment is shown in Table III. Yeast cells in sample A, the log phase control, had no patches, as expected. Cells that had been starved for about 5 hours (sample B) contained the two distinct populations of cells as described in section 2B. Cycloheximide treated cells had a relatively low population of crystalline patch containing cells, whereas cells starved in the presence of cycloheximide did not show a subpopulation of patch containing cells. Azide treated cells contained a relatively large subpopulation of patched cells which increased upon starvation in the presence of azide. The cell growth as determined by the A_{600} was measured before and after the addition of either cycloheximide or azide. Cell density increased slightly for about 1 hour after the addition of cycloheximide, whereas the cell density remained constant after the addition of sodium azide.

From this set of experiments, it was learned that new protein synthesis is a necessary condition for patch formation. The blocking of protein synthesis prevents patch formation not only in rich media,

TABLE III. SUMMARY OF INHIBITOR EXPERIMENTS

Sample	Description	% Cells With Patches	% Cells Without Patches	# Cells (Pictures)
A	Log Phase	0	100	20
B	Starved Cells	45	55	20
C1	Cycloheximide Treated Cells	5	95	20
C2	Cycloheximide Treated and Starved	0	100	22
D1	Azide Treated Cells	82	18	22
D2	Azide Treated and Starved	100	0	22

but also under starvation conditions. (Schindler and Davies, 1975). If only deprivation of metabolic energy was necessary to induce patch formation, then starvation should induce patches in cells which have been starved in the presence of cycloheximide. This did not happen. Cycloheximide interferes at the ribosomal level of protein synthesis and will interfere with DNA synthesis, as a secondary effect, after a first round of protein synthesis is complete (Schindler and Davies, 1975). Therefore, the formation of crystalline arrays can be blocked at the ribosomal (protein synthesis) level.

Metabolic energy inhibition by sodium azide does induce patch formation, but sodium azide inhibition may not inhibit all ATP synthesis, just aerobic ATP synthesis. It is possible that either protein synthesis can be completed with the pool of ATP remaining after azide inhibition or through completion of protein synthesis using anaerobic ATP synthesis. Patches can then form by the precipitation mechanism or also by the related mechanism of particle deactivation. A note of caution should be interjected here. The concentration of sodium azide was much higher than necessary and there is always the possibility of indirect effects. Also, the experiments on energy depletion were not well controlled, i.e. ATP levels were not measured and minimal conditions for energy depletion were not established. However, it was the intention of these experiments only to repeat and verify the experimental results of Osumi et al. (1979) and not to explain the effect of sodium azide upon paracrystal formation.

CHAPTER 3

Biochemical Isolation and Morphological Identification of the Crystalline Arrays

This chapter is focused on biochemical and morphological characterization of the crystalline arrays in the yeast plasma membrane. It describes 1) the creation of large paracrystals in protoplasts derived from log phase yeast cells which had no crystalline arrays, 2) the biochemical isolation of the crystalline arrays and the further purification of the crystalline arrays in the preparation, 3) biochemical versus morphological purity, 4) determination of the surface relief of these paracrystals, and 5) the morphological assay designed specifically for these paracrystalline arrays. Here freeze fracture techniques are used primarily because they are still the best way to assess the quality of the preparation of crystalline membranes.

A. Experiments on Protoplasts Containing Enlarged Crystalline Arrays

1. Patch Enrichment In Protoplasts by Starvation

As previously mentioned in Chapter 1, lytic enzymes used in isolation of the yeast plasma membrane do not have their enzymatic optimum at the same time as when crystalline arrays are found in the plasma membrane. It was known when the project was first started that starvation enhanced patch formation. It was thought that protoplasts made from late log phase cells could be induced into a starva-

tion condition in order to elicit patch formation. Late log phase cells were used in order to have a large yield of cells, but to still have cells whose wall materials would be digested by the lyticase. Fortunately, the result of starving yeast protoplasts far exceeded expectations and was the key to biochemically isolating the crystalline arrays.

a. Materials and Methods

Wild type yeast cells, type X2180-1a, were grown to stationary phase in the same way as described in chapter 2. A larger culture was inoculated at a dilution ratio of about 1/75. Cells were harvested by centrifugation after an OD_{600} of 14 was reached.

Spheroplasts (protoplasts) of X2180-1a were prepared using the purified zymolytic enzyme, lyticase. Lyticase, a β 1,3 glucanase derived from the culture supernatant of a soil bacterium grown on glucan or yeast as the substrate, removes the cell wall with far less proteolytic action than other enzymes used in previous preparations (Scott and Schekman, 1979). Cells were harvested in log phase because lyticase has its enzymatic optimum when yeast cells are in exponential growth. Cells were washed in a 50 mM potassium phosphate buffer (pH 7.5) and then in an isotonic buffer composed of 1.4 M sorbitol, 20 mM phosphate buffer, and 50 units/ ml of pen strep buffered to pH 7.5. The cells were incubated in the same volume as the original YEPD with 10 to 20 units of lyticase (purification fraction II)/10^7 cells and 20mM 2-mercaptoethanol. The addition of the mercaptoethanol to the lyticase incubation is an important step. When

mercaptoethanol was deleted from the enzymatic incubation, there was incomplete digestion of the cell walls, as visualized by deep etching techniques.

Spheroplasting was monitored at various times by appearance of the yeast cells by phase contrast light microscopy. Log phase cells are more irregularly shaped than spheroplasts. For example, cells in exponential phase are in the process of budding or have just finished budding and therefore, appear elongated on one side. Protoplasts appear perfectly circular. After an incubation at 30°C in the enzymatic medium, the osmotically fragile spheroplasts were collected by centrifugation. This incubation was typically longer than two hours to insure complete spheroplasting. The collected spheroplasts were then washed with the isotonic buffer and resuspended in an equal amount of the isotonic sorbitol buffer. The spheroplast suspension was placed on a shaker in a 30°C incubator overnight and allowed to proceed into a "starved" state. The spheroplasts were collected by centrifugation at 10,000 X g for 10 minutes.

In preparation for freeze fracture, protoplasts were fixed with 2% glutaraldehyde (final concentration) at room temperature for 30 minutes. Spheroplasts were cryoprotected by incubation in 20% glycerol overnight at 4°C. The cells were collected by centrifugation, resuspended in a minimum of 20% glycerol to make a paste, and 3 to 5 µl droplets were applied to 3 mm cardboard discs. The cardboard discs containing the cells were frozen in liquid nitrogen slush or liquid freon. Fracturing was done at a specimen temperature of -115

°C. Replication took place immediately after fracture. Electron beam gun emission was started before the knife was moved out of the way of the evaporation onto the fracture face in order to try to minimize water vapor condensation. About 25 Å of Pt-C shadow was deposited and backed with a rotary shadowed carbon layer. The replicas were cleaned in liquid bleach overnight and transferred to two water washes before mounting onto formvar coated carbon backed 200 mesh grids. The replicas were examined in the AEI 802 electron microscope.

b. Results

There are three major changes in the appearance of the yeast plasma membrane, as visualized by freeze fracture, when a whole yeast cell becomes a protoplast. The stationary state yeast cell contains an intact cell wall, which can be seen as a grainy ring around the outer surface of the cell (Figure 3.1). Second, there are small invaginations in the P face, which correspond to ridges in the E face. Third, the plasma membrane has small arrays of the hexagonally packed P face particles and their corresponding pits on the E face. When protoplasts of log phase cells are starved in the isotonic buffer, unusually large crystalline patches were formed which covered more than 50% of the cell surface (Figure 3.2). The grainy ring indicative of the cell wall is absent, the invaginations in the membrane are now more elongated, and the appearance of the protoplast is less spherical and in general, the cell itself appears much less rigid.

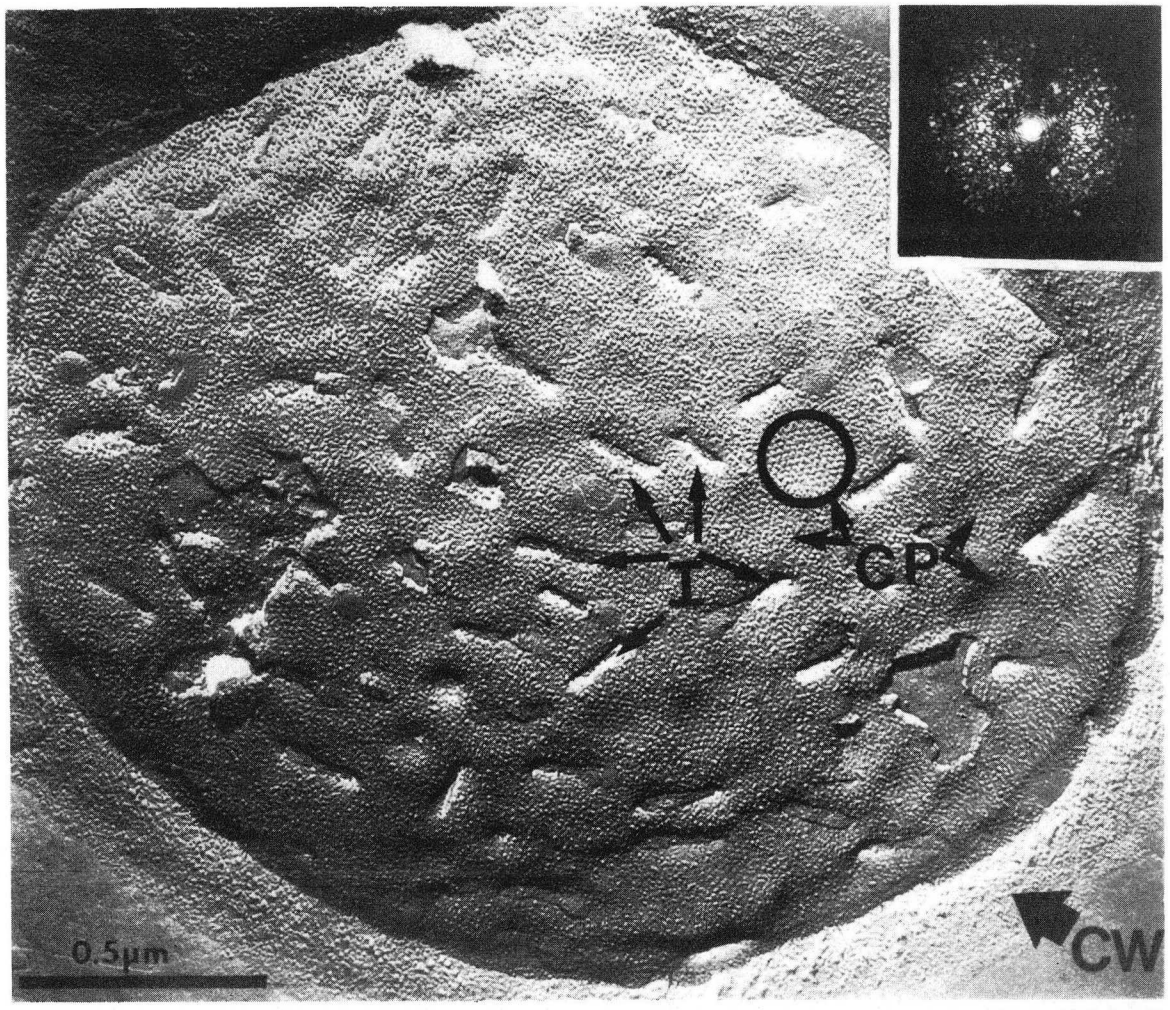

XBB 797-9886C

Figure 3.1. P face of a stationary state yeast cell. CW=cell wall, I=invaginations, CP=crystalline patches. The inset is the optical diffraction pattern from the crystalline patch that has been circled.

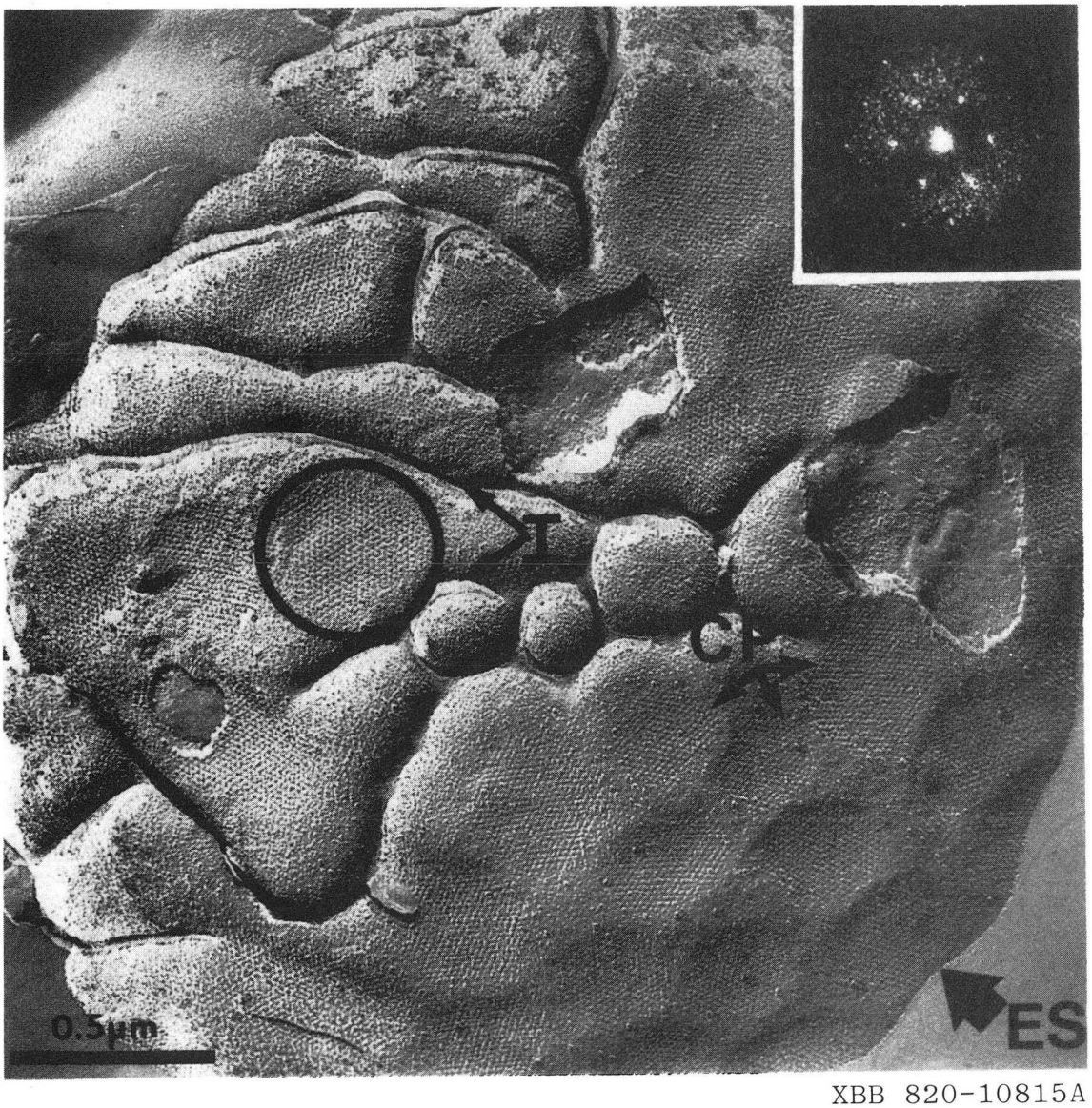

XBB 820-10815A

Figure 3.2. P face of a starved protoplast. ES=external surface. I and CP are the same as in Figure 3.1. The inset is the optical diffraction pattern from the circled crystalline patch.

2. Deep Etching of the External Surface of Yeast Protoplasts

Complete removal of the outer cell wall permitted the determination, by deep etching, of the extracellular surface (ES) relief of the crystalline arrays. Previous researchers had seen smooth surfaces on the ES (Kopp, 1973, Streiblova, 1968), but their experiments involved etching protoplasts with small patches. The small size of the crystalline patches used in previous studies has made it difficult to be certain that there really is a crystalline particular array in any given area that is being examined. Because the crystalline arrays from our starved protoplasts were so large and constituted most of the cell membrane surface area, there is no ambiguity whatsoever concerning the presence of a crystalline patch in the deep etched surface of the membrane.

a. Materials and Methods

Starved spheroplasts were prepared as described in the preceding section. Spheroplasts with large crystalline arrays were fixed with 2% glutaraldehyde for 30 minutes at room temperature. The spheroplasts were collected by centrifugation. The fixed cells were washed twice with double distilled water. The cells were spun down, applied to the cardboard discs, and frozen in liquid nitrogen slush. Specimens were deep etched by raising the specimen table temperature from -115°C to -90°C. The cold knife was placed over the table as a cold trap in order to minimize the water vapor condensation onto the fracture face. After 5 minutes at -90°C, the deep etched fracture face was replicated. The electron beam gun emission was started before

the knife was moved out of the way of evaporation of Pt-C onto the fracture face, in order to minimize water vapor condensation. About 25 Å of Pt-C was deposited and then, shadowed with a rotary shadowed carbon layer. The replicas were cleaned and mounted in the same way as for freeze fracture specimens.

Deep etched replicas were examined in the AEI 802 electron microscope. These replicas were also examined in the JEOL 100CX microscope at tilt angles of + and - 4^{o} to obtain a stereo view of the appearance of the membrane fracture face and surfaces.

Surface replicas of protoplasts and whole cells were produced by a modified monolayer technique. The method of surface replication of protoplasts and whole cells is discussed in detail in section 3D.

b. Results

The E surface of the yeast plasma membrane has a very smooth appearance with no trace of the crystalline arrays of membrane particles (Figure 3.3). The large hexagonally packed particles in the PF appear to form relatively flat plates, but when deep etched replicas are view in stereo, the patches appear more cup shaped than flat.

The absence of visible particle arrays on the ES was further confirmed by examination of shadowed replicas of freeze dried protoplasts. Obvious differences between replicas of freeze dried yeast and protoplasts are that in replicas of whole yeast, the cell wall appears fibrous, and contains large rings on a cell wall. Each ring is due to the budding off of a new daughter cell and is called a bud

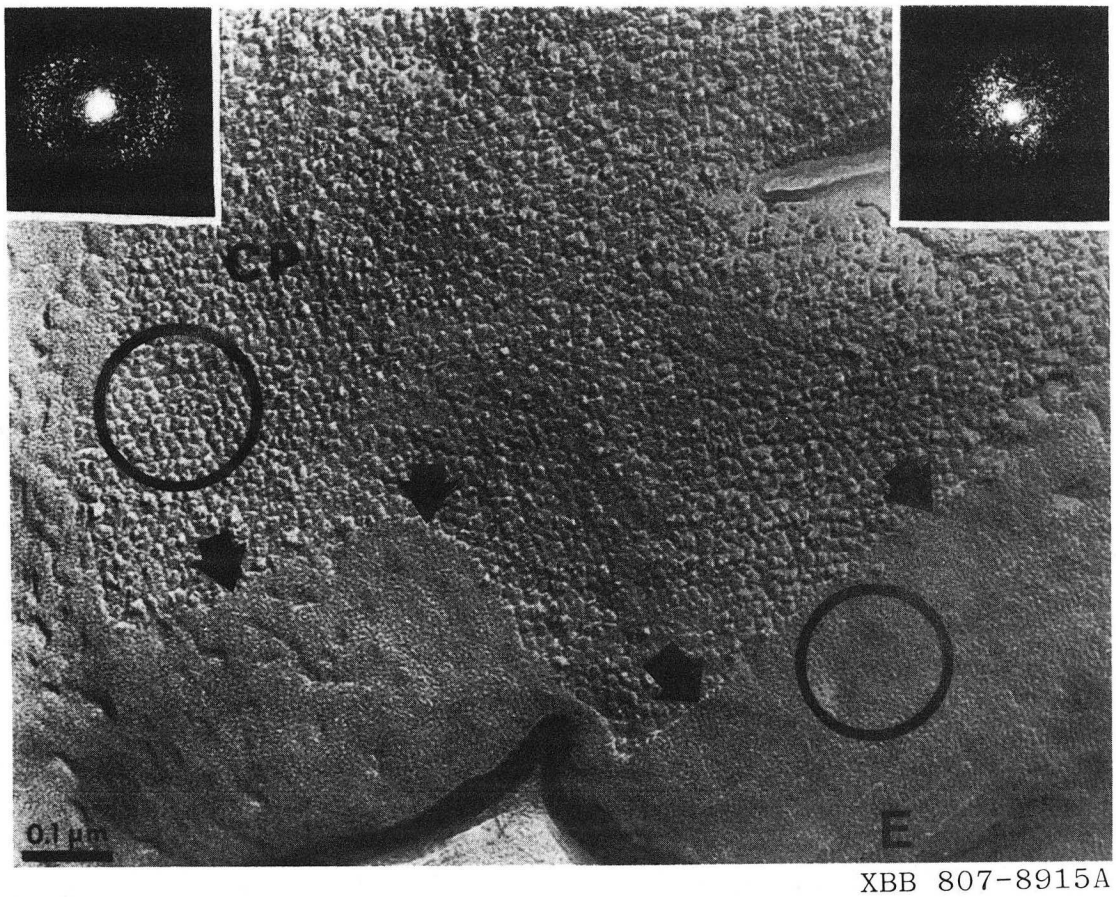

XBB 807-8915A

Figure 3.3. Deep etching of an extracellular surface of a yeast protoplast. The arrows indicate the fracture plane. E= extracellular surface and CP=crystalline PF particles. The right hand optical diffraction pattern is from the circled portion of the crystalline array. The left hand optical diffraction pattern is from the circled portion of the external surface. Note the smooth surface overlying the crystalline arrays and the lack of any diffraction intensities in the optical diffraction pattern from the ES as opposed to the obvious diffraction intensities in the optical diffraction pattern from the crystalline array.

or birth scar. These rings are never seen on the external surface of the protoplast.

3. Experiments Labeling Carbohydrate Groups on the External Surface

An experiment was performed to label the Con A receptors on the ES to see if the intramembranous particles comprising the crystalline arrays were glycoproteins. Deep etching of the labeled protoplasts should reveal a different ES texture than unlabeled protoplasts. The labeling procedure was adapted from Duran, Bowers, and Cabib (1975) with the following minor modifications. Labeling with Con A was done at 4°C to prevent patching which occurs in other eukaryotic cells at their physiological temperatures (Edelman, Yahara, and Wang, 1973). If patching of the Con A receptors occurred, this would lead to erroneous results.

a. Materials and Methods

In order to label mannose containing surface groups on the ES of the yeast plasma membrane, protoplasts were incubated overnight with 25 µg/ml of Con A in a buffer consisting of 1.4 M sorbitol, 50 mM Tris pH 7.5, and 10 mM magnesium sulfate at 4°C. The spheroplasts were washed with the same buffer and fixed for 30 minutes at 4°C with 2% glutaraldehyde (final concentration). The labeled protoplasts were washed twice with double distilled water and resuspended in double distilled water. The conditions for preparation of the labeled protoplasts for deep etching was the same as for unlabeled protoplasts.

b. Results

The results of this experiment were inconclusive because the Con A clusters were spread out over the cell surface. It was expected that the appearance of large patches of Con A clusters corresponding to the paracrystalline arrays or large areas devoid of clusters corresponding to the patch areas should have occurred. The experimental results did not support either expectation. Therefore, there may be approximately the same number of Con A receptors on the patch proteins and in the interpatch membrane areas.

4. Surface Replication of the PS of Protoplasts

An attempt was made to visualize the P surface of the yeast plasma membrane paracrystals and any cytoskeleton adhering to it by lysing a monolayer of starved protoplasts followed by surface replication. Protoplasts were lysed in a lysis buffer containing 10 mM Tris, 50 μM PMSF, and 0.5 mM EDTA (pH 6.5) after attachment to the treated glass substrate. Unfortunately, only the endoplasmic reticulum and its associated ribosomes were exposed. The endoplasmic reticulum is very closely associated with the plasma membrane in yeast cells. It should be noted that the small amount of cytoskeleton that is found in yeast may not be closely associated with the paracrystals or the plasma membrane (Schekman, personal communication).

To summarize, starvation of protoplasts made from log phase cells elicited the formation of patches of much larger size than in the original whole cells. The external surface of these large cry-

stalline arrays appears very smooth by replication techniques. So, at the limit of 20 Å resolution, there is no extensive surface relief of these crystalline arrays. This absence of an obvious surface relief, contrasted with the very obvious crystallinity in the individual fracture faces, indicates that the crystalline array particles span the membrane, but barely extend beyond the lipid bilayer. It is also possible that the intramembranous particles are glycoproteins whose glycocalyx obscures the crystallinity of the proteins.

B. Crude Membrane Preparations

The major difficulty in isolating the crystalline array-forming particles was the removal of the cell wall with a lytic enzyme at a time when the arrays were normally still dispersed. The problem was overcome by the use of lyticase to make protoplasts from log phase cells followed by starvation of the protoplasts. Once protoplasts containing these large arrays are made, an easy lysis procedure together with differential centrifugation techniques were used to separate the plasma membrane from other subcellular constituents.

1. Materials and Methods

Protoplasts with enlarged arrays were prepared as described in the previous section and collected by centrifugation at 10,000 X g for 10 minutes. The supernatant was discarded and the pellet was resuspended in 1/3 of the original volume in a hypotonic buffer composed of 5% Ficoll, 0.1 M sorbitol, 50 mM potassium phosphate, 50 µM phenyl methyl sulfonyl fluoride (PMSF), 1 mM sodium azide, and 10 mM

calcium chloride, buffered to pH 6.5. After 10 minutes at 0°C, the lysed cell suspension was centrifuged at 10,000 X g for 5 minutes. A pellet consisting of plasma membranes, endoplasmic reticulum membranes, mitochondria and/or mitochondrial membranes, and nuclei was collected. Again, the supernatant was discarded and the pellet was resuspended and washed with lysis buffer. The pellet was resuspended in 45% sucrose (in 50 mM potassium phosphate and 50 µM PMSF buffered to pH 6.5) by either vortexing or homogenization with a Dounce homogenizer if necessary and layered on top of an equal amount of 60% sucrose in the same buffer. The discontinuous gradients were centrifuged in a Beckman SW 41 rotor at 100,000 X g for 90 minutes at 4°C.

A crude membrane fraction was collected at the 45/60 interface. This membrane fraction appeared as a flocculent white band between the two sucrose layers. Unlysed mitochondria and nuclei were found at the bottom of the centrifuge tube, while lighter material, such as membranes with high lipid content, usually formed a pellicle at the top of the 45% sucrose. The membranes were washed with lysis buffer at 27,000 X g for 10 minutes. The supernatants were discarded and the pellets were then washed once again with a membrane buffer consisting of 10 mM TRIS, 50 µM PMSF, 1 mM sodium azide, and 0.5 mM EDTA. The membrane fraction was assayed for crystalline arrays by a modified monolayer freeze fracture technique. This technique will be described in greater detail in section 3D.

2. Results

An example of freeze fractured crude membranes are shown in Figure 3.4. Monolayer freeze fracture micrographs show very obvious crystalline P face particles. The crystalline plates of the plasma membranes remain intact after the lysis procedure, as seen by the large P face particles. There is very little mixture of the crystalline and noncrystalline areas, i.e. membranes are predominantly patch plasma membrane or predominantly nonpatch membranes. There is also a substantial amount of background material which appears clumped together like small balls of wool and produces very high shadows. By comparison, the crystalline patches appear flat and circular. Polyacrylamide gel electrophoresis (Laemmli, 1970) of the crude membrane fraction produced a pattern of about 36 distinct bands in the molecular weight range from 10,000 to 100,000.

C. Further Purifications of Crude Membrane Preparations

1. Detergent Treatments of Crude Membrane Preparations

It was clear from the protein gels and freeze fracture assay that patch purity needed to be improved. Since crystalline patches constituted most of the protoplast cell surface, the contamination was thought to be from other membranes besides the plasma membrane. One logical approach to improve the purity is to find a detergent which could dissolve away the extrapatch material but leave the crystalline arrays intact.

a. Materials and Methods

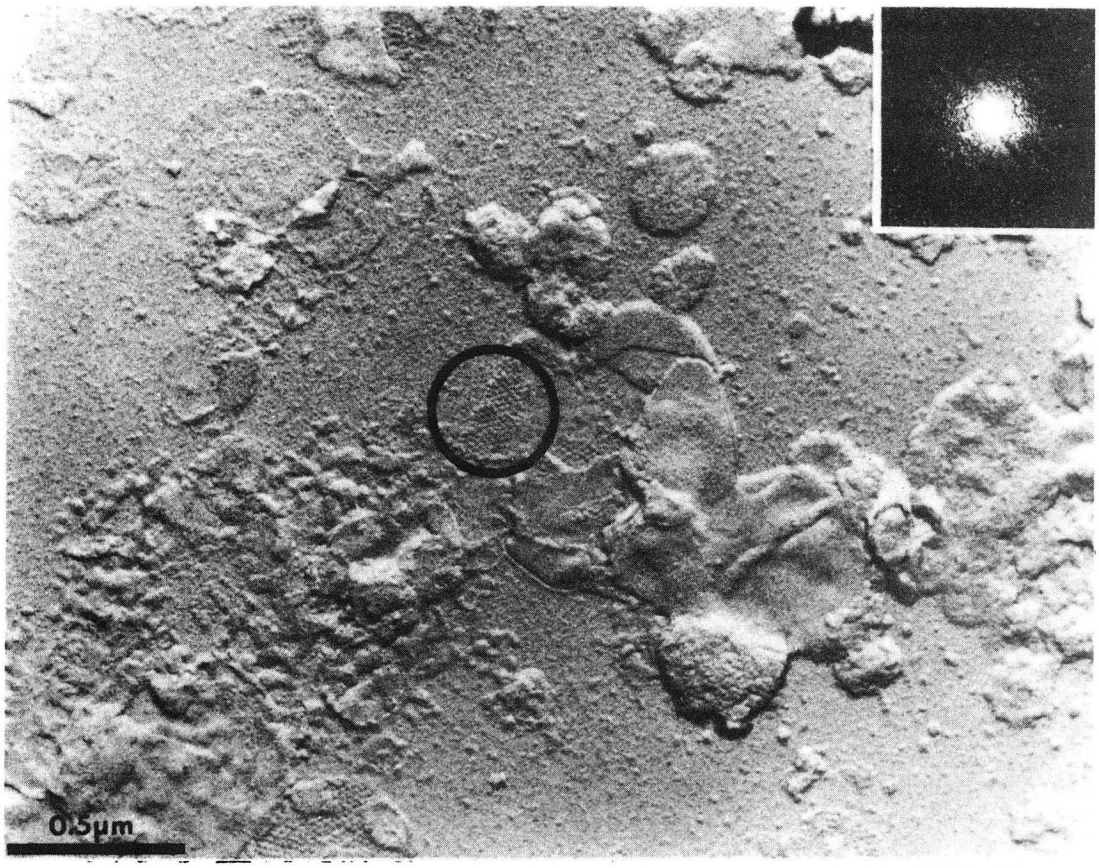

XBB 818-8121C

Figure 3.4. Monolayer freeze fractured crude membrane fraction. The optical diffraction pattern is from the circled portion of the membrane.

Several detergents were screened using the following method. Crude membranes (5 µl) and 5 µl of the detergent were mixed together on a piece of parafilm and incubated at room temperature for 15 minutes. The membrane and detergent solution (5 µl) was placed on a grid and the membranes were allowed to attach to the support film. The excess liquid was drained off, but the grid was not dried completely. Excess 1.5% phosphotungstic acid (PTA) pH 7.1 was applied to the grid. The excess PTA was drained off and the grid was flooded two more times with PTA. The grid was dipped into a small beaker of PTA to make sure that all of the detergent was washed off the grid. After the third PTA wash, the drained grid was allowed to dry completely. The grids were then examined in the AEI 802 electron microscope.

The following detergents were screened using this method: 10% deoxycholate (DOC), 1% sarkosyl, 1% octylglucoside, and 0.05% Triton-X100. Of membranes treated with these detergents, only crude membranes treated with DOC and Triton were left on the grid. From the results of this screening method, DOC and Triton appeared to be good candidates for detergent extraction of extra patch material. It should be noted that this procedure can produce misleading results because it does not exclude the possibility that membranes treated with sarkosyl and octylglucoside did not adhere to the grid.

Bulk detergent treatments using 0.025% Triton, 2% DOC, and more recently, 0.1% Brij 58 (all final concentrations) of the crude membranes were done in the following manner. Crude membrane stock (0.5

to 1.0 mg) was centrifuged in a Sorvall SS-34 rotor at 10,000 X g for 15 minutes. The pellet was then resuspended in the appropriate amount of detergent, mixed well, and incubated at room temperature for 30 minutes. For the case of the Triton treatment, the membrane suspension was centrifuged in the Beckman SW41 rotor at 20,000 X g for 90 minutes at 4°C and the pellet was washed twice with membrane buffer (following the procedure of Zampighi and Unwin, 1979). DOC treatment involved the membrane pellet being resuspended in sodium deoxycholate to give a final concentration of 2% (following the procedure of Henderson et al., 1979). After an incubation time of 20 minutes, the suspension was centrifuged at 20,000 X g for 15 minutes, and washed twice. For the Brij 58 detergent treatment (following the procedure of Fallon and Goodenough, 1981), the membrane suspension was centrifuged in the SW41 rotor at 100,000 X g for 2 hours at 4°C. The supernatant was removed and the pellet was resuspended in membrane buffer and centrifuged at 100,000 X g for 30 minutes. This wash was repeated. Pellets for all cases were resuspended by homogenization which was usually necessary because the pellet had been tightly packed. The membranes were then prepared for monolayer freeze fracture in order to assay the morphological purity of the specimen preparation.

b. Results

Patch purity, as assayed by freeze fracture, was enhanced by the incubation of the crude membrane fraction with 0.05% Triton X-100 at a 1/1 volume ratio (Figure 3.5). Because of the Triton treatment,

the pellet size of the crude membranes decreased to about 70% of its original volume. This decrease in the amount of membranes is reflected in the monolayer freeze fracture micrographs. The small clumps of background material have become even smaller, and the bulkier extra-patch material is less evident. There is a higher concentration of patches found on the substrate.

The Triton-treated membranes were layered on top of a finer discontinuous gradient composed of 45%/50%/55%/60% sucrose. The membranes were centrifuged in the SW41 rotor at 100,000 X g for 90 minutes. The membranes were found exclusively at the 55/60 interface. Therefore, the buoyant density of the Triton-treated membranes was measured to be approximately 1.27 gms/cc. This density suggests that the amount of protein and lipid in the crystalline arrays is approximately 80% and 20%, respectively, when the values for protein and lipid densities for purple membrane (Unwin and Henderson, 1975) were used. Polyacrylamide gel electrophoresis (PAGE) of the 55/60 fraction exhibited the same 35 distinct protein band pattern. Higher concentrations of Triton X-100 (5%, 1%, 0.5%, 0.1%) incubated at a 1/1 volume ratio had no effect in reducing the number of bands found in the gel patterns.

DOC-treated membranes when freeze fractured by the monolayer technique did not resemble crystalline arrays. Gel electrophoresis was not done in this case because no initial crystallinity in this membrane fraction was found.

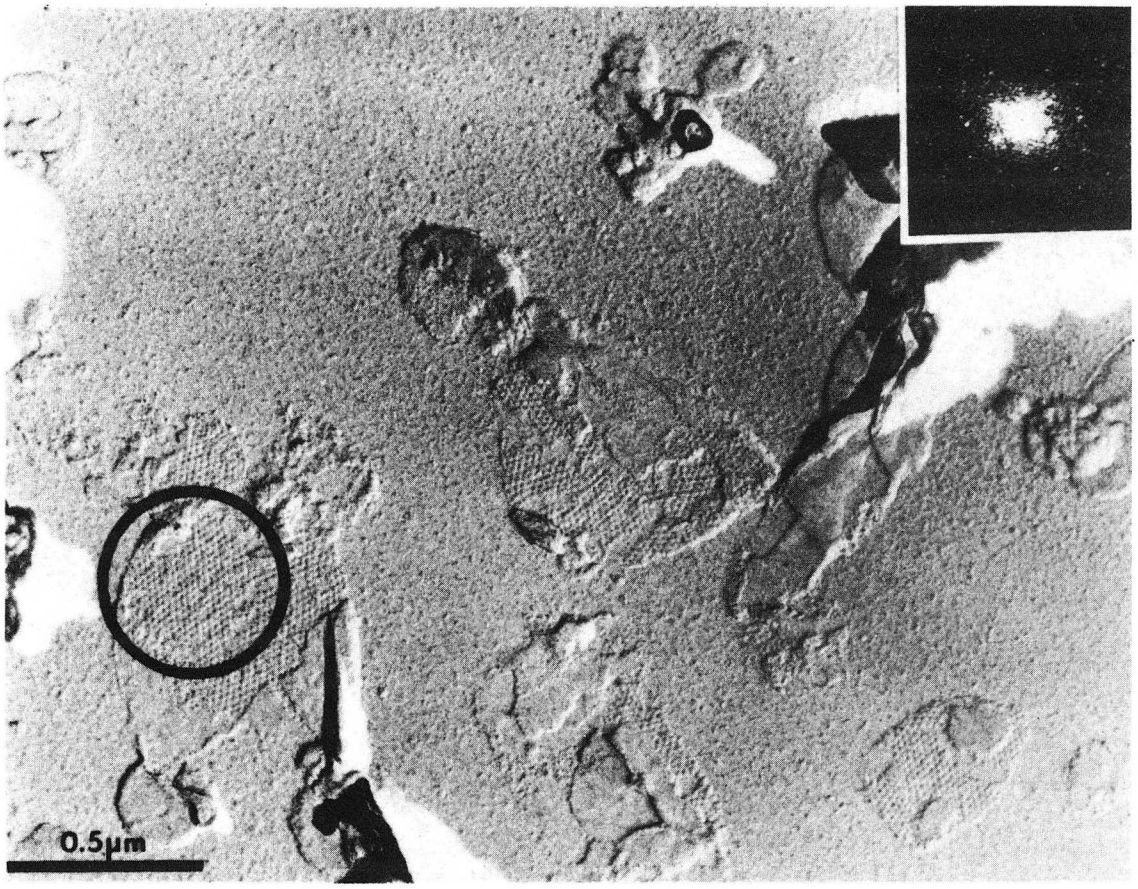

XBB 818-8121D

Figure 3.5. Monolayer freeze fractured Triton X-100 treated membrane fraction. The optical diffractogram is from the circled area of the membrane.

The treatment of the membranes with Brij 58 detergent also enhanced the morphological patch purity. Figure 3.6 is a monolayer freeze fracture micrograph of the Brij-treated membranes. As was the case with the Triton membranes, the amount of background material is significantly decreased, but once again, the number of protein bands in the PAGE did not decrease. The Brij-treated membranes appear to be better ordered than the Triton-treated membranes, as judged qualitatively from the freeze fracture micrographs. Figure 3.7 is an example of a gel comprised of Triton and Brij membranes showing cross-contamination from other membrane species. Figure 3.8 is a summary of the best isolation procedure devised to date using detergent extractions.

2. Guanidine Hydrochloride Treatment of Crude Membrane Preparations

It was hypothesized that a number of bands on the polyacrylamide gels might be due to peripheral membrane proteins which were adhering to the crystalline membranes. In order to test the hypothesis that the extra proteins were due to peripheral membrane proteins, crude plasma membranes were treated with guanidine hydrochloride.

a. Materials and Methods

The procedure for treating membranes with guanidine hydrochloride was adapted from Steck (1972). Pelleted crude membranes were suspended in 6 M guanidine hydrochloride (GuHCl) (pH 7.4) and the suspension was reduced with 0.01 M dithiothreiotol (final concentration) for 15 minutes at 37^{o}C. The membranes were centrifuged at

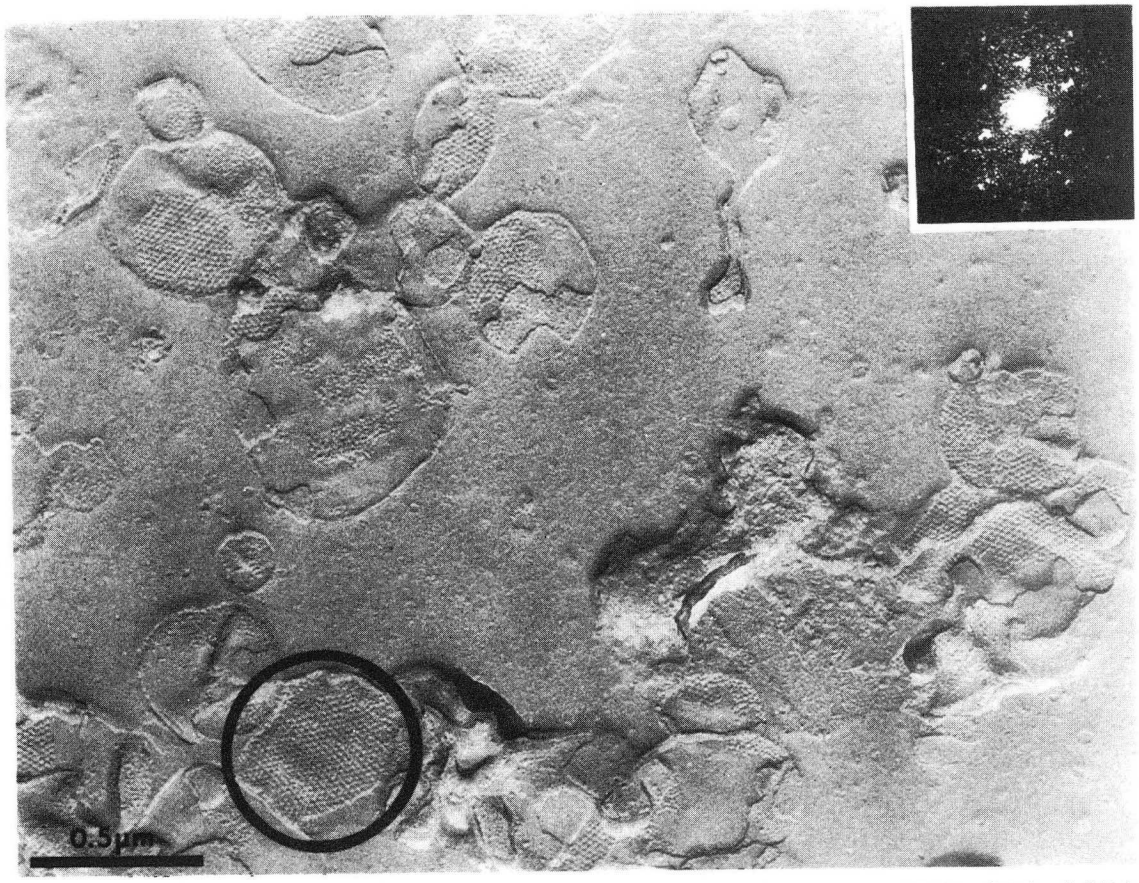

XBB 831-105A

Figure 3.6. Monolayer freeze fracture Brij 58 treated membrane fraction. The optical diffraction pattern is from the membrane that has been circled. The Brij-treated membranes appear to be more coherently ordered than the Triton-treated membranes.

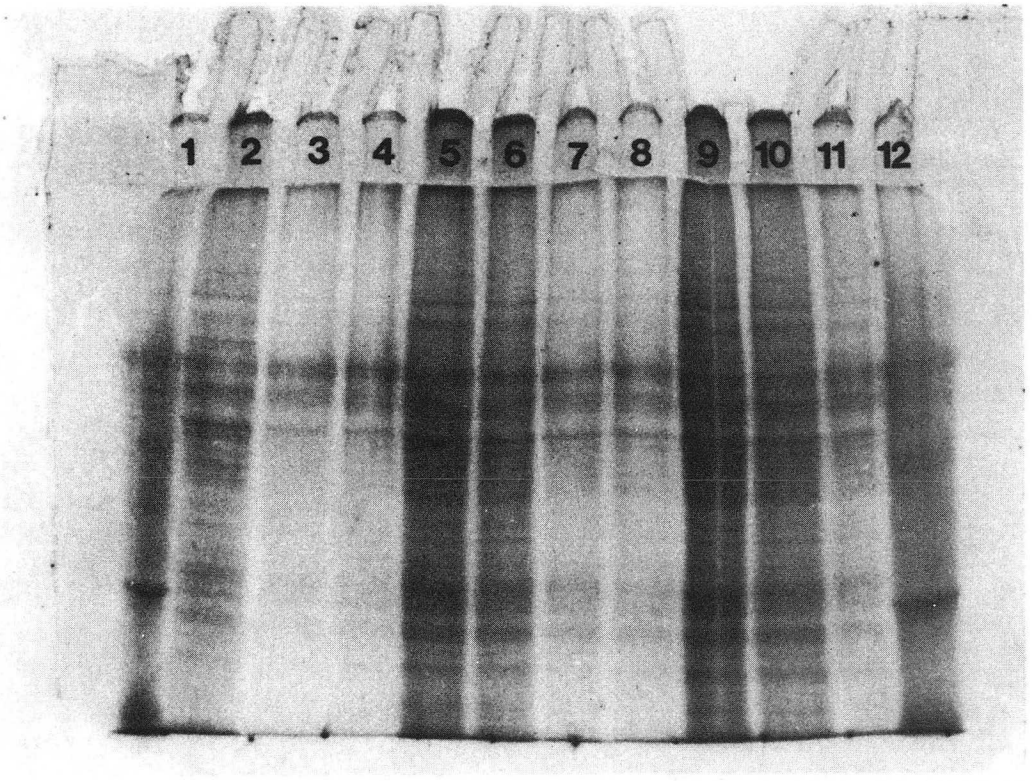

XBB 820-10814A

Figure 3.7. Polyacrylamide gel electrophoresis of the three different preparations of yeast plasma membranes. Lanes 1 and 12 are the standards (cytochrome c, β-lactoglobulin, α-chymotrypsinogen, ovalbumin, bovine serum albumin, phosphorylase B, and Myosin). Lanes 2 through 4 and 9 through 11 are varying concentrations of Triton-treated membranes. Lanes 5 through 8 are varying concentrations of Brij-treated membranes. The banding pattern of the membranes are very similar, in spite of the fact that the Brij-treated membranes appear to be morphologically more pure.

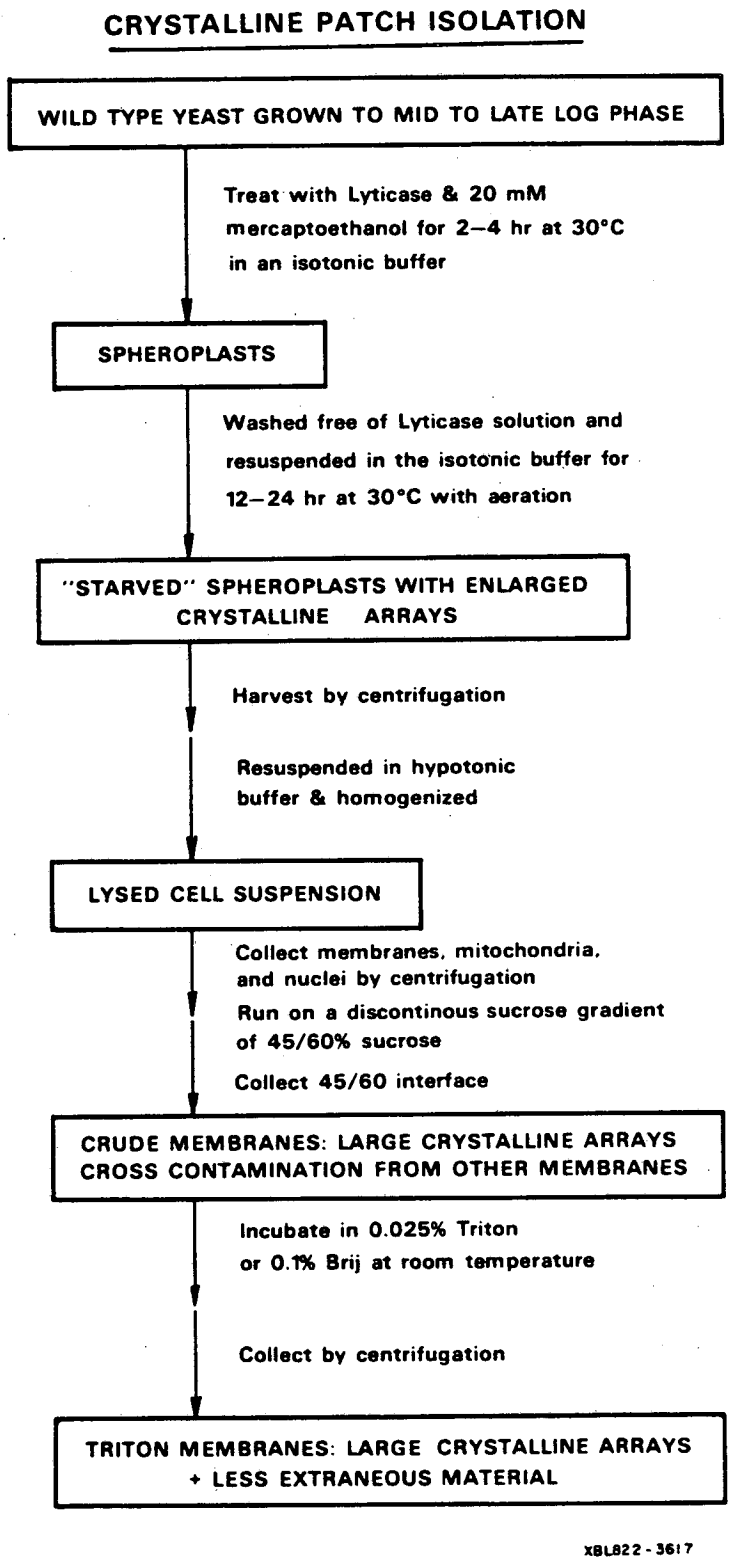

Figure 3.8. A summary of the protocol for obtaining the best preparations of crystalline yeast membranes by detergent extraction.

15°C for 5 hours at 70,000 X g in order to pellet the membranes from the very dense GuHCl solution. The pellet was collected as well as the supernatant. The GuHCl was removed from the supernatant by dialysis against distilled water, during which time there was a flocculation of white material out of solution. The pellet was washed twice with membrane buffer. An acetylation step included in the original procedure by Steck was eliminated from this protocol. The pH of the iodoacetamide incubation was reported to drop from about pH 6.8 to pH 2.7 and it was felt that this was too drastic a pH change for this membrane system (Dufour et al., 1978).

b. Results

The results of treatment with guanidine HCl were as follows: a) a small pellet, which was about 10 to 30% of the original crude membrane pellet, sedimented at high g forces and contained two protein bands of molecular weights of approximately 50,000 and 45,000, b) no pellicle formed at the top of the centrifuge tube, and c) when the guanidine was dialysed out of the supernatant, a white flocculent appeared. If a pellicle had formed, it would be composed of membranes with a high percentage of lipids, as is the situation with guanidine hydrochloride treatment of red blood cell membranes (Steck, 1972). The banding pattern of the supernatant material closely matched that of the Triton-treated membrane preparations. The morphological appearance of the pellet from the guanidine treatment was that of membranes clumped into small balls, which resembled the background material of the crude membranes and definitely not the flat

circular patches indicative of Triton-treated membranes.

The failure of the membranes to sediment in 6 M guanidine hydrochloride seems to be inconsistent with the buoyant density measurements as determined by discontinuous sucrose gradients. The density of 6 M guanidine hydrochloride is approximately 1.15 gm/cc (Kawahara and Tanford, 1966), and a membrane of this density would be composed of about 45% protein and 55% lipid. As stated earlier in Chapter 3, the crystalline-patch containing membranes banded at a sucrose density between 55% and 60% sucrose, and thus is it presumed that they contained 80% protein and 20% lipid. These two measurements might be reconciled, however, if we postulate that guanidine denatured the peripheral membrane proteins and released them from the membranes, thereby decreasing the the density of the membranes from 1.27 gm/cc to 1.15 gm/cc. If the density of the "cleaned" crystalline membranes matched the density of the 6 M guanidine hydrochloride, the membranes would never sediment in the 6 M guanidine hydrochloride. However, we can further imagine that when the guanidine was dialyzed out of the supernatant, the peripheral membrane proteins would adhere back onto the membranes. The PAGE protein banding pattern of the guanidine supernatant would then be almost the same as the gel pattern as the original crude membrane. The only other reasonable alternative would be to hypothesize that there may be an unknown reaction between the membrane and the guanidine in which the membrane particles become dispersed (solubilized) in the guanidine hydrochloride and would never sediment. As is the case with the red cell membrane, guanidine

hydrochloride denatures soluble proteins, but is believed to leave lipophilic membrane proteins intact (Steck, 1972). Other membranes may not necessarily behave similarly.

To summarize, the likely contaminant is cross contamination from any membrane whose protein to lipid composition closely reflects that of the yeast paracrystals, i.e. 80% and 20%. The most probable candidate for this sort of contamination would be the inner mitochondrial membrane, because it has a high protein to lipid ratio and cross contamination from this membrane has been previously reported (Fuhrmann et al. 1974). The effect of detergent treatments of the plasma membrane was to dissolve away membranes containing high percentages of lipid to protein membranes (e.g. plasma membranes, endoplasmic reticulum, and outer mitochondrial membranes) while leaving the densely packed crystalline arrays intact. At the pH these preparations were done, it is possible that the clumped material in the background of the freeze fracture micrographs are inner mitochondrial membranes (see Dufour et al., 1978) and hence, any biochemically pure preparation of crystalline membranes needs to be prepared according to an isolation procedure which would separate out the patches from the inner mitochondrial membranes. Contamination from peripheral membrane proteins is also a consideration.

D. Development of a Freeze Fracture Monolayer Technique

When membranes are fractured using the conventional droplet technique, there are two main problems in obtaining large crystalline membrane fracture planes. As the fracture plane traverses through

the droplet, it may follow a random course through the ice matrix. This ice is formed by water that is trapped in the void volume of the pellet. If the fracture plane is random, then the areas of membrane fracture are likely to be small. As a result, the replicas will be made up of large areas of ice spaces rather than membrane fracture faces.

In order to use freeze fracture as the assay for a given membrane preparation, a different fracturing technique needed to be developed to survey the morphological purity of the sample. The qualities that such an assay must have are 1) large fields of membranes need to be surveyed for crystalline arrays, 2) the membranes must lay fairly flat on the substrate in order to assess the quality of the crystalline order and flatness of the membranes.

1. Adaptation of the Fisher Monolayer Technique to the Yeast Plasma Membrane

A freeze fracture technique which embodied just these qualities was the membrane monolayer technique developed by Fisher for red blood cells and purple membrane (Fisher, 1975). In this technique, a 12 mm glass cover slip is scrupulously cleaned so a solution of 1000 to 4000 molecular weight polylysine can be applied. The excess polylysine is washed with a stream of double distilled water and the excess liquid is drained off. The result is a substrate with a positively charged surface. Both red blood cells and purple membrane contain a relatively large number of negative surface charge groups on their membranes so both will stick spontaneously to the glass

(Fisher, 1978). A solution of purple membranes or red blood cells is then applied to the positively charged glass. A monolayer of sample reacts with the polylysine and will lay flat against the glass. A minute or so later the excess specimen is washed off with distilled water or buffer for purple membrane or red blood cells, respectively. Excess liquid is drained off by blotting the edges of the coverslip. A copper top with a pull ring is placed on top and frozen as a sandwich. The sandwich is then placed on a precooled stage of a Balzers 301. The stage contains a specialized stage head which will fit a 12 mm coverslip exactly. By pulling this copper lid off with the cooled microtome arm, the fracture plane follows the "plane of least resistance" and should fracture along the plane of the membrane.

Early on in the adaptation of this technique to the yeast plasma membrane paracrystals, it was discovered that although red blood cells stuck to the polylysine treated glass, yeast membranes did not stick nearly as well. It was suggested that a better substrate for this particular system would be one in which polylysine glass had been treated with concentrated (50%) glutaraldehyde (J. Heuser, personal communication). The aldehyde groups of the glutaraldehyde would readily react with the amino groups of the polylysine resulting in free aldehyde groups especially if concentrated glutaraldehyde was used. By using concentrated glutaraldehyde, there is very little chance that both ends of the glutaraldehyde molecules would react with the polylysine, thereby forming closed loops. These free

aldehyde groups could then react with any free amino groups from exposed membrane proteins. The membranes would then be covalently bonded to the glass in a monolayer.

An added benefit of this procedure is that additional proteins can be layered on top of the glutaraldehyde-polylysine-glass (glu-PL-cs) to orient specimens preferentially or to bind ones which would not necessary bind to either polylysine or glutaraldehyde. For example, whole yeast cells could be fractured in a monolayer using this technique if Concanavalin A was layered on top of the glu-PL-cs. Whole yeast cells do not have proteins exposed on the surface of the cell wall, but do have mannose residues which will bind to Con A.

It was observed initially that the best binding of monolayers of membranes occurred when the membranes were left to settle onto the substrate overnight under the force of one g. Therefore, it was thought that centrifugation would enhance this effect in a shorter amount of time. Plastic Sorvall centrifuge tubes (12 ml) were modified in the following manner: a leveled 12 mm lucite cylinder was epoxied into the bottom of the tube. The diameter of these centrifuge tubes is slightly larger than the diameter of the 12 mm glass coverslip. The coverslip will lie flat against the lucite and will be supported during low speed swinging bucket centrifugation. Because the diameter of the tubes closely matches the diameter of the coverslip, there is very little side-to-side motion and, therefore, the coverslip will be less likely to shatter under the centrifugal force. Centrifugation enhanced immensely the deposition onto the

coverslip of the material being assayed.

2. Summary of the Monolayer Technique

The protocol for freeze fracturing membranes according to the monolayer technique is as follows. Coverslips are cleaned with mild soap, rinsed with warm water, and then distilled water. The glass coverslips are then cleaned with acetone or 100% alcohol in order to render them free of hydrocarbons, hydrophilic, and thereby, responsive to polylysine. A cleaned coverslip, stored in acetone or alcohol, was air dried for a couple of minutes. One side of the coverslip was marked as the bottom in order to know which side would be used as the substrate. An aliquot (100 µl) of a 10 mg/ ml solution of 1000 to 4000 molecular weight polylysine was applied and after a couple of minutes, the excess was washed off with double distilled water. Glutaraldehyde (100 µl of 50%) was then applied and after a couple of minutes, the excess was washed off with a stream of double distilled water. The coverslips pretreated with polylysine and glutaraldehyde are placed into the modified tubes and covered with either buffer or distilled water depending on the experiment. It should be noted that a Tris buffer or any other amino-group-containing buffer will react with the glutaraldehyde to form a Schiff base. This reaction will negate the advantage of using glutaraldehyde to cross-link proteins to the substrate. In spite of this, successful monolayers were produced using Tris in the membrane buffer. An aliquot of membrane solution (0.2 to 0.5 ml of a 0.1 to 0.5 mg/ml) is added to the tube, and then centrifuged at 2000 X g for 3 to 4 hours

in a Beckman J-6 centrifuge. The length of the centrifugation is rather long in order to get all the membranes in solution onto the substrate. Excess membranes are washed off the coverslip by vortexing the glass in a small amount of the supernatant in the centrifuge tube. The mem-glu-PL-glass monolayer is removed from the centrifuge tube and the back is dried off completely. A copper top was fabricated from 20 mil copper and comprised an approximately 9 mm diameter circle with a smaller ring soldered to it. The copper top was sanded with medium course sand paper, cleaned with nitric acid, rinsed with double distilled water, and dried. The copper lid is placed on top of the mem-glu-PL-glass. The exposed edge of the coverslip is blotted with filter paper and the excess liquid between the lid and the coverslip is drained. The sandwich is frozen in liquid nitrogen slush and mounted onto the special Balzer's stage head designed to fit the 12 mm coverslip. The fracturing is done at -115 ^{o}C by knocking off the copper lid with the cold knife.

The sample is completely freeze dried to expose the maximum amount of replica area possible. Freeze drying was done by raising the sample temperature over the course of two to four hours and finally turning off the liquid nitrogen flow. The Balzers stage would act like a cold block freeze drier and warm slowly to room temperature under vacuum. The knife is always kept colder than the stage and kept over the stage to act as a cold trap.

The sample was left overnight and replicated the next day. Approximately 25 $\mathring{A}$ of platinum and carbon was deposited on the

coverslip and the sample was backed by a layer of rotary shadowed carbon. Replicas were stripped off the glass by immersing the coverslip at a 45° angle into approximately 20% hydrofluoric acid. The replica was immediately transferred to a water rinse followed by rinses in liquid bleach, and two more transfers into distilled water for a minimum time of twenty minutes each. The replicas were picked up on formvar carbon coated grids and examined. A schematic of this protocol is shown in Figure 3.9. Figures 3.4, 3.5, and 3.6 are examples of crude, Triton-treated, and Brij-treated membranes respectively, prepared with this technique.

3. Identifying the Fractured Areas on Monolayer Replicas

It was observed that freeze fractured areas occurred in those areas of the replicas which appeared extremely smooth and shiny. Surface replicated areas may also occur, if before freezing, the layer of liquid between the copper lid and the coverslip is too thick or uneven. As the fracture plane traverses the specimen, in areas where the ice was too thick, the ice will fracture rather than the membrane. In these areas the membranes were surface replicated after freeze drying. Alternatively, there are areas where the buildup of buffer salts occurs because the ice had been extremely thick and developed salt deposits after freeze drying.

4. Surface Replication using the Monolayer Technique

The surface replication described in section 3A was done using the same monolayer preparatory technique as was used for isolated

MONOLAYER FREEZE FRACTURE AND SURFACE REPLICATION TECHNIQUE

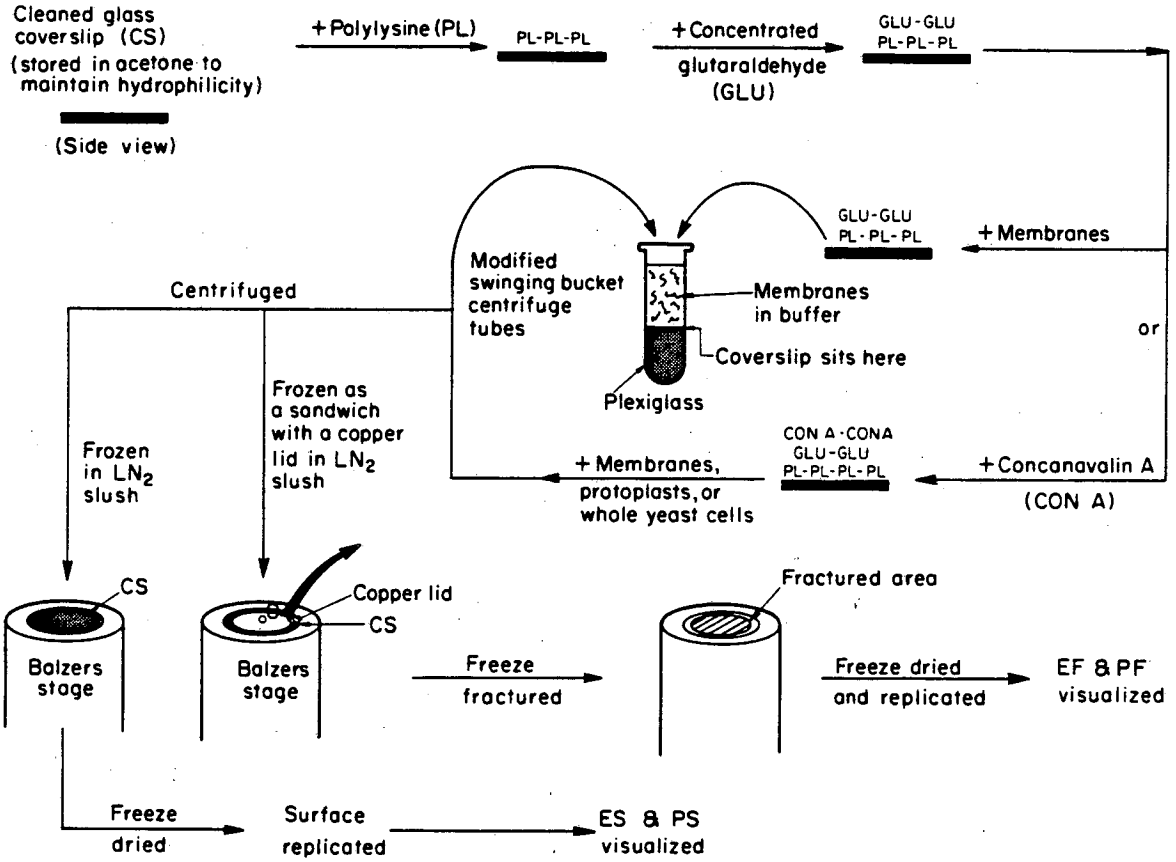

Figure 3.9. Summary of the monolayer freeze fracture and surface replication technique.

membranes. In the case of whole cells and protoplasts, a layer of Concanavalin A was applied to the glu-PL-cs substrate. A concentrated Con A solution (10 mg/ml in 0.01 M potassium phosphate and 1 M sodium chloride, pH 7.0) was prepared fresh and centrifuged to remove any aggregated material. The solution was layered on top of the glu-PL-cs and the excess was washed off with the 0.1 M potassium phosphate and 1 M sodium chloride buffer. The substrate was placed into the bottom of the monolayer centrifuge tubes, a solution of fixed cells or protoplasts were added, and centrifuged. Alternatively, a solution of cells or protoplasts could be layered on top of the substrate and allowed to attach for times greater than two hours. Excess cells were rinsed off. The monolayer was blotted and immediately frozen. The temperature rise and the time involved for freeze drying whole cells and protoplasts was much slower, usually involving a time period of over 6 hours before the nitrogen flow was turned off. Times shorter than this combined with too rapid a temperature rise resulted in freeze drying collapse.

E. Surface Morphology of Triton-Treated Membranes

1. Surface Replication of the ES and PS

To reemphasize the Triton freeze fracture results, large crystalline arrays were present in the membrane preparations. It was known already from the results of the deep etching of starved protoplasts that the external surface was devoid of any obvious crystalline array. Lysing protoplasts did not appear to be a viable method

to view the inner surface, but monolayer preparations of membranes could also be freeze dried and shadowed to reveal whether surface detail could be seen on the cytoplasmic side.

a. Materials and Methods

A monolayer of membranes was prepared in the exact same manner that a membrane monolayer would be prepared for freeze fracture with the exception that no copper top was used. The same sample of membranes was freeze fractured and surface replicated as a separate control experiment to be sure there would not be any variable due to the membrane preparation. The mem-glu-PL-cs was freeze dried in the same way as a freeze fractured sample would be and then, surface replicated (see the schematic in Figure 3.9).

b. Results

When replicas were examined, there was no surface relief found on any of the membranes (Figure 3.10). Figure 3.10 is an example of a typical field of membranes. The crystalline array membranes are probably the circular patches which in some cases are puckered. Many fields of membranes were surveyed and no surface relief was ever seen.

2. Surface Replication of the PS of the Isolated Membranes using an Oriented Substrate

An additional control was devised in order to make sure that the substrate had not biased the sampling of the replicated membranes.

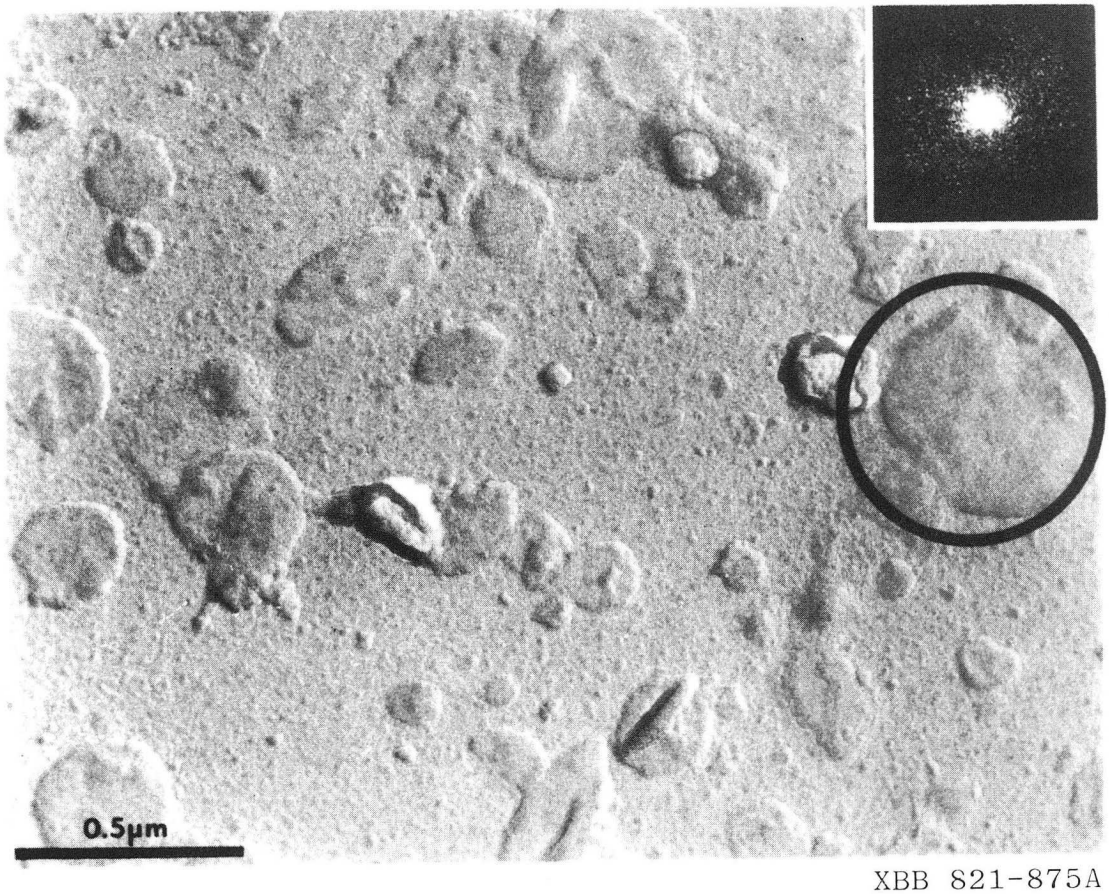

XBB 821-875A

Figure 3.10. Surface replicated Triton X-100 treated membranes. The optical diffraction pattern is from the circled membrane and is typical of optical diffraction pattern from the other membranes in the field of view. The absence of a surface relief is reflected in the lack of any hexagonal diffraction intensities in the diffractogram.

If the sample was biased so that all the ES were facing up, then all the replicated surfaces would appear smooth. Therefore, a substrate was devised so that a biased sampling would occur in which the PS would be facing up for replication. Since Con A labeling of yeast protoplasts did not show Con A markers totally exclusive of patch areas, it was likely that the crystalline arrays might have Con A receptors.

a. Materials and Methods

In order to orient the membranes so the external surface would be bound to the glass and the cytoplasmic surface would be facing up, the coverslip was prepared with Con A as the top layer of the substrate. Preparation of the Con A-glu-PL-cs was the same as the one used for whole cells and protoplasts. The mem-Con A-glu-PL-cs was freeze dried in the same way that the freeze fractured specimens were, again using the same preparation of membranes.

b. Results

The membrane surfaces still appeared smooth by this replication technique (Figure 3.11). Again, many grids were scanned for any obvious surface relief. No surface relief was ever found. It is interesting to note the difference between the background in the Con A substrate, which contains very noticeable Con A aggregates, while the background in Figure 3.10 is much smoother.

To summarize, no surface relief was found on the P or E surface within the limits of replication technique, i.e. 20 Å. It is still

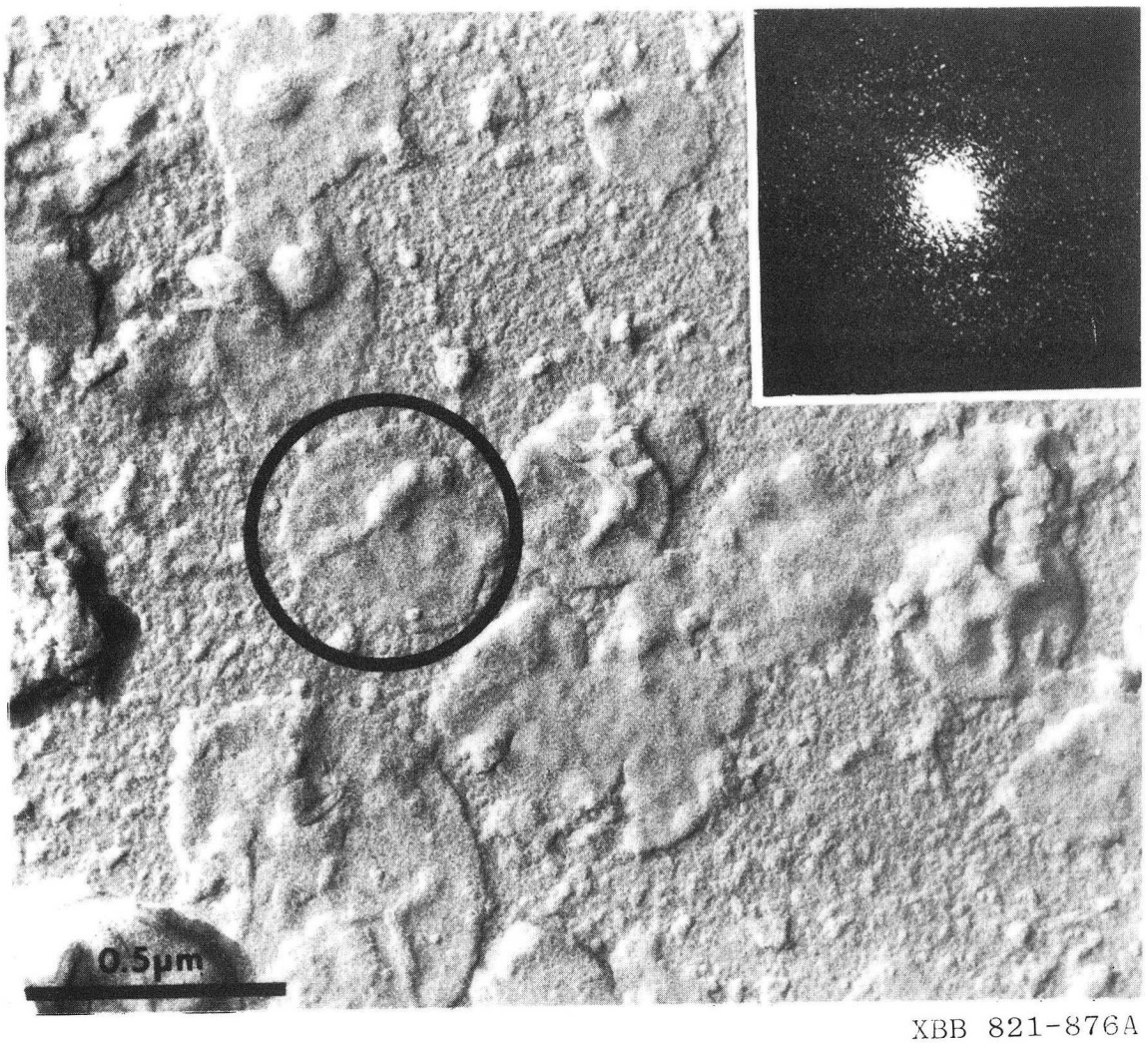

XBB 821-876A

Figure 3.11. Surface replicated Triton X-100 treated membrane on a Con A substrate. There are no hexagonal diffraction spots in the optical diffraction inset. The inset is from the circled membrane.

possible that there is a very slight surface relief not detected, but it is also possible that the exposed areas of these membrane particles are very flat with respect to the lipid components. This became an important result when other microscopic techniques other than freeze fracture, such as negative staining, were applied in order to ascertain the crystallinity of isolated membranes. The amount of surface relief, if no pores or channels are present, may determine the available water spaces for negative staining.

CHAPTER 4

High Resolution Imaging of the Yeast Paracrystals

Once crystalline membranes are isolated, fairly standard electron microscopic techniques combined with computer processing can be applied. It was an exciting prospect to attempt to visualize this membrane, which had been the subject of so much freeze fracture study.

Negative staining was the first electron microscopic technique to be attempted. Negative staining of these membranes will outline the membranes and fill in spaces where the heavy metal ions can penetrate. Because these membranes are crystalline, spatial averaging techniques can be applied to negatively stained membranes that optically diffract, hopefully to the same or higher resolution as images of freeze fracture replicas. It was not known at the outset, however, if the membrane subunits would be accessible to negative stain. Accessibility of the stain to channels or surface structures was questionable in light of the results from the surface replication experiments described in Chapter 3.

Other high resolution imaging techniques could also be applied to this particular system. Frozen hydrated imaging techniques and subsequent spatial averaging applied to unstained hydrated crystalline membranes might provide a projection of the subunits in the crystalline membrane. This goal was equally as exciting, if not more,

as obtaining processed images of negative stained paracrystals, because it would directly compare the projection of the membrane proteins with the reconstructions of the membrane morphology that had been arrived at previously from the distribution of the intramembranous particles obtained from freeze fracture replicas.

A. Negative Staining of the Membranes

1. Materials and Methods

Membranes were negatively stained by thoroughly mixing 5 µl of membrane suspension with 5 µl of the negative stain on a piece of parafilm. An aliquot (5 µl) of this droplet was placed on a grid containing carbon coated formvar as the support film. The membranes were allowed to attach to the support film for about 5 minutes. The bulk water was drawn off with a piece of filter paper and allowed to air dry. The grid was then examined in either the AEI 802, JEOL 100B, or JEOL 100CX at a magnification of 40,000. Micrographs were scanned on a linear optical diffractometer setup in our laboratory.

2. Results

No obvious crystalline arrays were seen in micrographs of negatively stained Triton or Brij-treated membranes. Over 200 membranes were examined under varying conditions of negative staining. Among the negative stains tested were phosphotungstic acid, uranyl acetate, uranyl formate, and ammonium molybdate. Different buffer conditions i.e. distilled water used rather than membrane buffer, did not reveal any stainable material. The failure to see periodic structure in

negatively stained samples was not surprising because surface replication of the paracrystals had shown no obvious channels or surface relief in the membranes.

Negatively stained Triton or Brij-treated membranes were scanned with an optical diffractometer to pick up crystalline order not visible to the eye. Only one membrane ever showed hexagonal optical diffraction intensities. Figure 4.1 is the phosphotungstic acid (PTA) stained Triton-treated membrane. The inset is the optical diffraction pattern from the membrane. No obvious crystallinity is seen in the image, yet this membrane shows hexagonal diffraction intensities which closely match the lattice spacings seen in freeze fracture electron micrographs. There is the slight appearance of doughnut shapes in this image. The highest order reflection in this image is the 2,0 (82.5 Å) reflection. The 1,0 set of reflections may be absent.

There are two hypotheses that can explain why this particular membrane shows hexagonal optical diffraction intensities. The first is that this particular membrane patch was more coherently ordered than others in any preparation. The second explanation is that the membrane may have been slightly delipidated by the Triton-treatment and, therefore, weak stain-filled channels were created. The second explanation is the more likely one since negatively stained Brij-treated membranes, which appear to be better ordered than the Triton-treated membranes, did not show any stronger or clearer optical diffraction intensities than this particular Triton-treated mem-

XBB 821-877A

Figure 4.1. Phosphotungstic acid stained Triton-treated membrane showing weak hexagonal diffraction spots (inset). The highest order diffraction spot visible on the optical diffraction pattern is the 2,0.

brane. Purple membrane is known to optically diffract more intensely (better penetration of the negative stain) after it has been delipidated with 10% deoxycholate (Hwang and Stoeckenius, 1977).

B. Frozen Hydrated Imaging

Since negative staining did not work with these crystalline membranes, the next step was to try the technique of frozen hydrated imaging in conjunction with image processing. Purple membrane is an example of a crystalline membrane which does not stain well, but whose structure has been successfully determined to greater than 4 Å resolution using this cryomicroscopic technique. By analogy, it was thought that the frozen hydrated technique would reveal crystalline optical diffraction intensities in the yeast plasma membrane.

1. Materials and Methods

a. Specimen preparation

The frozen hydrated specimen preparation technique used to image the paracrystals, unstained and hydrated, was the double carbon film technique. The basis of this technique is a sandwiching of the specimen between two thin carbon films (Jaffe, 1982). Carbon was evaporated onto freshly cleaved mica. The "right" thickness of the carbon film was measured by its surface reflectance by an incandescent light bulb after being floated off on double distilled water. If the carbon film was too thin, the film usually broke up on the water surface. If the carbon film was too thick, then it appeared to have a very rough surface. Preferable carbon films were those that

had a very smooth reflective appearance. Carbon films of this "best" thickness were found to be reproducibly produced by directly evaporating 3/4 of a 3.1 mm carbon point at a distance of about 12 to 14 cm from the carbon source.

In the original technique, a grid was brought up through a carbon film which had been floated off on double distilled water in a crystallizing dish. The carbon coated grid was then allowed to dry. The specimen was applied to the carbon coated grid and allowed to attach. The specimen-grid was plunged into the distilled water and shaken to rinse off the excess specimen. The specimen-grid was brought back up through the carbon film to produce the specimen sandwich. The back of the grid was quickly wiped off with a piece of filter paper. Blotting the back side of the grid eliminated the excess water and pieces of the carbon film which wrap around the grid as it is pulled up through the floating carbon film.

Maintaining hydration of the specimen is based on controlled evaporation of the bulk water from the specimen before freezing. The correct amount of water in the sample was monitored by the reflectance of the surface of the grid when illuminated by an incandescent light bulb. The grid will undergo reflectance changes as the water evaporates from between the two carbon layers. When it is extremely wet, the top carbon layer will appear very shiny. As the bulk water evaporates, the top carbon film dries down onto the grid. The rims of the copper grid then begin to appear tarnished, as the rim is often the first part of the grid to dry. Dried regions of the grid

appear matted rather than shiny. Usually there will be one edge of the grid which will dry first. The shiny to mat transition usually starts at one edge of the grid and moves in a wave-like motion across the grid. Best results were obtained when the grid was frozen at the point when half of the grid appeared matted and half shiny. It is interesting to note that when thicker carbon films were used as the top or bottom layer, the grid undergoes the following transformation: very shiny (watery) to mat to shiny (dry) again. In these cases, grids frozen halfway through the mat to shiny transition were thin enough for the beam to pass and contained specimens which were frozen hydrated.

Yeast membranes did not stick spontaneously to carbon films, unlike our experience with purple membrane or catalase crystals. Yeast membranes will adhere onto the grid, but only after long periods of time. Centrifugation had earlier been found to greatly enhance the deposition of crystalline membranes onto the treated glass in the freeze fracture monolayer technique and by analogy, centrifugation should enhance the deposition of membranes onto pretreated carbon coated grids. First attempts of preparing frozen hydrated grids mimicked this protocol. In these first attempts, the carbon grids were found to be sufficiently sticky so that a polylysine-glutaraldehyde treated substrate was not necessary.

The double carbon film technique was therefore changed from the original procedure by the use of thicker and more continuous support films and by the use of centrifugation. Thick carbon films were eva-

porated onto freshly cleaved mica. Reproducible thick carbon films were produced by directly evaporating about 2/3 of a 4.7 mm carbon point at a distance to the source of 12 cm. The carbon films were again floated off onto double distilled water in a crystallizing dish. Several submerged 200 mesh tabbed grids lay on a piece of very smooth filter paper at the bottom of the crystallizing dish. The water was suctioned off so that the carbon film lay on the grids. The carbon coated grids were completely dried. The tab of the grid was cut in half, so that the grid would fit into the back of the 50 µl well of the insert to the Airfuge EM-90 rotor. The membranes are centrifuged for 30 minutes at 15 psi (about 45,000 x g). An aliquot (50 µl) of an appropriate concentration of membrane suspension was then inserted into the chamber. A grid was quickly taken out of the rotor and immersed into a crystallizing dis.h containing the second carbon film. The second film was usually much thinner than the support film and was prepared by the Jaffe method. The grid was shaken to wash off excess material and brought up through the second carbon film. The grid was frozen when the evaporation was considered complete. The grid was then transferred into the 100B electron microscope for frozen hydrated imaging of the membranes. Figure 4.2 is a summary of the procedure for the specimen preparation.

An advantage of using centrifugation is that more than one grid could be centrifuged and kept hydrated in the rotor chamber. At a later time, the second carbon film would be applied, frozen, and inserted into the cold stage of the 100B.

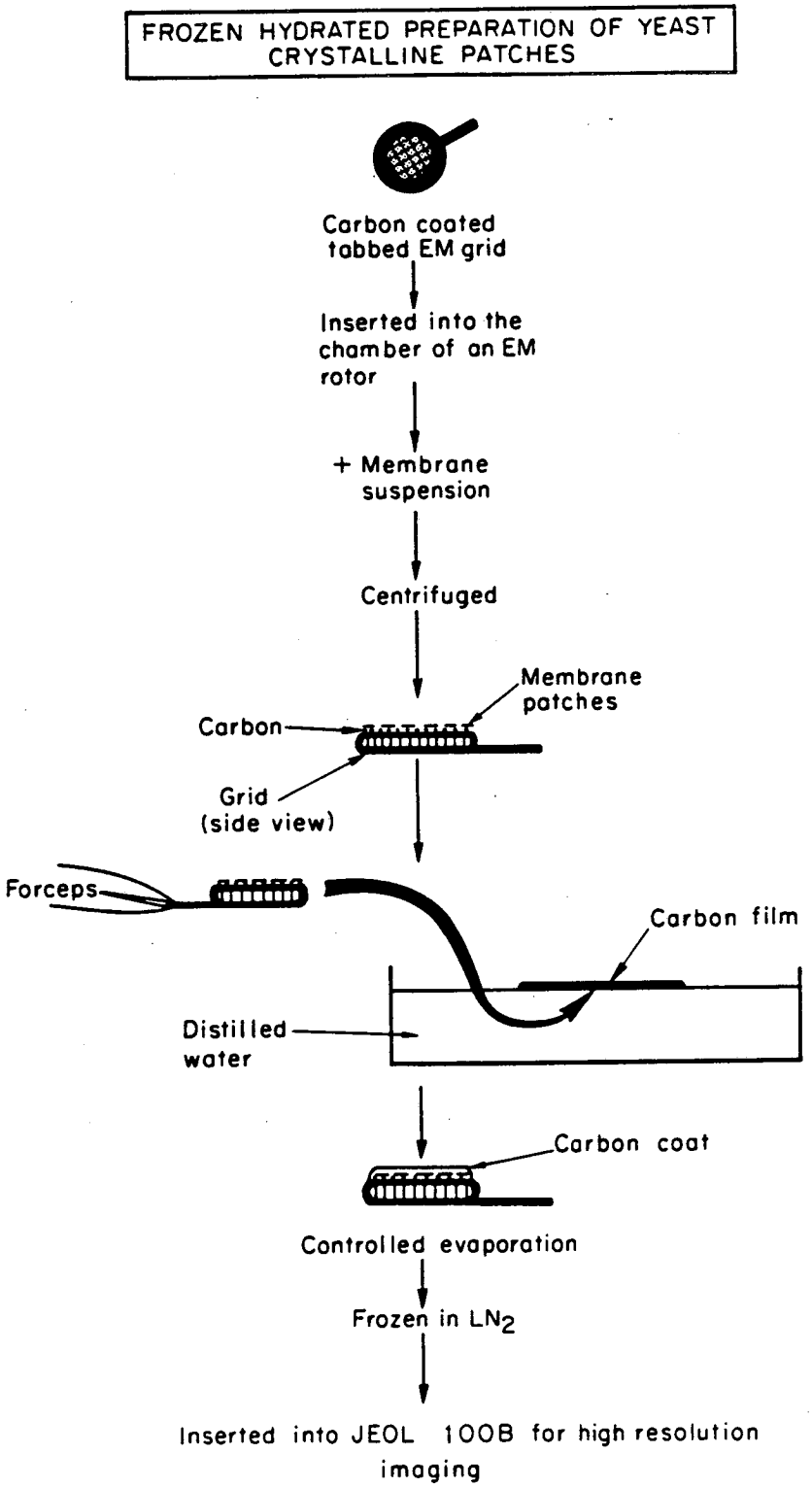

Figure 4.2 A summary of the protocol for the modified double carbon film technique preparation of frozen hydrated specimens.

b. Electron Microscopy (Imaging conditions)

Since not all yeast membranes were necessarily the same, it was preferable to look at the membranes in an extremely low dose scanning mode. When a suitable specimen was found, one would then switch to the higher dose picture mode to take an image with a dose of approximately 5 to 10 e-/$\AA^2$. Ice condensation buildup onto the grid, which is due to residual water in the microscope column, limited the time one could spend looking at a particular grid.

The Remote Condensor Lens Control (RCLC) on our 100B microscope has two channel settings. Channel 2 was set to allow scanning at a low dose rate and Channel 1 was set to record the image. Focusing was carried out on a separate fluorescent screen, which in the 100B microscope is set just in front of the regular fluorescent screen. The dark field imaging system was used for focusing the image by using the dark field translation controls to deflect a condensed electron beam onto the front fluorescent screen. The focusing area, corresponding to the front screen, is just off of the picture area. Therefore, the specimen in the picture area will never see the highly condensed electron beam. The RCLC channel 2 was set to give a dose rate of about 1-2 e-/$\AA^2$/min, as measured by a lithium drifted solid state electron detector.

The RCLC channel 1 was set for image dose at a rate of 100 to 300 e-/$\AA^2$/min, equivalent to 1700 to 5100 cts/sec at a magnification of 200,000. The exposure time typically was set to 2 or 3 sec for picture taking.

Scanning of the specimen grid was done in diffraction mode by defocusing the diffraction spot with the P1 controls. A defocused diffraction spot provides a low magnification image of the specimen, but one that is extremely out of focus and, therefore, contains better specimen contrast than a low magnification image in image mode. There is one drawback to scanning with the low dose channel 2 setting. The defocused diffraction image at these low electron doses can appear distorted and care must be taken to have the image illumination areas in both channels aligned to the center of the screen. If these two image illumination areas are not aligned, it is possible that the specimen may not be in the image area when switching from diffraction to image mode.

A typical low dose image was taken in the following manner: a suitable specimen as seen in diffraction mode was placed on a mark in the center of the screen. The gun shutter was tripped so that the beam was deflected by coils located in the electron gun. The microscope mode setting was changed from diffraction to image mode at a magnification of 40,000. The RCLC current was turned off, the beam was switched to the dark field deflection coils, and the shutter was turned off. The condensed dark field beam, if properly aligned, would fall on the front screen. The image was focused to as an exact focus as one can obtain at 40,000 magnification by minimization of the amorphous carbon granularity and then, defocused from that reference position by the amount of defocus desired. The shutter was again closed. The deflection system was returned to bright field.

The RCLC was switched to Channel 1 and a setting called "One Shot" was used, which will delay the beam current for a few seconds and then provide an exposure of a chosen time to give the specimen a dose of 5 to 10 e-/Å^2. A film was advanced into the camera. A few more minutes were waited in order to minimize specimen drift. The screen was raised and the "FEG START" button was tripped. The "FEG START" controls the time exposure of the electron beam. After the exposure of 2 to 3 seconds, the screen was lowered.

A second, low magnification image of the highly defocused diffraction spot was taken after the low dose image. An image of the defocused diffraction spot can help ascertain not only the shape and size of the membrane whose "high resolution" image had just been taken, but also the amount of hydration in the specimen area. This second image was taken by defocusing the diffraction spot of channel 1 to the size of the screen and exposing for 0.5 seconds. After readjusting the image illumination areas so that fields seen in channel 1 and 2 are coincident (if necessary), the channel setting was returned to 2 and scanning of the grid resumed.

c. Detection of Crystalline Membranes (Scanning Images by Optical Diffraction)

Frozen hydrated membranes are not usually expected to show obvious crystallinity as do some frozen hydrated specimens, e.g. the outer cell wall of Spirillum serpens (Taylor, 1978). Therefore, all frozen hydrated images were scanned for areas that would produce optical diffraction intensities arising from the membranes. The

membrane outlines were not always visible because of ice condensation onto the grid and therefore, plates were scanned thoroughly with an aperture that was large enough to produce detectable diffraction spots, but minimized so that the contrast transfer function from the carbon film would not overwhelm the signal from the yeast membrane.

2. Results

a. Purple Membrane as a Test Specimen

The purple membrane bears a resemblance to the yeast plasma membrane in many ways. Purple membrane is about 80% protein, forms large naturally crystalline arrays, and has only a slight surface relief. Purple membrane does not negatively stain well. There has also been a great deal of work on the structure of purple membrane by electron microscopy (see Chapter 1). Therefore, because of its similarities to the yeast plasma membrane and because so much effort within this laboratory has been dedicated to the technique of frozen hydrated imaging of this membrane, purple membrane was chosen as the test specimen for the double carbon specimen preparation technique.

Good quality electron diffraction patterns of purple membrane had been obtained using the double carbon film technique (Jaffe, 1982), but good quality images of purple membrane had not previously been attempted using this specimen preparation technique. As expected, the double carbon film technique proved to be a very effective specimen hydration technique for imaging purple membrane, as well as for electron diffraction. Figure 4.3a is a low dose image of a frozen hydrated native purple membrane. Although no obvious

crystallinity can be seen, the inset in Figure 4.3 shows an optical diffraction pattern with crystalline diffraction intensities. The arrows in the optical diffraction inset indicate the strong 2,2 reflection corresponding to a resolution of 15.5 Å. Weaker higher resolution spots can also be seen in this optical diffraction pattern. Figure 4.3b is the low magnification image (defocused diffraction spot) of the image of the membrane in 4.3a. The box indicates the low dose image area.

The best images of purple membrane, those images whose optical diffraction patterns contain hexagonal sharp spots beyond 20 Å, were usually from membranes with clear crisp outlines or membranes, such as the one in Figure 4.3b, which were not well delineated but did not "bubble" after prolonged electron irradiation. Unfortunately, air dried membranes also have distinct outlines, so it is not always possible to tell the difference when scanning in diffraction mode between air dried and frozen hydrated membranes. Frozen hydrated membranes with greater amounts of ice usually contained indistinct outlines and "bubbled" after prolonged exposure to the electron beam (electron beam dose on the specimen of greater than 30 e-/Å^2). In these cases the ice covering the membranes, between the two carbon films, was thick enough so that upon prolonged electron exposure, radiolysis products were formed, which created the bubbled appearance. Images with thicker amounts of ice such that the membranes bubbled also showed crystalline optical diffraction. Diffraction spots were not as clearly defined above the noise and often did not

Figure 4.3. A low dose and low magnification pair of images of a frozen hydrated purple membrane. 4.3a. is the low dose image. The inset is the optical diffraction pattern of the membrane. The arrow indicate the 2,2 reflection at a resolution of 15.3 Å. 4.3b is the low magnification (defocused diffraction spot). The box indicates the image area in 4.3a. The asterisk indicates the focusing area on the front screen of the 100B. The purple membrane is not readily apparent due to water vapor condensation as ice on the grid (the small dark blobs seen on 4.3a and b). If the reader holds Figure 4.3b further back, the membrane is more obvious.

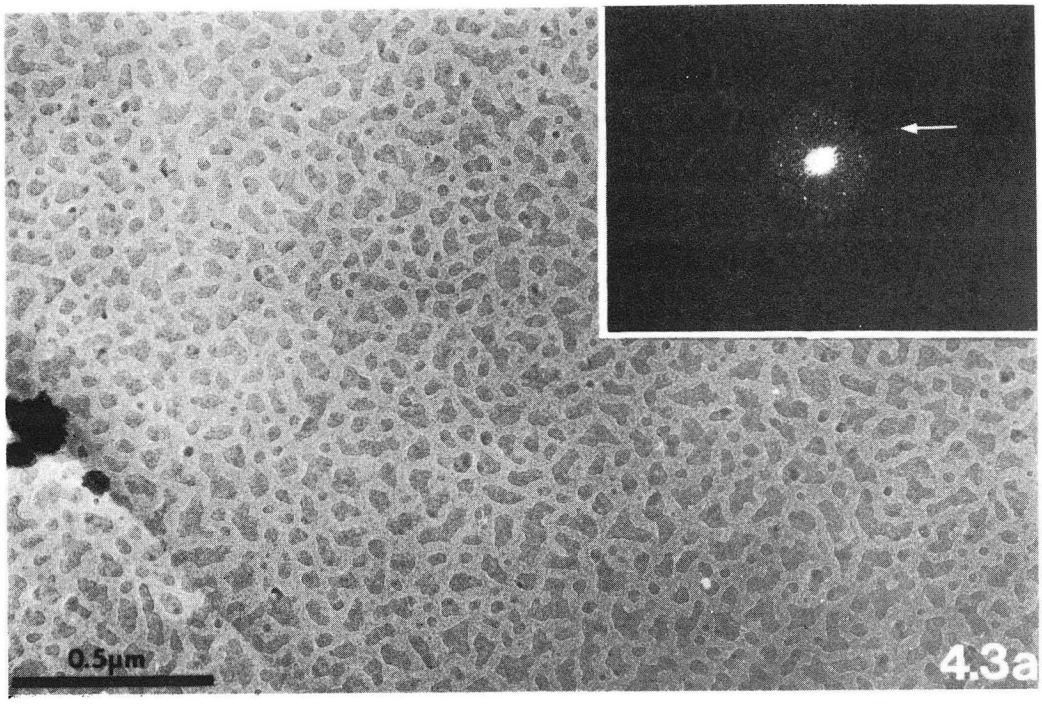

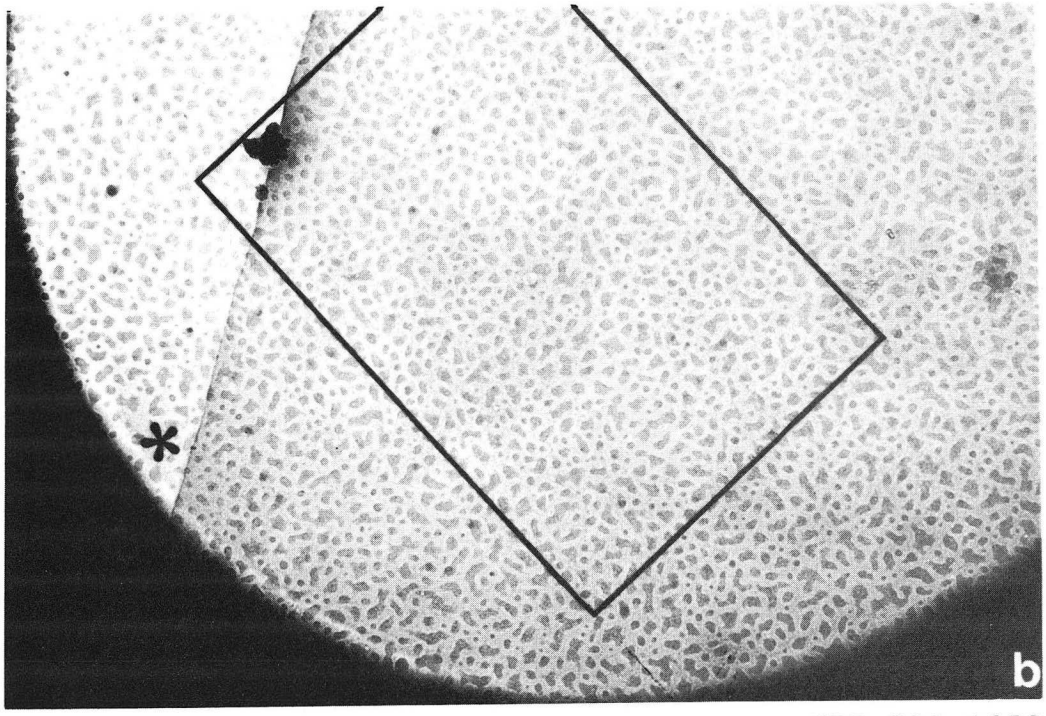

XBB 832-1653

extend to as high a resolution as membranes which did not bubble.

Figure 4.4 is a low dose and low magnification pair of images of frozen hydrated purple membranes that bubbled upon prolonged electron irradiation. Again, no obvious crystallinity can be seen, but the optical diffraction inset shows crystalline diffraction intensities. The arrow indicates the strong 2,2 reflection, but higher resolution diffraction spots are absent. Figure 4.4b is the defocused diffraction spot, which shows the mottled appearance (bubbling phenomenon) of the purple membranes in the irradiated area due to prolonged electron beam exposure of doses greater than 30 $e^-/\text{Å}^2$.

There are three advantages to using the double carbon film technique. The first is the ease of preparation of the frozen hydrated specimen. The second advantage in using the double carbon film technique is that if a particular grid or grid area was hydrated, almost all images of specimens taken on that grid or grid square would show the appropriate optical diffraction intensities. The double carbon film technique is, therefore, an extremely consistent and reproducible technique. The degree of sharpness of the spots and order of the highest resolution spot varied depending on the degree of hydration and the crystalline order of the particular membrane. Another advantage is the easy visibility of the contrast transfer function as seen in the optical diffraction insets. From the contrast transfer function, the defocus can easily be calculated.

b. Imaging of the Yeast Plasma Membrane

Figure 4.4. A low dose and low magnification pair of images of frozen hydrated purple membranes. Figure 4.4a is the low dose image. The optical diffraction is from a portion of the low dose image. The arrow indicates the 2,2 reflection at the same resolution as in Figure 4.3. Figure 4.4b is the low magnification image of the irradiated area. The box indicates the image area in 4.4a and the asterisk indicates the focusing area.

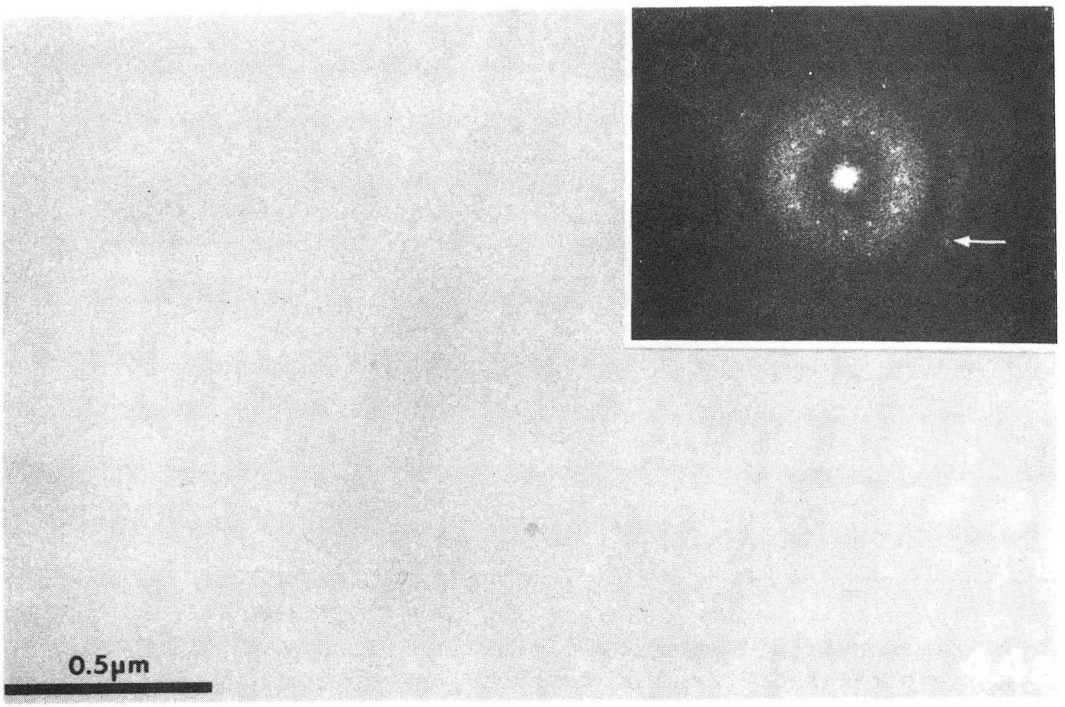

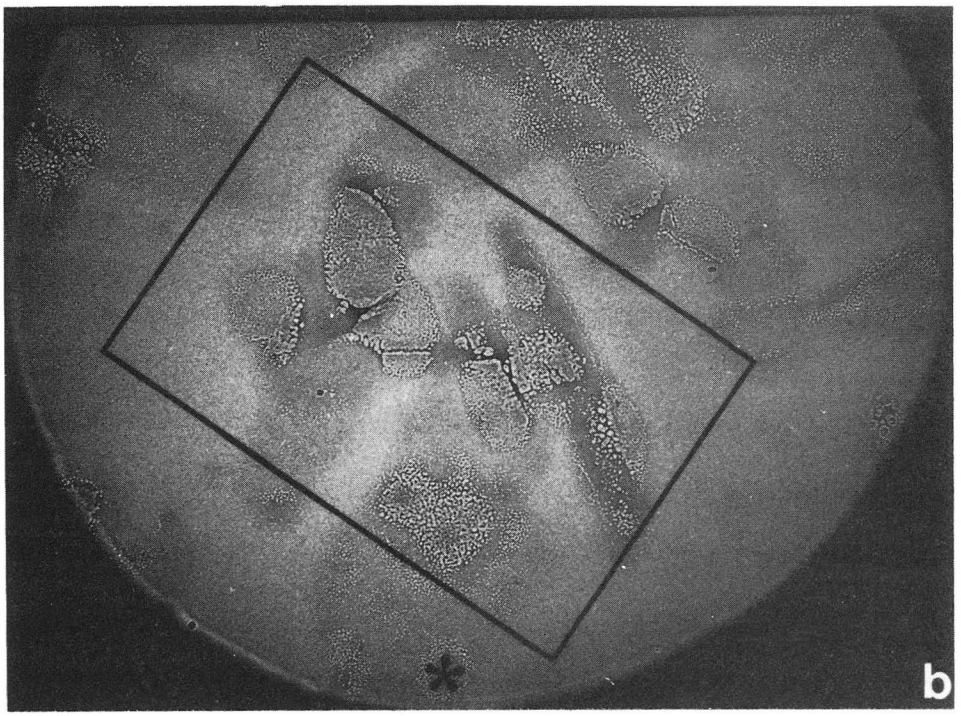

XBB 832-1657

Over 300 images were taken and of these images of yeast plasma membranes very few ever showed crystalline optical diffraction. Imaging of both Triton-treated and Brij-treated yeast plasma membranes was attempted. Brij-treated membranes were thought to be preferable to the Triton-treated membranes because the preparations of Brij-treated membranes were morphologically more pure and therefore, easier to scan for individual membranes in diffraction mode. The appearance of the size and shape of the Brij-membranes correlated well with those seen in the monolayer freeze fracture electron micrographs.

Figure 4.5 is a pair of images of Brij-treated membrane with no crystalline optical diffraction. Figure 4.5a is the low dose image. The inset shows no crystalline diffraction. Figure 4.5b is the defocused diffraction spot and shows an area containing air dried membranes and frozen hydrated membranes. The box in Figure 4.5b is the image area. Air dried membranes never bubbled under prolonged electron exposure and never showed any hexagonal optical diffraction pattern. Those membranes covered by the carbon film were clearly in a frozen hydrated condition, because these membranes bubbled. The yeast plasma membranes bubbled at a faster rate than the purple membranes had, which is probably due to thicker layers of ice trapped between the two carbon layers. The yeast plasma membrane is about 80 Å thick versus 45 Å thick for purple membrane. Hexagonal optical diffraction intensities were never seen from yeast membranes that bubbled after prolonged irradiation.

Figure 4.5. A low dose and low magnification pair of images of Brij-treated yeast plasma membranes. Figure 4.5a is the low dose image. The inset is the optical diffraction pattern from one of the membranes which appeared bubbled in 4.5b (the defocused diffraction spot). There do not seem to be any obvious hexagonal diffraction intensities. The circle indicates the membrane which gave rise to the optical diffraction pattern in the inset. The box in 4.5b indicates the low dose image area. The asterisk indicates the focusing area on the front screen.

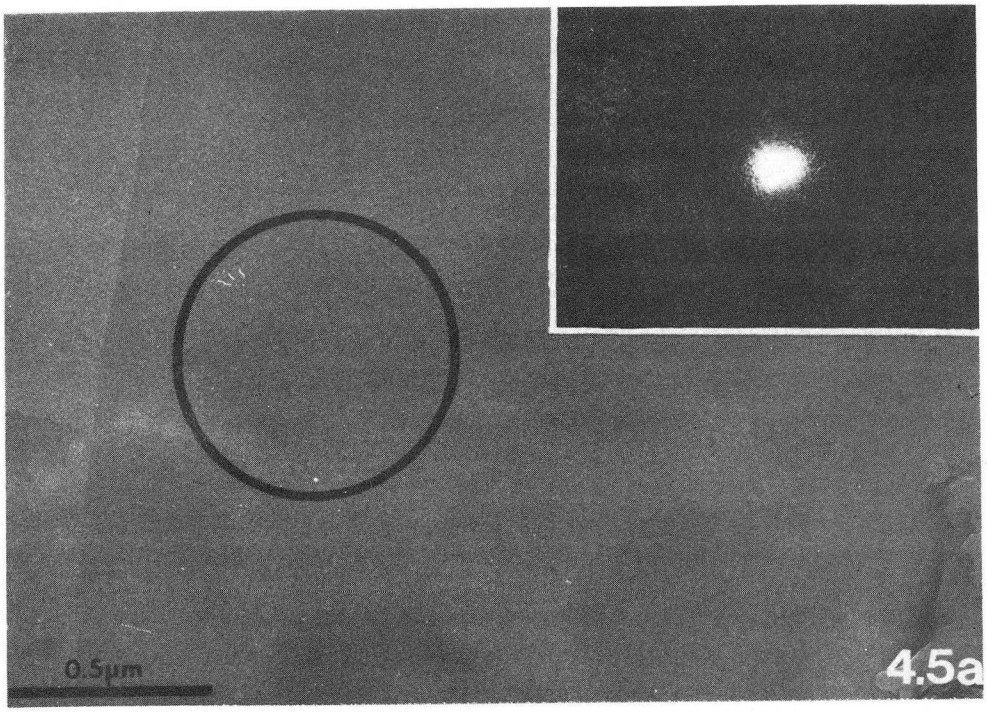

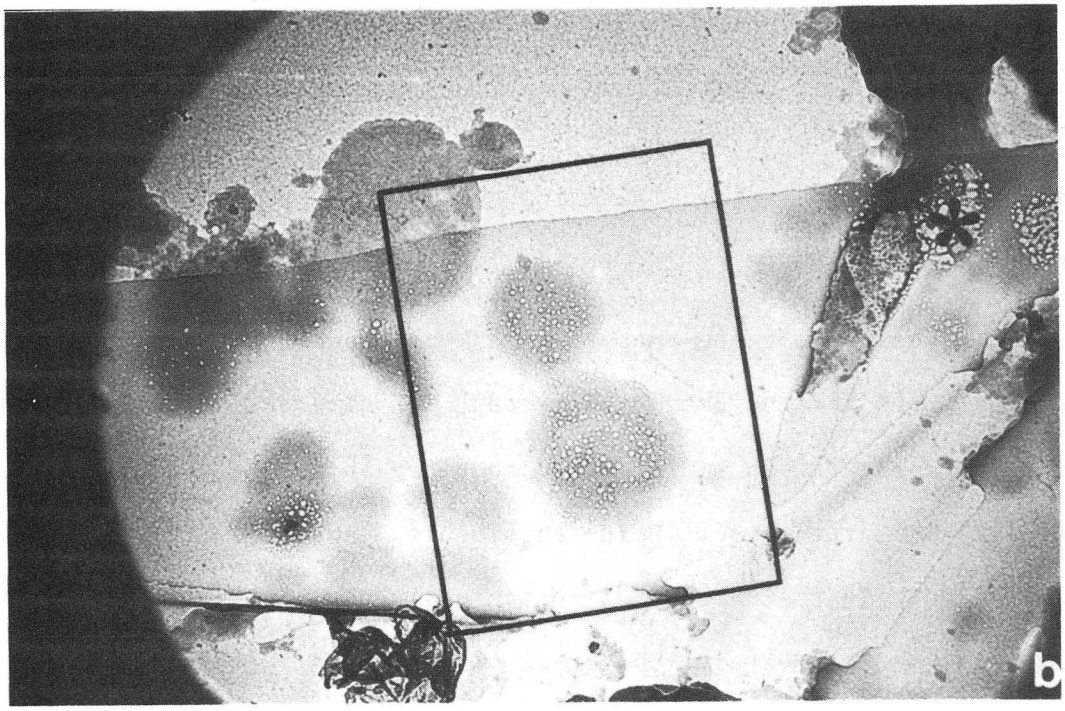

XBB 832-1654

Figure 4.6a is a low dose image of a Brij-treated membrane whose outline on the defocused diffraction spot (Figure 4.6b) is clear and crisp. This area is probably frozen hydrated, because even though the membranes themselves did not bubble, higher water content material in the illuminated area bubbled. It suggests that these particular membranes had the "correct" amount of water bound to the membrane to be frozen hydrated, but not so little as to be air dried. The optical diffraction inset shows no obvious optical diffraction intensities. The box indicates the image area.

Figure 4.7a is a low dose image of a membrane that showed weak hexagonal optical diffraction intensities corresponding to the lattice spacings found in freeze fracture electron micrographs. The membrane itself can be seen in the low dose image area as well as in the defocused diffraction spot (4.7b). The arrows indicate the 2,0 reflection. The six-fold diffraction spots are not very well defined.

The yeast membranes that gave weak hexagonal diffraction spots were measured for the patch coherence. The size of the optical diffraction aperture was minimized so that the spots could just barely be seen above the noise. Using this minimal aperture, the image was scanned both in the x and y dimension until the hexagonal diffraction intensities disappeared. The areas on the plates across which optical diffraction intensities were observed were converted into the specimen areas. Four images that diffracted gave a linear coherent patch size of about 0.28 to 0.48 μm. This is about the size of the

Figure 4.6. A low dose and low magnification pair of images of Brij-treated membranes which probably had the "correct" amount of bound water. These membranes never bubbled after prolonged electron irradiation, but there was extraneous material present in the irradiated area which did bubble (see 4.6b). The inset is the optical diffraction pattern from the membrane indicated by the circle. The optical diffraction inset reveals no obvious hexagonal intensities which would correspond to the spacings measured by freeze fracture.

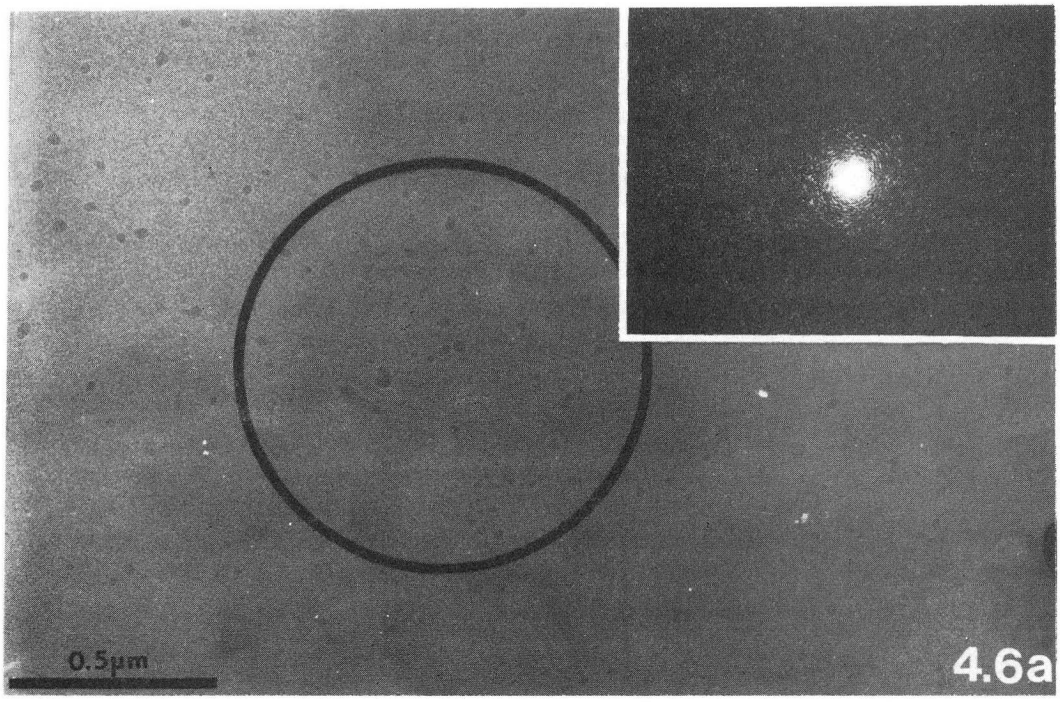

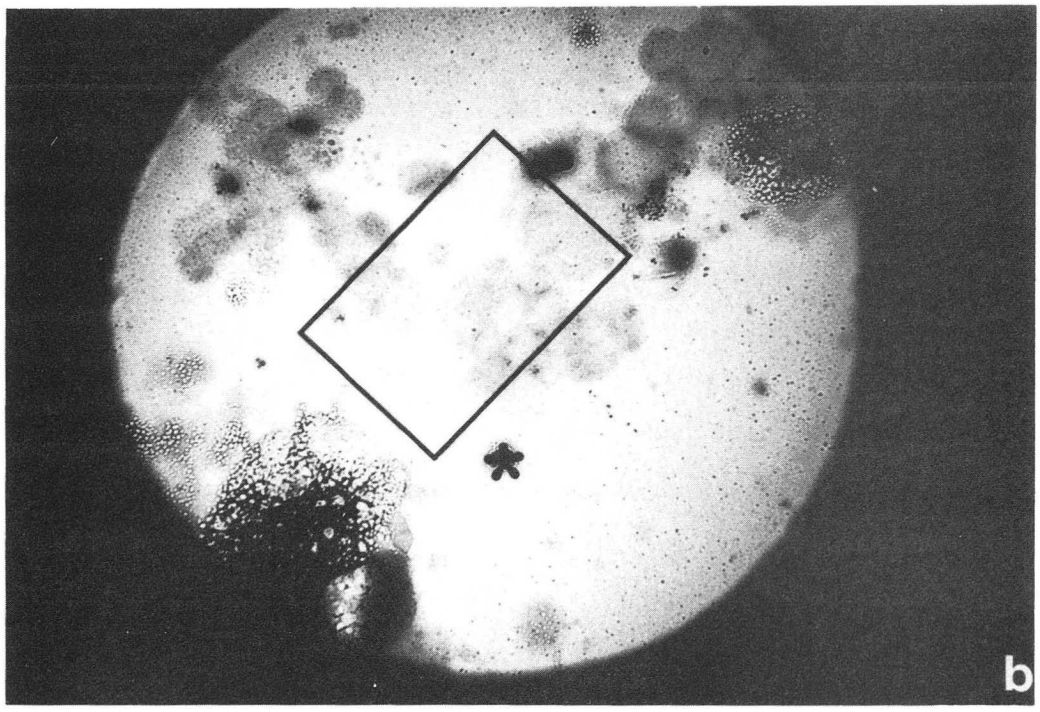

XBB 832-1655

Figure 4.7. A low dose and low magnification pair of images of a Brij-treated membrane which showed hexagonal diffraction intensities corresponding to the lattice spacings found in freeze fracture electron micrographs. This membrane is very well defined in both the defocused diffraction spot and the low dose image. The arrows on the optical diffraction pattern indicate the 2,0 reflection and the circle on the low dose image (4.7a) indicates the membrane that gave rise to this pattern.

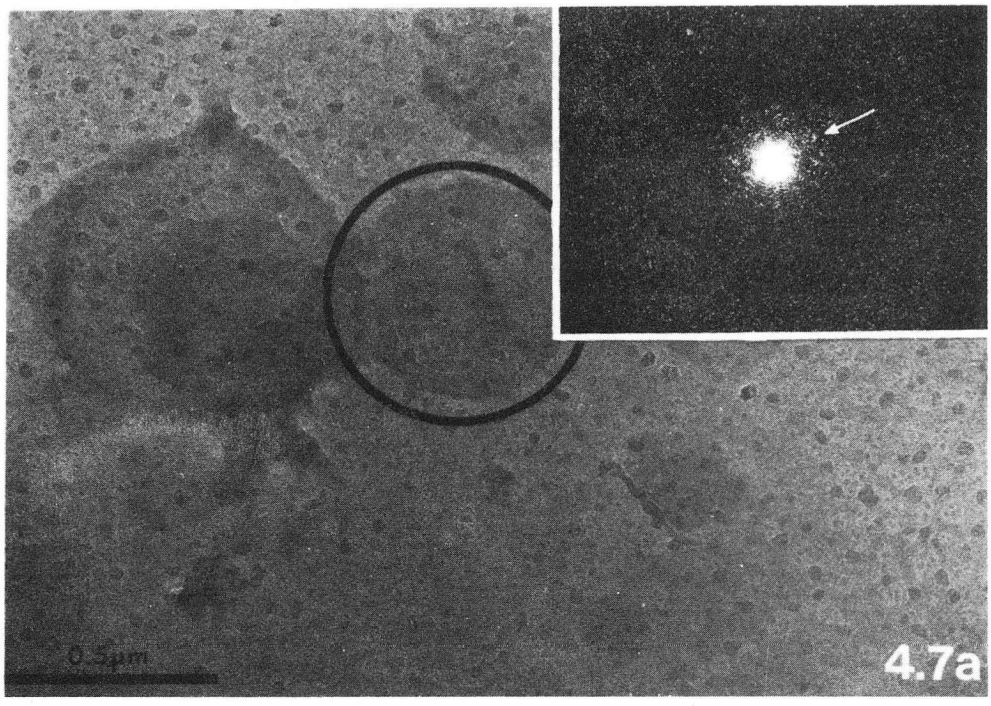

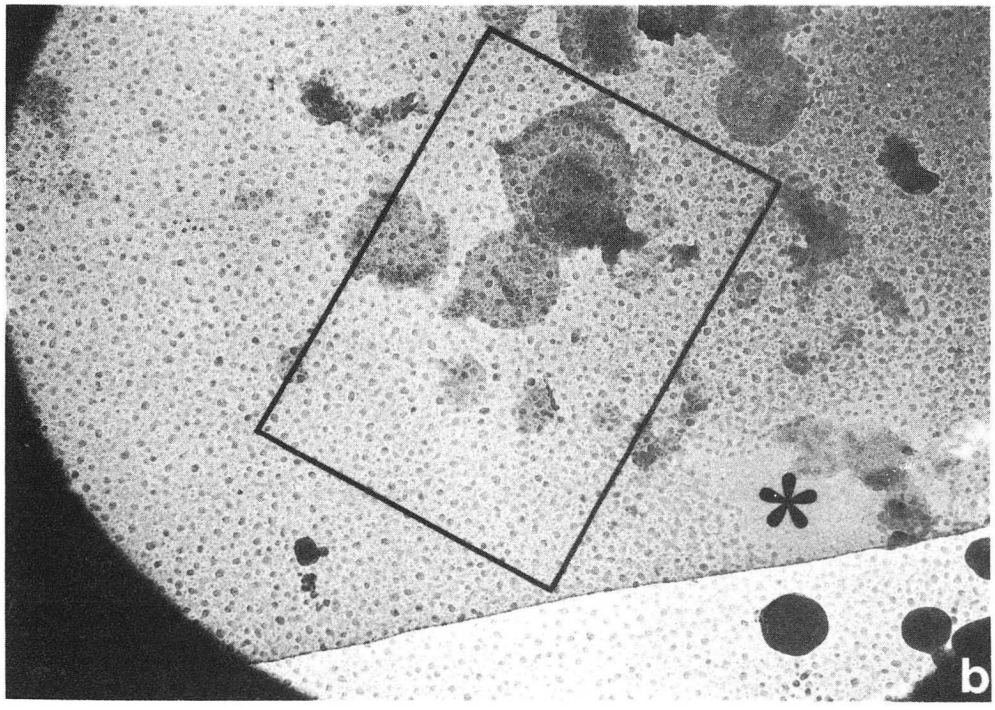

XBB 832-1656

average crystalline array as seen in the freeze fracture micrographs. Therefore, it would appear that in cases where optical diffraction intensities were observed, the whole patch was coherent.

Image processing was not pursued because few structural details could be resolved at the resolution that existed in the optical diffractograms in the best images of yeast membranes. Although these images were very disappointing, the results of the frozen hydrated imaging did contain information about the membrane and the direction that the continued research should go. The next chapter will discuss the meaning of these "negative" results and integrate that information into the present structural model of the paracrystals.

CHAPTER 5

Discussion of Thesis Results and Conclusions

In the previous three chapters, the three problems studied were the crystallization of the intramembranous particles in vivo, the biochemical isolation of the membranes, and the high resolution structure of the membrane. This chapter discusses and interprets the results of the last three chapters and compares our interpretations with the work of previous researchers.

A. Mechanism of Crystallization

The data in Chapter 2 have shown that the patches present in stationary phase are not present in log phase. Furthermore, a smooth transition occurs during lag phase, in which the intramembranous particles move apart within the membrane.

If a cold shroud apparatus were available on our Balzers freeze fracture machine, particle counting could be done to see if the number of volcano particles per unit area of membrane changes as a function of time within the cell growth cycle. The real advantage of having a cold shroud on a freeze fracture machine has been shown by Steere, Erbe, and Moseley (1980). They showed that in exponential phase the particles can be seen as discrete volcanoes even when they are not in hexagonal arrays. In unshrouded systems, the only definitive test of having "volcano particles" is if they are in crystalline arrays. With an adequate shrouding system, one can accurately count

not only the volcano particles within the arrays, but how many volcanoes are in interstitial areas. In the small selected areas of the micrographs in the paper by Steere et al. of stationary state yeast cells, there are volcano particles in the hexagonal arrays and not in the inter-patch areas, however, Bullivant et al. (1979) show micrographs of P faces where there are clear volcano particles in the inter-patch membrane areas. If there were clear volcano particles in the interpatch areas, it might argue for a mechanism in which a solubility limit existed in the membrane. Larger fracture face areas and statistical counting of the volcano particles in the fracture faces would provide a quantitative measurement of the solubility constant of these particles.

In summary, our experiments with inhibitors and those of Osumi, Nagano, and Yanagida (1979) show that sodium azide and dinitrophenol induce crystalline patch formation, while oligomycin, ouabain, and cycloheximide do not induce crystalline arrays in a yeast cell in an exponential phase of cell culture. It is well known that sodium azide and dinitrophenol are both inhibitors of oxidative phosphorylation (Boyer et. al. 1977), oligomycin inhibits the mitochondrial ATPase (Dujon, 1981), and ouabain is an inhibitor only of the Na^+/K^+ ATPase (Dujon, 1981). It was assumed by Osumi, Nagano, and Yanagida that these ATPase inhibitors had no effect on patch formation because no induction of crystalline arrays occurred. However, this conclusion is based on incomplete experiments and remains to be further tested. Drugs and metabolic inhibitors can either induce the forma-

tion of crystalline patches or they can prevent the formation of crystalline patches under the "starvation conditions" in which formation would normally occur. For example, in our experiments, cycloheximide did not induce patches in pre-treated cells, but it still had a demonstrable effect on patch formation in that starvation in the presence of cycloheximide failed to induce patches. If the yeast cells had been pre-treated and then starved in the presence of oligomycin or ouabain, and still did not reveal hexagonal arrays, then those inhibitors would also be considered to have had an effect. On the other hand, if no patches are formed in pre-treated cells but normal patches do form in pre-treated, starved cells, then one could indeed conclude that oligomycin and ouabain were unable to influence patch formation in yeast. The results from treating yeast cells with additional inhibitors and starving them in the presence of the inhibitors can help us to discern which of the three mechanisms seems the most probable.

It has long been hypothesized that the reason why paracrystals were found in stationary state yeast cells was that metabolic starvation occurred when the yeast cells reached stationary phase. The experiments in Chapter 2 have shown that metabolic starvation by itself was not a sufficient basis for crystal formation, but that protein synthesis was also necessary. The most probable mechanism for patch formation is the saturation of the membrane with these particular proteins and the subsequent precipitation of these membrane proteins as crystalline patches in the plasma membrane. Since meta-

bolic starvation was observed to lead to crystallization, it is possible that yeast cells can only form these crystalline arrays in a certain phase of the cell cycle. Stationary phase cells are known to arrest in G1 Pringle and Hartwell, 1981), so G1 would be the phase of the cell cycle in which crystalline arrays would form.

Although the precipitation mechanism is the most probable, other crystallization mechanisms cannot be ruled out. Protein synthesis may indirectly be an integral step in other mechanisms, i.e., other proteins may be involved without which the patches cannot form. The precipitation mechanism is just the simplest and most direct hypothesis that can account for the results of patch inducement with inhibitors. Other data is also accounted by this hypothesis, i.e. the timing of the disappearance of patches in late lag phase correspond to the point in which the total cell surface area begins to increase.

B. Evaluation of The Patch Isolation Method

The paracrystalline membrane isolation described in this thesis provides good morphological purity as shown by the monolayer freeze fracture assay. The ease of isolation of the crystalline membranes is a definite advantage. Two detergents tested, Brij 58 and Triton X-100 dissolve many of the contaminants from extraneous membranes. An extensive use of detergents has yet to be fully exploited. Brij 58-treated crude membranes appear by electron microscopic techniques to be less contaminated by other subcellular materials and better ordered than Triton-treated membranes. The Triton treated-membranes

appear to show good morphological purity, but for frozen hydrated imaging the Brij-treated membranes were preferred. The isolation method described in this thesis is believed to be selective for the crystalline patches. The membrane sheets that are isolated predominatly consist of crystalline arrays instead of mixed areas of patches and nonpatches.

The role that lyticase plays in the isolation of the crystalline arrays cannot be emphasized enough. This enzyme has so much less proteolytic activity than commercially available lytic enzymes that the isolated membrane proteins can be assumed to be intact.

This membrane isolation has the advantage of isolating intact sheets rather than vesicles. This is an advantage in imaging the crystalline membrane proteins by negative staining or frozen hydrated electron microscopy. Flat membranes are desirable because an image of a patch may optically diffract better if the patch laid flat on the support film. If one were interested in functional studies, e.g. pumping protons across a membrane, a preparation of vesicles might be more advantageous. The isolation of vesicles may not be possible using this membrane isolation procedure because, in the intact protoplast, the patches form fairly rigid plates. If cross contamination from other proteins was eliminated, reconstitution of the membrane proteins into lipid vesicles would be possible. Other membrane preparations contained vesicles as the predominant species (for example Fuhrmann et al., 1976, Maurer and Mühlethaler, 1981a, b). Their vesicles were composed of a mixture of nonpatch and patches (Maurer

and Mühlethaler, 1981a, b), thereby allowing closure of the membranes into vesicles.

The exact molecular weight of these proteins has yet to be determined. There is still so much cross contamination from other proteins that there are too many bands on the gel to determine which belong to the yeast plasma membrane. It is probable there are more than three proteins involved in the paracrystals because fracturing of the arrays yields three types of particles. Fracturing of the membrane would not break intra-protein bonds, but would fracture along the hydrophobic surface between proteins.

The cross contamination is deleterious not only because molecular weights can not be determined, but exact lipid and carbohydrate compostion also cannot be accurately determined. Some authors (Matile, 1970, Kramer et al., 1978, Schibechi, Rattray, and Kidby, 1973, and Garcia-Mendoza et al., 1967) have tried to measure the lipid composition of the plasma membrane. Although the composition seems to be relatively independent of the cell wall removal method, all preparations had cross contamination from other membranes and the areas of the plasma membrane devoid of hexagonal arrays. Therefore, one cannot draw conclusions on the lipid composition of crystalline arrays from the published results on the lipid composition of plasma membrane fractions which merely contained crystalline arrays.

The possibility that the paracrystal proteins contain carbohydrate groups such as mannose is somewhat less speculative than the estimate of lipid composition, mainly because of the results of Con A

labeling studies (Maurer and Mühlethaler, 1982, Sosinsky and Glaeser, unpublished results). There is good evidence that there may be mannose residues on the crystalline arrays of the proteins. At the concentration of Con A used when labeling was attempted in this thesis, all the mannose residues were probably not saturated, but labeling of the receptors probably did occur.

C. Current Model of the Structure of the Yeast Plasma Membrane Paracrystals

The experiments reported in this thesis show that the surface relief, as determined by surface replication and negative staining of isolated membranes and deep etching of yeast protoplasts, is minimal. This is in contrast to the findings of Maurer and Mühlethaler (1981a). These authors report a crystalline structure on the PS. This crystalline relief was never seen in any of the methods we used for exploring the crystalline structure. So how can we explain their observations in light of our results?

What may have occurred was that their plasma membrane vesicles absorbed to the alcian blue-treated glass were of an inside-out orientation. Upon freezing in liquid propane, some of the vesicles prefractured and the PF was exposed. Prefracturing is common with another similar freezing agent, liquid freon (Steere, Erbe, and Moseley, 1980). The large crystalline particles that they believed were on the PS therefore could actually have been on the the PF. The strands they observed, which they thought were cytoskeleton, might be the same as the strands seen on the PF, which are known to be due to

plastic deformation of the membrane particles (Sletyr and Robards, 1974). This conjecture explains the fact that their PS particles not only had the same lattice constant as the PF particles, but almost exactly the same size. If a large crystalline array is located on the PS and rises 50 Å above the membrane, negative stains should be readily able to penetrate the spaces between the particles in the array. An example of a membrane where the surface portions of the integral proteins rise significantly above the membrane and where negative stains can also penetrate quite successfully is the chloroplast a/b light harvesting complex membrane (McDonnel and Staehelin, 1980). Therefore, our current model of the structure of the membrane is seen in Figure 5.1. Figure 5.1 is another version of Figure 1.1 modified according to our results.

Seeing no surface relief by replication techniques does not necessarily mean that there is absolutely no surface exposure of the paracrystal proteins. It is possible that exposed regions of the proteins are flush with respect to the lipid bilayer or rise just a few Å above the bilayer or have so much carbohydrate content that the crystallinity is obscured.

Membrane fracture faces imaged by the freeze fracture monolayer assay will not show volcano-like structures because of freeze drying collapse. The monolayer freeze fracture assay was never designed to assay the structure of the crystalline arrays, but only the morphological purity of the membrane sample. The crystalline membranes are instantly recognizable from the micrographs in spite of the ultras-

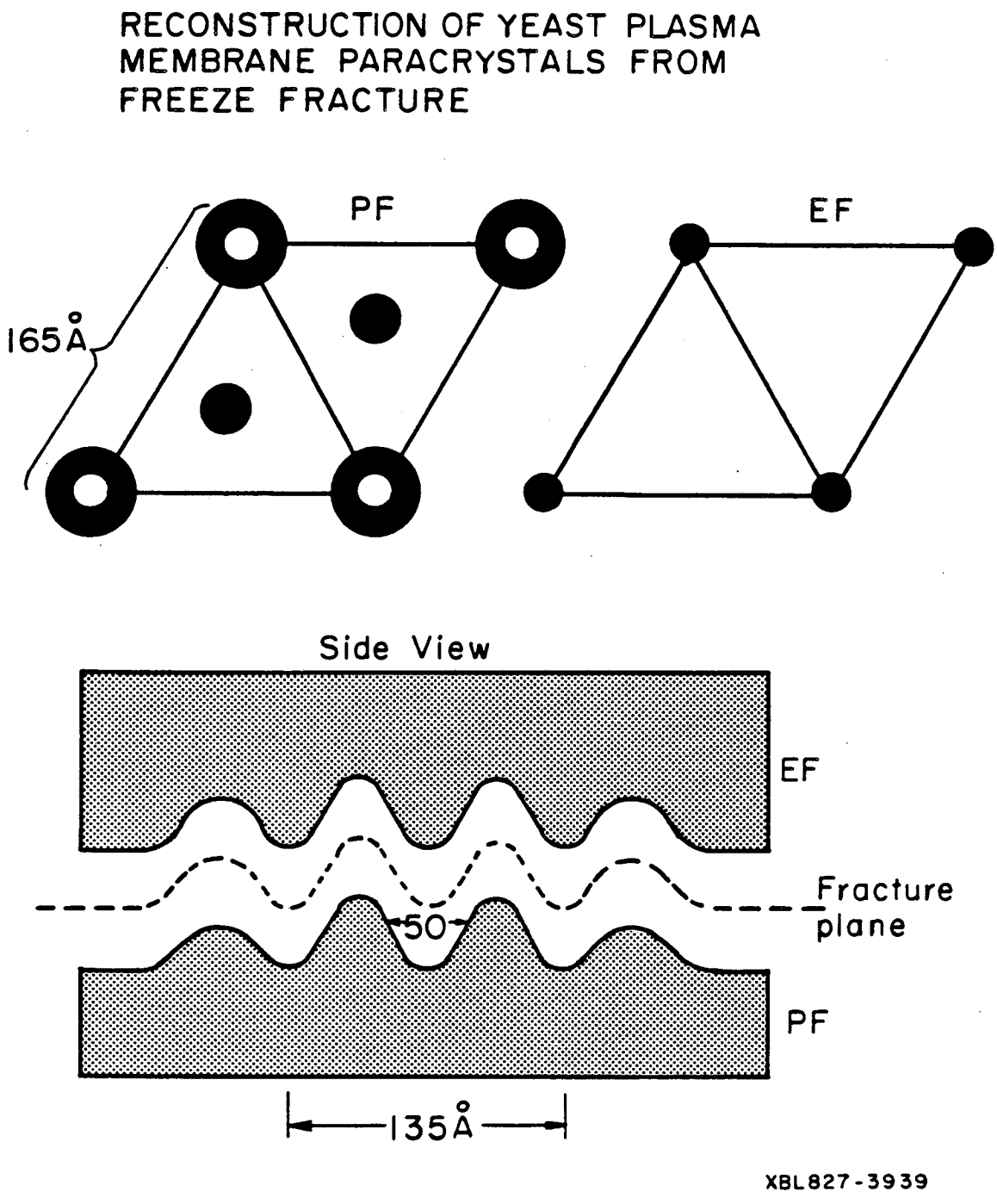

Figure 5.1. A reconstruction of the paracrystal structure modified by the results presented in this thesis.

tructural artifacts introduced by the monolayer technique itself.

In order to achieve greater resolution than can be provided by the monolayer freeze fracture and freeze fracture in general, negative staining and the frozen hydrated imaging technique were applied. Although both gave disappointing optical diffraction results, those "negative results" are additional evidence for the hypothesis that the surface structure is minimal. The contrast of a frozen hydrated specimen is better (and will produce better optical diffraction intensities for a small number of unit cells, e.g. the number of unit cells as found in the yeast plasma membrane) if there are greater amounts of water channels in the structure. The density of the ice versus the protein in the structure is about 0.9 gm/cc for ice and 1.35 gm/cc for proteins. The periodicity in frozen hydrated specimens such as protein crystals (for example, crotoxin and catalase) and Spirillum serpens surface layers is visible by direct imaging, i.e. no image processing is necessary to see the repeating structure, because of the difference in densities. These specimens have large water channels between each of the unit cells. This was not the case with frozen hydrated yeast plasma membranes.

There are three possible reasons why the images of yeast plasma membranes did not show optical diffraction intensities arising from the periodicity within the membrane. The first hypothesis is based on the amount of hydration of the sample. Images of the yeast plasma membrane will not show crystalline optical diffraction if the specimen was dried before it was frozen. On the other hand, if the amount

of ice surrounding the specimen is too thick, diffraction spots may not be detectable. The second reason that the membrane did not reveal optical diffraction is that the membrane being photographed was the "wrong type" of membrane, i.e. that the membrane was derived from either the mitochondrial membrane or the interpatch area of the plasma membrane. The third reason is that the coherent patch size was not large enough, or is too disordered to give good optical diffraction.

Of these hypotheses, the third is the most probable. Figures 4.4, 4.5, and 4.6 showed membranes under varying conditions of hydration. The membranes imaged in Figure 4.5 are indicative of membranes that were sure to be frozen hydrated, but still did not diffract. Therefore, hydration of the membranes does not seem to be the cause of the absence of optical diffraction spots. The crystalline membranes constitute a large percentage of the preparation and enough images were taken so that it is unlikely that all images contained the wrong kind of membrane. The coherent patch size was measured for images of membranes which diffracted and showed that the whole patch was coherent in those cases where the membrane did show diffraction spots. The second half of this hypothesis, that the lattice is too disordered in most cases, or the coherent patch size does not cover the whole membrane to give good optical diffraction intensities, is untestable at the present time.

What can be ascertained from these negative results is the confirmation that the contrast across the membrane is very low. By

analogy, purple membrane has a very low specimen contrast, but has a very large coherent patch size. Native purple membrane has about the same size membrane patches, but its unit cell size is only about 63 Å, as opposed to the yeast paracrystals which has a unit cell size of about 165 Å. If we can assume that the buoyant density of the yeast plasma membrane is 1.27 gm/cc (80% protein and 20% lipid) from the sucrose density gradient data, such that the contrast is similar to purple membrane, then the coherent crystalline area needed to produce as strong spots as an equivalent area of purple membrane will have to be about 7 times as large. Optical diffraction intensities of yeast plasma membrane images can be expected to be, for most cases, 1/7 as strong as those of the same-sized piece of purple membrane, and therefore, the diffraction spots from the yeast membranes may be lost in the background of the contrast transfer function.

D. Future Directions in Studying the Paracrystals

More physiological studies need to be done with other inhibitors in order to unequivically determine the mechanism of crystallization. Experiments with synchronous cells may be able to test the hypothesis that the crystalline arrays only form in G1.

The next step in isolating the paracrystals is to obtain biochemically pure preparations of membranes. It is essential to separate the plasma membrane from mitochondrial membrane. A combination of an acid precipitation of mitochondrial membranes (Dufour and Goffeau, 1978), subsequent low speed differential centrifugation, and a detergent treatment of the plasma membrane to dissolve the

interpatch areas could be the answer to isolating a pure preparation of crystalline proteins. If peripheral proteins are still a problem, the plasma membranes (hopefully devoid of contaminating mitochondrial membranes) can be suspended in 3 to 5 M Gu HCl or in the less dense, but powerful Gu thiocynate. At lower concentrations of guanidine salts, the peripheral proteins may still be denaturated, but the density of the resulting "stripped" membranes will be heavier than the guanidine hydrochloride density, and therefore, it will still be possible to sediment the membranes.

There are several reasons for pure biochemical preparations of the paracrystal membrane proteins being the next goal. In terms of the structural work, reconstitution of the membrane proteins into larger crystalline arrays than can normally be isolated by the present procedure is necessary in order to increase the signal-to-noise in the optical diffraction patterns from the images of the frozen hydrated crystalline membranes. It is also essential to eliminate the possibility that the "wrong" membrane was being imaged. Once cross contamination is cleared up, it is possible that the function of the membrane proteins may be investigated in a more systematic process. For example, if one were given gels with three or four distinct protein bands, Maurer and Mühlethaler's claim that the intramembranous particles are membrane bound invertase could be either eliminated or substantiated by testing the protein bands for invertase activity. Similarly, these proteins can be tested for ATPase activity to see if the particles contain the Mg^{++}-ATPase and

if this ATPase has the same function as the proton pump ATPase found in Schizosaccharomyces pombe by Dufour et al. (1978).

Given the results in this thesis, there is hope that in the future, there will be a great deal more information forthcoming on the structure and function of these particles themselves, and they will no longer be relegated merely to serving as test objects for artifacts of the freeze fracture technique. The fact that the yeast cell makes so many copies of these intramembranous particles makes one wonder about the functional importance. One would hope that the question of why the yeast cell has expended so much energy into synthesis of these particular proteins would stimulate our curiousity about these crystalline membranes.

REFERENCES

1. Anderson, T.F. "Steroscopic Studies of Cells and Viruses in the Electron Microscope." Amer. Natural. 136, 91-100 (1952).

2. Arnold, W.N. "Enzymes." in Yeast Cell Envelopes: Biochemistry, Biophysics, and Ultrastructure. Vol. II. Arnold W.N. eds., 1-46, CRC Press, Inc. (1982).

3. Baumgartner,B., Lambillotte, M., and MŰhlethaler, K. "Immunochemical Analysis of the Plasma Membrane from Baker's Yeast" Saccharomyces cerevisiae. Eur. J. Cell Biol. 23, 6-15 (1980).

4. Boulton, A. "Some Observations on the Chemistry and Morphology of the Membranes Released from Yeast Protoplasts by Osmotic Shock." Exp. Cell Res. 37, 343-359 (1965).

5. Boyer, P.D., Chance, B., Ernster, L., Mitchell, P., and Racker, E., and Slater, E.C. "Oxidative Phosphorylation and Photophosphorylation." Ann. Rev. Biochem. 46, 955-1026 (1977).

6. Branton, D., Bullivant, S., Gilula, N.B., Karnovsky, M.J., Moor, H., MŰhlethaler, K., Northcote, D.H., Packer, L., Satir, B., Satir, P., Speth, V., Staehlin, L.A., Steere, R.L., and Weinstein, R.S. "Freeze-Etching Nomenclature." Science 190, 54-56 (1975).

7. Bullivant, S. "Freeze-Etching and Freeze Fracturing." in Advances in Biological Electron Microscopy, Koehler S., ed., 67-112, Springer-Verlag, (1973).

8. Bullivant, S., Metcalf, P., and Warne, K. "Fine Structure of

Yeast Plasma Membrane After Freeze Fracturing in a Simple Shielded Device." in Freeze Fracture: Methods, Artifacts, and Interpretations, Rash, J.E. and Hudson, C.S., eds., 141-147, Raven Press (1979).

9. Dobbs, B.C., Pangborn, W.A., and Parsons, D.F. "Electron Diffraction of Wet, Unstained, Unfixed Rat Hemoglobin." Proceedings from the Electron Microscopy Society of America, 33rd annual meeting, 216-217, (1975).

10. Dorset, D.L. and Parsons, D.F. "Electron Diffraction from Single, Fully Hydrated, Ox-Liver Catalase Microcrystals." Acta Cryst. A31, 210-215 (1975).

11. Dufour, J.P. and Goffeau, A. "Solubilization by Lysolecithin and Purification of the Plasma Membrane ATPase of the Yeast Schizosaccharomyces pombe." J. Biol. Chem. 253, 7026-7032 (1978).

12. Dujon, B., "Mitochondrial Genetics and Functions." in The Molecular Biology of the Yeast Saccharomyces Life Cycle and Inheritance, Strathern, J.N., Jones, E.W., and Broach, J.R., eds., 97-142. Cold Spring Harbor, (1981).

13. Duran, A., Bowers, B., and Cabib, E. "Chitin Synthetase Zymogen is Attached to the Yeast Plasma Membrane." Proc. Nat. Acad. Sci. 72, 3952-3955 (1975).

14. Edelman, G.M., Yahara, I., and Wang, J.L. "Receptor Mobility and Receptor-Cytoplasmic Interactions in Lymphocytes." Proc. Nat. Acad. Sci. 70, 1442-1446 (1973).

15. Fallon, R.F. and Goodenough, D.A. "Five-Hour Half-Life of Mouse Liver Gap-Junction Protein." J. Cell Biol. 90, 521-526 (1981).

16. Fisher, K.A. "Half "Membrane" Enrichment: Verification by Electron Microscopy." Science 190, 983-985 (1975).

17. Fisher, K.A. "Split Membrane Lipids and Polypeptides." Procedings from the 9th International Congress on Electron Microscopy, Vol. III, 521-532, Toronto, Canada (1978).

18. Fuhrmann, G., Wehrli, E., and Boehm C. "Preparation and Identification of Yeast Plasma Membrane Vesicles." Biochem. Biophys. Acta 363, 295-310 (1974).

19. Fuhrmann, G., Boehm, C., and Theuvenet, A. "Sugar Transport and Potassium Permeability in Yeast Plasma Membrane Vesicles." Biochem. Biophys. Acta 433, 583-596 (1976).

20. Garcia-Mendoza, C., and Villaneuva, J.R. "Preparation and Composition of Protoplast Membranes of Candida utilis." Biochem. Biophys. Acta 135, 189-195 (1967).

21. Glaeser, R.M. "Limitations to Significant Information in Biological Electron Microscopy as a Result of Radiation Damage." J. Ultrastruc. Res. 36, 466-482 (1971).

22. Glaeser, R.M. and Taylor, K.A. "Radiation Damage Relative to Transmission Electron Microscopy of Biological Specimens at Low Temperature: a Review." J. of Micros. 112, 127-138 (1978).

23. Gross, H., Kübler, O., Bas, E., and Moor, H. "Decoration of Specific Sites on Freeze-Fractured Membranes." J. Cell Biol. 79, 646-656 (1978).

24. Gross, H., Bas, E., and Moor, H. "Freeze Fracturing in Ultrahigh Vacuum at -196°C." J. of Cell Biol. 76, 712-728 (1978).

25. Gross, H. "Advances in Ultrahigh Vacuum Freeze Fracturing at Very

Low Specimen Temperature." in Freeze Fracture: Methods, Artifacts, and Interpretations, Rash, J.E. and Hudson, C.S., eds., 127-139, Raven Press, (1979).

26. Hayward, S.B., Grano, D.A., Glaeser, R.M., and Fisher, K.A. "Molecular Orientation of Bacteriorhodopsin within the Purple Membrane of Halobacterium halobium." Proc. Nat. Acad. Sci. 75, 4320-4324 (1978).

27. Hayward, S.B. and Glaeser, R.M. "Radiation Damage of Purple Membrane at Low Temperature." Ultramicros. 4, 201-210 (1979).

28. Hayward, S.B. and Glaeser, R.M. "Use of Low Temperatures for Electron Diffraction and Imaging of Biological Macromolecular Arrays." in Electron Microscopy at Molecular Dimensions. Baumeister, W. and Vogell, W., eds., 226-233, Springer-Verlag (1980).

29. Hayward, S.B. and Stroud, R.M. "Projected Structure of Purple Membrane Determined to 3.7 Å Resolution by Low Temperature Electron Microscopy." J. Mol. Biol. 151, 491-517 (1981).

30. Henderson, D., Eibl, H., and Weber, K. "Structure and Biochemistry of Mouse Hepatic Gap Junctions." J. Mol. Biol. 132, 193-218 (1979).

31. Henderson, R. and Unwin, P.N.T. "Three-Dimensional Model of Purple Membrane Obtained by Electron Microscopy." Nature 257, 28-32 (1975).

32. Hui, S.W., Matricardi, V.R., and Parsons, D.F. "Electron Diffraction of Wet Retina Rod Disc Membranes." Proceedings from the Electron Microscopy Society of America, 31st annual meeting,

602-603, (1973).

33. Hui, S.W., and Parsons, D.F. "Electron Diffraction of Wet Biological Membranes." Science 184, 77-78 (1974).

34. Hwang, S.B. and Stoeckenius, W. "Purple Membrane Vesicles: Morphology and Proton Translocation." J. Mem. Biol. 33, 325-350 (1977).

35. Jaffe, J. "A Difference Fourier Comparison between Frozen Hydrated and Glucose Embedded Purple Membrane." Berkeley, California, University of California, Dissertation, (1982).

36. Kalman, E., Havlik, L., Eke A., Kovacs, P., and Palinkas, G. "In Vitro Investigation of Biological Specimens By Electron Microscopy." Acta Biol. Acad. Sci. Hung. 27, 177-182 (1976).

37. Kawahara, K. and Tanford, C. "Viscosity and Density of Aqueous Solutions of Urea and Guanidine Hydrochloride." J. Biol. Chem. 241, 3228-3232 (1966).

38. Kellenberger, E. and Kistler, J. "The Physics of Specimen Preparation." in Advances in Structure Research by Diffraction, Band VII, Hoppe and Mason, eds., 48-81, Weisbaden, Friedr. Viewig. E. Sohn. (1979).

39. Kistler, J., and Kellenberger, E. "Collapse Phenomena in Freeze Drying." J. of UltraStruc. Res. 59, 70-75 (1977).

40. Kistler, J., Aebi, U., and Kellenberger, E. "Freeze-Drying and Shadowing a Two-Dimensional Periodic Specimen." J. of UltraStruc. Res. 59, 76-86 (1977).

41. Kopp, F. "Morphology of the Plasmalemma of Baker's Yeast (Saccharomyces cerevisiae)." in Freeze-Etching Techniques and

Applications, Benedetti, E.L. and Favard, P. eds., 181-185, Societe Francaise de Microscopie Electronique (1973).

42. Kramer, R., Kopp, F., and Niedermeyer, W., and Fuhrmann, G. "Comparative Studies of the Structure and Composition of the Plasmalemma and the Tonoplast in Saccharomyces cerevisiae." Biochem. Biophys. Acta 507, 369-380 (1978).

43. Kübler, O., Gross, H., and Moor, H. "Complementary Structures of Membrane Fracture Faces Obtained by Ultrahigh Vacuum Freeze-Fracturing at -196°C and Digital Image Processing." Ultramicroscopy 3, 161-168 (1978).

44. Laemmli, U.K. "Cleavage of Structural Proteins during the Assembly of the Head of Bacteriophage T4." Nature 227, 680-685 (1970).

45. Lepault, J., and Dubochet, J. "Preservation of Biological Specimens After Freezing." Proceedings from the European Congress of Electron Microscopy, vol. 2, 648-649 (1980).

46. Longley, R., Rose, A., and Knights, B, "Composition of the Protoplast Membrane from Saccharomyces cerevisiae." Biochem. J. 108, 401-412 (1968).

47. Matile, Ph. "Properties of the Purified Cytoplasmic Membrane of Yeast." in Membrane Structure and Function, FEBS Symposium, 20, Villaneuva, J.R. and Ponz, F., eds., 39-49, Academic Press (1970).

48. Matile, Ph., Moor, H., and Mühlethaler, K. "Isolation and Properties of the Plasmalemma in Yeast." Arch. of Microbiol. 58, 201-211 (1967).

49. Matile, Ph., Moor, H., and Rabinow, C. "Yeast Cytology." in The

Yeasts. vol. I, Rose, A.H. and Harrison, J.S., eds., 219-302, Academic Press, (1971).

50. Maurer, A., and Mühlethaler, K. "Isolation and Characterization of the Paracrystalline Arrays of the Plasma Membrane of Baker's Yeast Saccharomyces cerevisiae." Eur. J. Cell Biol. 24, 216-225, (1981a).

51. Maurer, A. and Mühlethaler, K. "Specific Labeling of Glycoproteins in the Yeast Plasma Membrane with Concanavalin A." Eur. J. Cell Biol. 25, 58-65 (1981b).

52. Maurer, A., and Mühlethaler, K. "Isolation and Localization of Plasma Membrane-Bound Invertase in the Yeast Saccharomyces cerevisiae." Eur. J. Cell Biol. 26, 219-227 (1982).

53. McDonnel, A. and Staehelin, L.A., "Adhesion Between Liposomes Mediated By the Chlorophyll a/b Light-Harvesting Complex Isolated from Chloroplast Membranes." J. Cell Biol. 84 40-56 (1980).

54. McNutt, N., and Weinstein, R. "Useful Resolution Standards for Freeze-Cleave and Etch Replication Techniques." Proceedings from the Electron Microscopy Society of America. 29th annual meeting, 444-445 (1971).

55. Moor, H. "Recent Progress in the Freeze-Etching Technique." Phil. Trans. Roy. Soc. Lond. B 261, 121-131 (1971).

56. Moor, H., and Mühlethaler, K. "Fine Structure in Frozen-Etched Yeast Cells." J. of Cell Biol. 17, 609-628 (1963).

57. Osumi, M., Nagano, M., and Yanagida, M. "Structure of Paracrystalline Arrays in the Cell Membrane of Yeasts." J. Electron Microsc. 28, 301-307 (1979).

58. Parsons, D.F., Matricardi, V.R., Subjeck, J., Uydess, I., and Wray, G. "High-Voltage Electron Microscopy of Wet Whole Cancer and Normal cells. Visualization of Cytoplasmic Structures and Surface Projections." Biochem. Biophys. Acta 290, 110-124 (1972).

59. Parsons, D.F., Uydess, I., and Matricardi, V.R. "High Voltage Electron Microscopy of Wet Whole Cells: Effect of Different Wet Cell Preparation Methods on the Visibility of Structures." J. of Micros. 100, 153-167 (1974).

60. Pringle, J.R. and Hartwell, L.H. "The Saccharomyces cerevisiae Cell Cycle." in: The Molecular Biology of the Yeast Saccharomyces: Life cycle and Inheritance. Stathern, J.N., Jones, E.W., and Broach, J.R. 97-142, Cold Spring Harbor (1981).

61. Schibechi, A., Rattray, J.B.M., and Kidby, D.K. "Electron Microscopy of Autoradiography of Labeled Yeast Plasma Membrane." Biochem. Biophys. Acta 323, 532-538 (1973).

62. Schindler, D. and Davies, J. "Inhibitors of Macromolecular Synthesis in Yeast." in Methods in Cell Biology, 17-38, Prescott, D., ed. Academic Press (1975).

63. Scott, J.H. and Schekman, R. "Lyticase: Endoglucanase and Protease Activities That Act Together in Yeast Cell Lysis." J. of Bact. 142, 414-423 (1980).

64. Sleytr, U.B., and Messner, P. "Freeze-Fracturing in Normal Vacuum Reveals Ringlike Yeast Plasmalemma Structures." J. Cell Biol. 79, 276-280 (1978).

65. Sleytr, U.B., and Robards, A.W. "Plastic Deformation during Freeze Cleavage: A Review." J. of Microsc. 110, 1-25 (1977).

66. Sleytr, U.B., and Robards, A.W. "Understanding the Artifact Problem in Freeze-Fracture Replication: a Review." J. of Micros. 126, 101-122 (1982).

67. Sletyr, U.B. and Umrath, W. "A Simple Device for Obtaining Complementary Fracture Planes at Liquid Helium Temperature in the Freeze Etching Technique." J. of Micros. 101, 187-195 (1974).

68. Steck, T.L. "Selective Solubilization of Red Blood Cell Membrane Proteins with Guanidine Hydrochloride." Biochem. Biophys. Acta 255, 553-556 (1972).

69. Steere, R.L. "Electron Microscopy of Structural Detail in Frozen Biological Specimens." J. Biophs. and Biochem. Cytol. 3, 43-60 (1957).

70. Steere, R.L., Erbe, E.F., and Moseley, J.M. "Prefracture and Cold-Fracture Images of Yeast Plasma Membranes." J. Cell Biol. 86, 113-122 (1980).

71. Streiblova, E. "Surface structure of Yeast Protoplasts." J. of Bact. 95, 700-707 (1968).

72. Takeo, K. "Ultrastructural Features Underlying the Hexagonal Arrangement of Plasma Membrane-Intercalated Particles of Saccharomyces cerevisiae." J. of Gen. Microbiol. 97, 331-334 (1976).

73. Takeo, K., Shigeta, M., and Takagi, Y. "Plasma Membrane Ultrastructural Differences Between the Exponential and Stationary Phases of Saccharomyces cerevisiae as Revealed by Freeze-Etching." J. of Gen. Microbiol. 97, 323-329 (1976).

74. Taylor, K.A., and Glaeser, R.M. "Electron Microscopy of Frozen

Hydrated Biological Specimens." J. Ultrastruc. Res. 55, 446-456 (1976).

75. Taylor, K.A. "Structure Determination of Frozen Hydrated Crystalline Biological Specimens." J. of Micros. 112, 115-125 (1978).

76. Unwin, P.N.T. "Electron Microscopy of the Stacked Disc Aggregate of Tobacco Mosaic Virus Protein." J. Mol. Biol. 87, 657-670 (1974).

77. Unwin, P.N.T., and Henderson, R. "Molecular Structure Determination by Electron Microscopy of Unstained Crystalline Specimens." J. Mol. Biol. 94, 425-440 (1975).

78. Williams, R.C., and Fisher, H.W. "Electron Microscopy of Tobacco Mosaic Virus Under Conditions of Minimal Beam Exposure." J. Mol. Biol. 52, 121-123 (1970).

79. Zampighi, G. and Unwin, P.N.T. "Two Forms of Isolated Gap Junctions." J. Mol. Biol. 135, 451-464 (1979).

TECHNICAL INFORMATION DEPARTMENT
LAWRENCE BERKELEY LABORATORY
UNIVERSITY OF CALIFORNIA
BERKELEY, CALIFORNIA 94720